Head and Neck

8

Head and Neck

HEAD AND NECK

8.1. SKULL: ANTERIOR VIEW

8.2. SKULL: ANTEROPOSTERIOR X-RAY

8.3. SKULL: ANTEROPOSTERIOR CALDWELL PROJECTION AND FACE/ORBIT DETAIL

8.4. SKULL: LATERAL VIEW

8.5. SKULL: MIDSAGITTAL SECTION

8.6. LATERAL X-RAY

8.7. CALVARIA

8.8. CRANIAL BASE: INFERIOR VIEW

8.9. CRANIAL BASE: SUPERIOR VIEW

8.10. SKULL OF THE NEWBORN

8.11. MANDIBLE

8.12. CERVICAL VERTEBRAE AND LATERAL X-RAY

8.13. ATLAS AND AXIS

8.14. IMAGING OF CERVICAL TRAUMA AND PATHOLOGY

8.15. SUPERFICIAL VESSELS, NERVES, AND MUSCLES OF THE NECK

8.16. ARTERIES OF ORAL AND PHARYNGEAL REGIONS

8.17. AXIAL CT AND CROSS SECTION OF THE NECK THROUGH C7 AND THE THYROID GLAND

8.18. AXIAL CT THROUGH C5 AND THE LARYNX

8.19. AXIAL CT THROUGH C3 AND THE HYOID BONE

8.20. SEARCH STRATEGY: NECK IMAGING OF LARYNGEAL TUMOR

8.21. CROSS AND CORONAL SECTIONS OF THE TONGUE AND SALIVARY GLANDS

8.22. AXIAL CT AT C2 AND C1

8.23. IMAGING PATHOLOGY OF THE ORAL CAVITY

8.24. LATERAL WALL OF THE NASAL CAVITY

8.25. THE NOSE, NASAL CAVITY, AND MAXILLARY SINUSES IN THE TRANSVERSE PLANE

8.26. PARANASAL AIR SINUSES

8.27. IMAGING OF THE PARANASAL SINUSES

8.28. CROSS AND CORONAL SECTIONS OF THE ORBIT

8.29. IMAGING OF THE ORBIT

8.30. IMAGING OF SINUS AND ORBIT PATHOLOGY

8.31. IMAGING OF SINUS AND ORBIT PATHOLOGY (CONT'D)

8.32. CORONAL SECTION OF THE HEAD THROUGH THE ORBIT, SINUSES, AND ORAL CAVITY: OVERVIEW

8.33. MIDSAGITTAL SECTION OF THE NASAL CAVITY, PHARYNX, ORAL CAVITY, AND NECK: OVERVIEW

8.34. T1 AND T2 MRI OF THE HEAD AND NECK IN MIDSAGITTAL SECTION

8.35. DURAL VENOUS SINUSES

8.36. DURAL VENOUS SINUSES (CONT'D)

8.37. the CAVERNOUS SINUS

8.38. SUPERIOR SAGITTAL SINUS, MIDDLE MENINGEAL ARTERY, AND SUPERFICIAL CEREBRAL VEINS

8.39. IMAGING OF EPIDURAL AND SUBDURAL BLEEDING

8.40. ARTERIES FROM THE NECK TO THE BRAIN

8.41. VASCULAR STUDIES

8.42. EXTERNAL, MIDDLE, AND INNER EAR

8.43. CT OF THE TEMPORAL BONE AND EAR COMPARTMENTS

8.44. IMAGING OF TEMPORAL BONE/EAR PATHOLOGY

BRAIN

8.45. MIDSAGITTAL SECTION OF BRAIN; MEDIAL VIEW OF CEREBRUM

8.46. MIDSAGITTAL T1 MRI

8.47. VENTRICLES OF THE BRAIN

8.48. CIRCULATION OF CEREBROSPINAL FLUID AND HYDROCEPHALUS

8.49. FOURTH VENTRICLE AND SECTIONS OF THE CEREBELLUM

8.50. BRAINSTEM

8.51. CEREBELLUM

8.52. T1 SAGITTAL MRI NEAR THE MIDLINE

8.53. T1 SAGITTAL MRI THROUGH THE TEMPORAL LOBE

8.54. T1 SAGITTAL MRI THROUGH THE TEMPORAL LOBE (CONT'D)

8.55. T2 FLAIR CORONAL MRI THROUGH THE CEREBELLUM

8.56. T2 FLAIR CORONAL MRI THROUGH THE BRAINSTEM

8.57. T2 FLAIR CORONAL MRI THROUGH THE PONS AND THIRD VENTRICLE

8.58. T2 FLAIR CORONAL MRI THROUGH THE OPTIC CHIASM

8.59. T2 FLAIR CORONAL MRI THROUGH THE TEMPORAL LOBES

8.60. T2 FLAIR CORONAL MRI THROUGH THE FRONTAL LOBES

8.61. T1 AND T2 AXIAL MRI THROUGH THE MEDULLA

8.62. T1 AND T2 AXIAL MRI THROUGH THE CEREBELLUM, TEMPORAL LOBES, AND EYE

8.63. T1 AND T2 AXIAL MRI THROUGH THE UPPER CEREBELLUM

8.64. ARTERIES OF THE BRAIN: INFERIOR VIEW

8.65. CEREBRAL ARTERIAL CIRCLE (OF WILLIS)

8.66. T1 AND T2 AXIAL MRI THROUGH THE OPTIC CHIASM

8.67. T1 AND T2 AXIAL MRI THROUGH THE THALAMUS AND THIRD VENTRICLE

8.68. TRANSVERSE (AXIAL) SECTION OF THE BRAIN AT THE LEVEL OF THE BASAL NUCLEI

8.69. T1 AND T2 AXIAL MRI THROUGH THE THALAMUS AND LATERAL VENTRICLES

8.70. THALAMUS

8.71. HIPPOCAMPUS AND FORNIX

8.72. T1 AND T2 AXIAL MRI THROUGH THE LATERAL VENTRICLES

8.73. T1 AND T2 AXIAL MRI THROUGH THE MIDDLE OF THE CEREBRAL HEMISPHERES

8.74. T1 AND T2 AXIAL MRI THROUGH THE THALAMUS AND LATERAL VENTRICLES

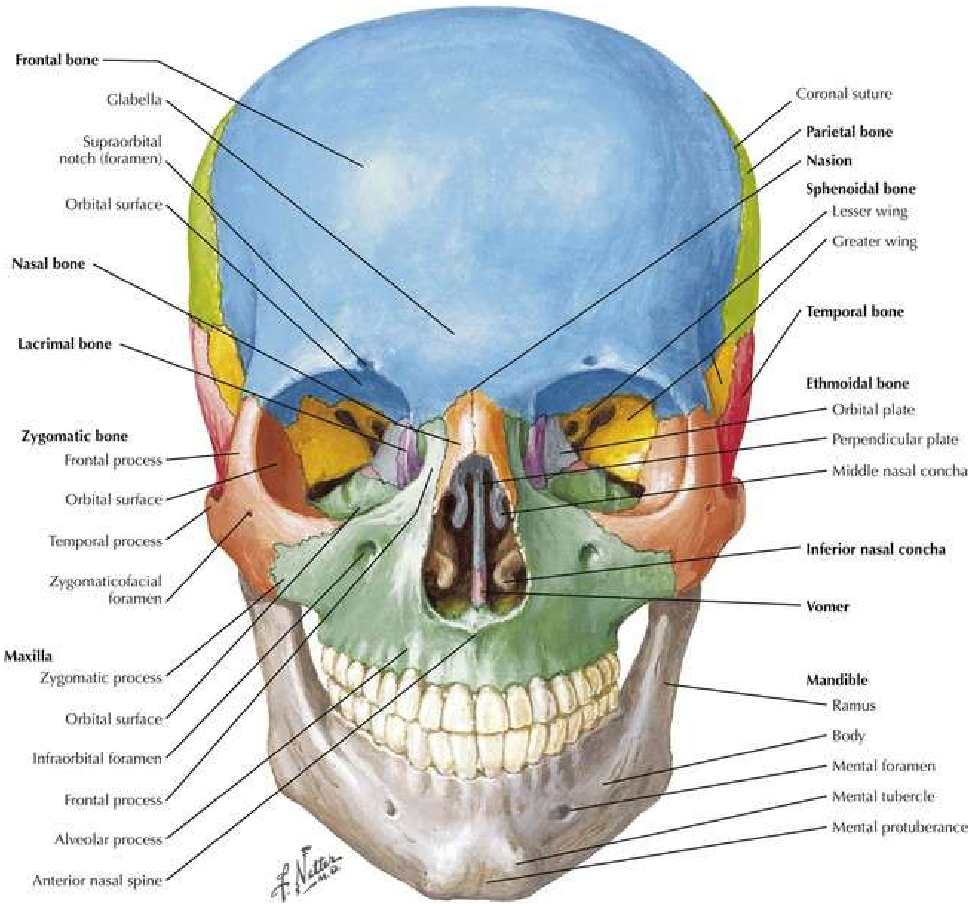

8.1 Skull: Anterior View

The prominent bones of the skull in an anterior view are the frontal bone forming the anterior calvarium and roof of each orbit, nasal bones, zygomatic bones of the cheek and lateral wall of the orbit, maxilla, and mandible. The upper part of the nasal septum and middle nasal conchae are parts of the ethmoid bone; the lower part of the septum is the vomer.

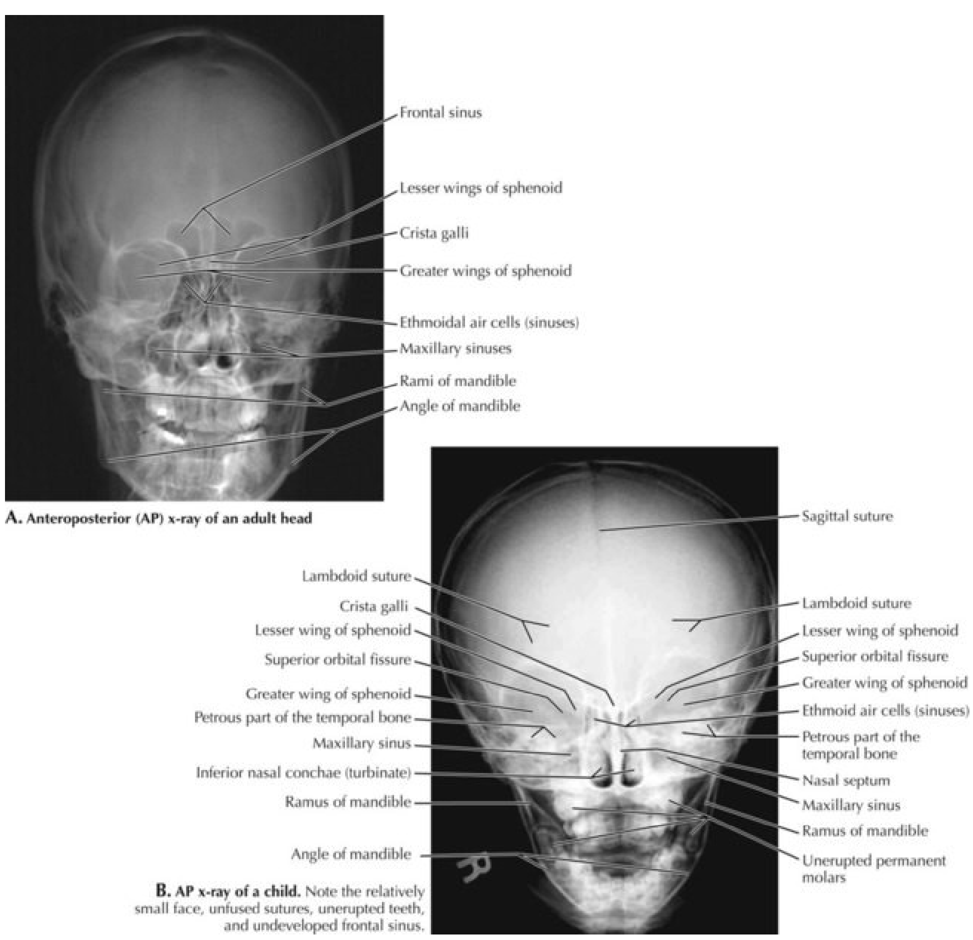

A. **Anteroposterior (AP) x-ray of an adult head**

B. **AP x-ray of a child.** Note the relatively small face, unfused sutures, unerupted teeth, and undeveloped frontal sinus.

8.2 Skull: Anteroposterior X-Ray

The most radiopaque (whitest) parts of the skull in an anterior x-ray are the petrous parts of the temporal bone and the overlap of the molar row of teeth in the maxilla and mandible. The head is positioned to superimpose the petrous temporal on the lower parts of the orbits to better view the inferior parts of the maxillary sinuses for fluid or blood (e.g., from trauma). The most radiolucent (darkest) areas are from air in the mastoid air cells, nasal cavity, and paranasal sinuses (frontal, maxillary, and ethmoid). The ethmoid sinuses appear darker; they are superimposed on the sphenoid sinus behind it. Also note the increase in density where x-rays pass end-on through the flat bones at the periphery of the neurocranium and through the cribriform plate of the ethmoid bone.

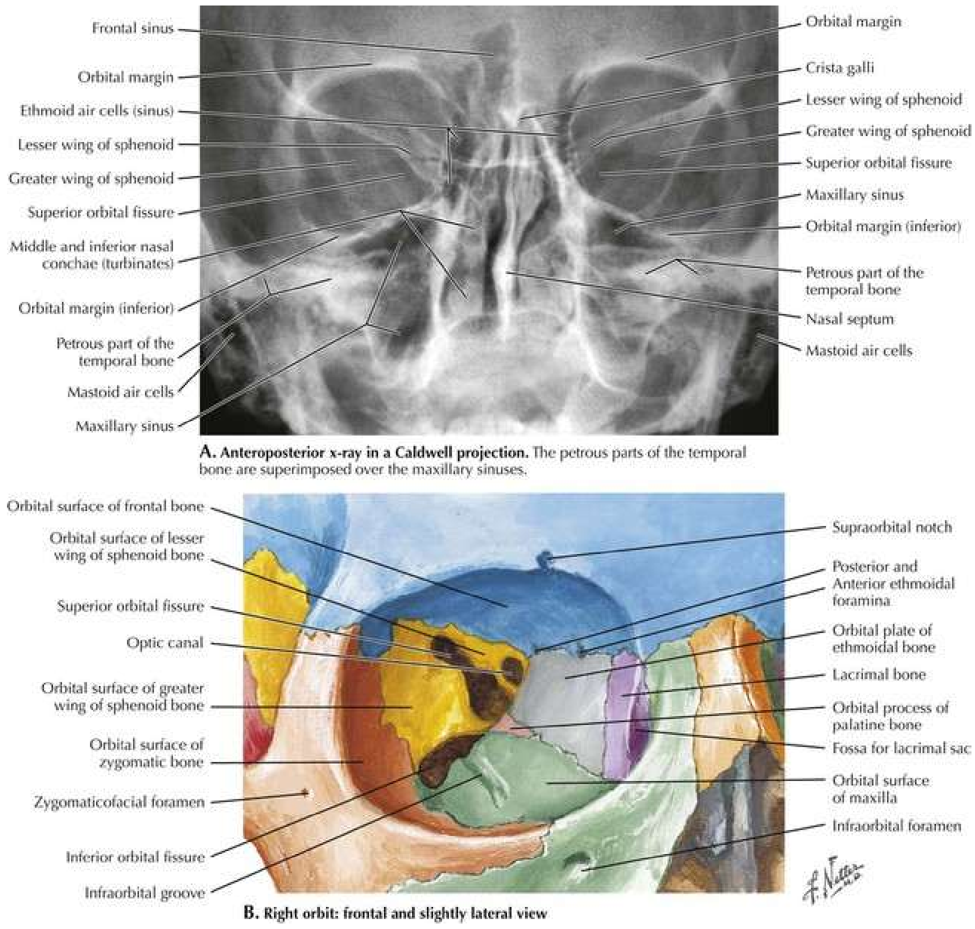

A. Anteroposterior x-ray in a Caldwell projection. The petrous parts of the temporal bone are superimposed over the maxillary sinuses.

B. Right orbit: frontal and slightly lateral view

8.3 Skull: Anteroposterior Caldwell Projection and Face/Orbit Detail

In an anteroposterior (AP) Caldwell view of the skull, the head is positioned so the petrous parts of the temporal bone are projected through the maxillary sinuses rather than the orbits. Orbital anatomy and pathology are better seen here; maxillary sinuses are better studied (e.g., for "blow-out" fractures) in a conventional film. A dominant feature of the orbit is the superior orbital fissure separating the greater and lesser wings of the sphenoid bone. The lateral surface of the greater wing of the sphenoid bone in the infratemporal fossa behind the orbit is also prominent.

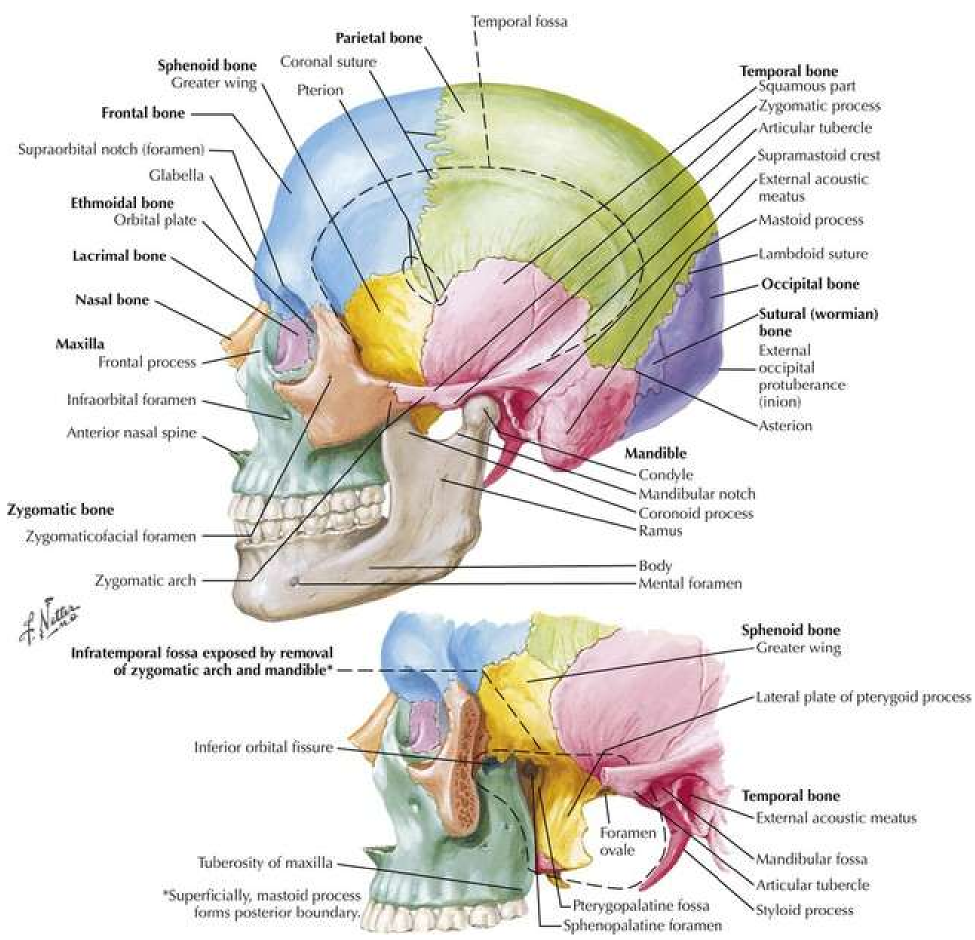

8.4 Skull: Lateral View

The skull consists of a neurocranium surrounding the brain and a viscerocranium consisting of upper and lower jaws and the orbits. The coronal suture separates the frontal and parietal bones, the lambdoidal suture the parietal and occipital bones, and the squamous suture the parietal and temporal bones. Following the contour of the lateral surface of the neurocranium from superficial to deep are three fossae: the temporal fossa for the temporalis muscle; the infratemporal fossa for the pterygoid muscles, mandibular nerve, and maxillary artery; and the pterygopalatine fossa for the maxillary nerve and sphenopalatine artery.

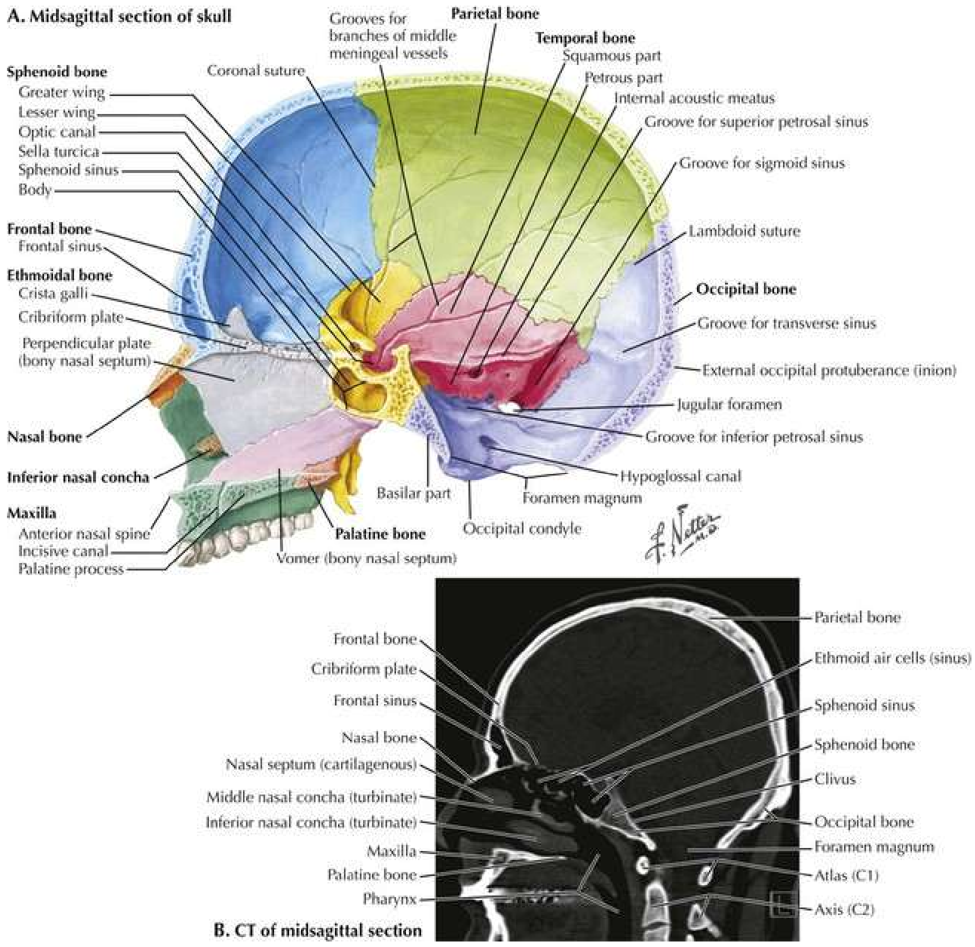

8.5 Skull: Midsagittal Section

The frontal sinus and sphenoidal sinus are cut in section. The sella turcica (“Turkish saddle”) housing the hypophysis of the brain is an important landmark at the junction of the anterior and posterior cranial base between the viscerocranium and neurocranium. The petrous parts of the temporal bone separate the middle and posterior cranial fossae. Grooves on the neurocranial bones contain the middle meningeal vessel branches that supply these bones and the dura mater surrounding the brain.

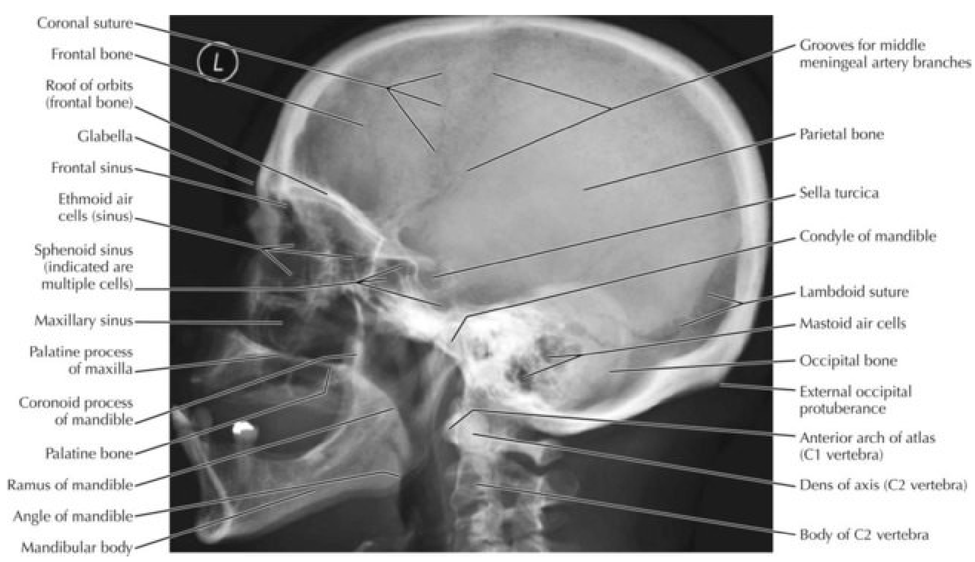

8.6 Lateral X-Ray

Radiolucent air is apparent as dark areas in the mastoid air cells, paranasal air sinuses, and pharynx. The very dense opacity represents the petrous parts of the temporal bones superimposed on each other. Note the sella turcica, coronal and lambdoidal sutures, and atlas (C1) and axis (C2). The squamosal suture is not visible because the thin bones overlap at their articulation unlike the end-to-end articulations of thicker bone at the other sutures. Also note in the neurocranial bones the outer and inner tables of compact bone and the diploë (trabecular bone) in between.

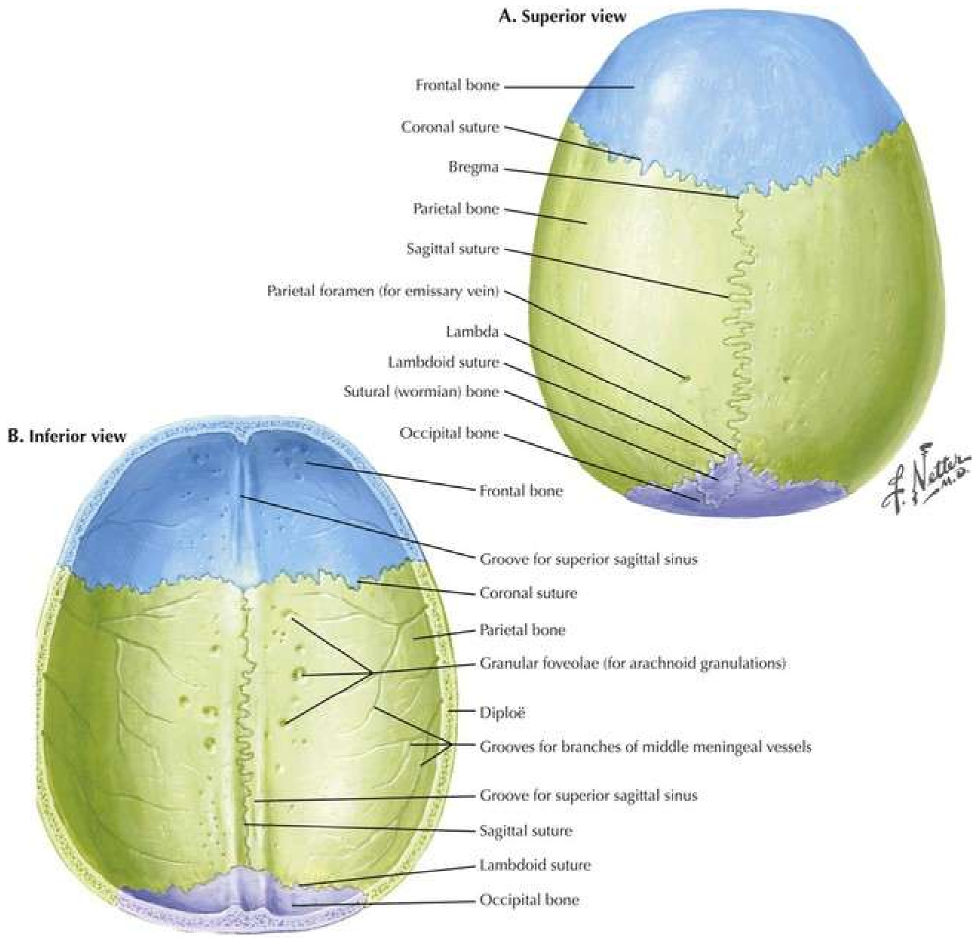

8.7 Calvaria

The sagittal suture separates the left and right parietal bones. From the frontal bone to the occipital bone is a groove for the superior sagittal sinus, a venous channel in the dura mater that receives blood from the brain. All dural sinuses converge on the internal jugular vein. Depressions on the parietal bone are for arachnoid granulations that penetrate lacunae, lateral extensions of the superior sagittal sinus. This is where cerebrospinal fluid (CSF) reenters the circulation. The parietal foramina and smaller foramina along the midline are for emissary veins that connect the scalp veins to the superior sagittal sinus.

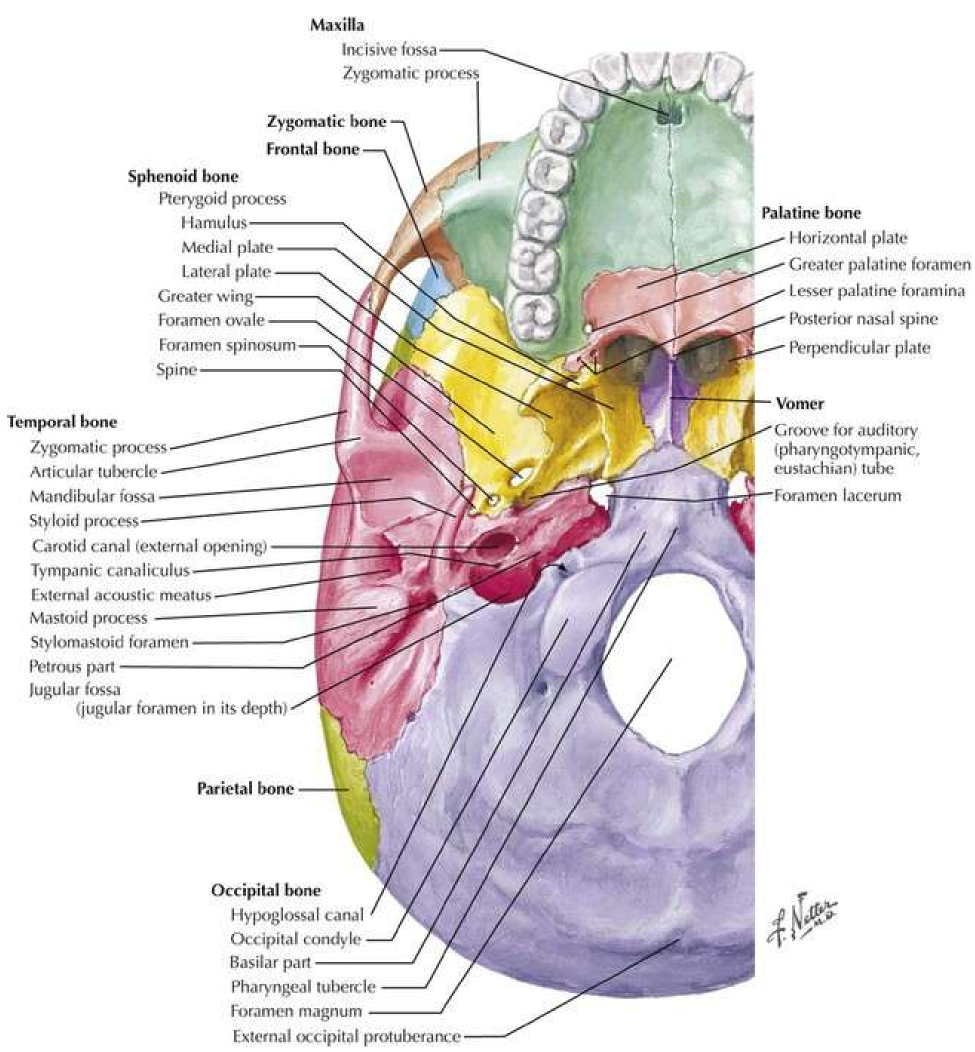

8.8 Cranial Base: Inferior View

The cranial base is the inferior portion of the neurocranium that is the interface with the viscerocranium (facial skeleton) anteriorly. The petrous parts of the temporal bones extend medially between the occipital and sphenoid bones. The inferior extent of the upper jaw is the bony palate consisting of the maxilla and horizontal plate of the palatine bones. Behind the upper jaw are the medial and lateral pterygoid plates of the sphenoid bone. The nasal septum is the vomer posteriorly. Note the mandibular fossa of the temporal bone, the carotid and jugular canals, and the occipital condyles flanking the foramen magnum.

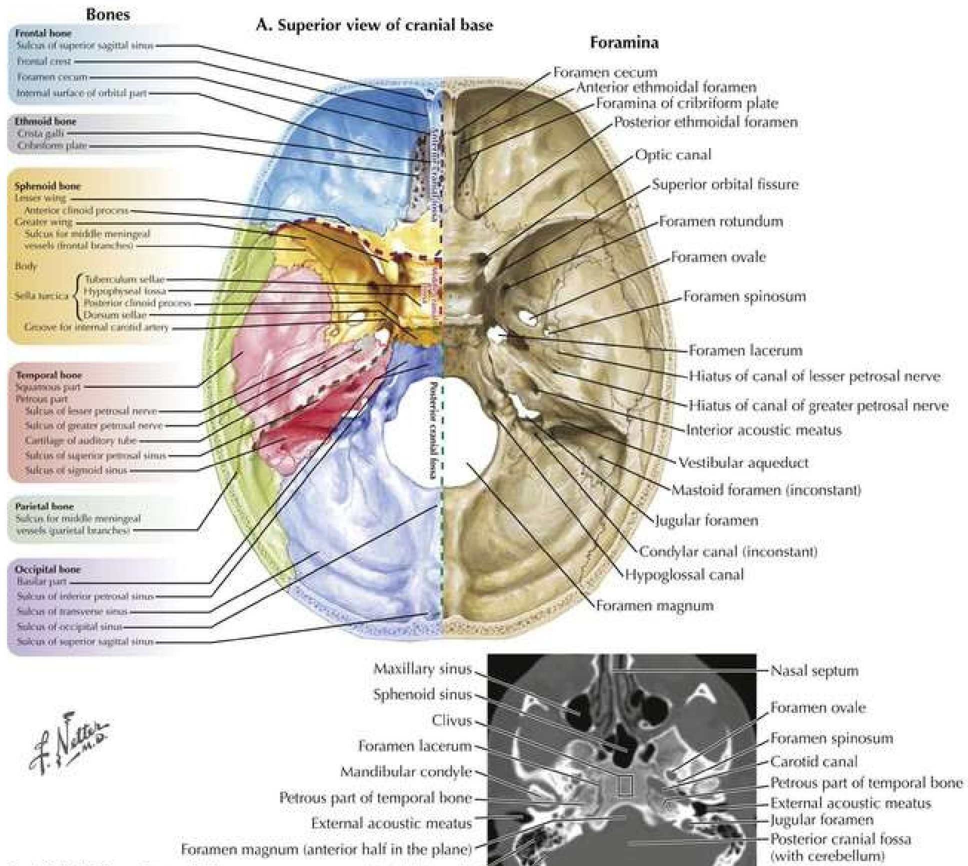

B. Axial CT through cranial base and posterior cranial fossa. The anterior cranial base is above the plane of section.

8.9 Cranial Base: Superior View

The lesser wings of the sphenoid divide the anterior and middle cranial fossae, and the petrous parts of the temporal bone separate the middle and posterior cranial fossae. From anterior to posterior along the cranial base are the ethmoid bone (between the orbits), body of the sphenoid bone, and basilar part of the occipital bone. The anterior cranial fossa contains the cribriform plate of the ethmoid bone (for the olfactory nerve). The middle cranial fossa has the three openings for the three divisions of the trigeminal nerve: superior orbital fissure, foramen rotundum, and foramen ovale. Next to the foramen ovale is the foramen spinosum for the middle meningeal artery.

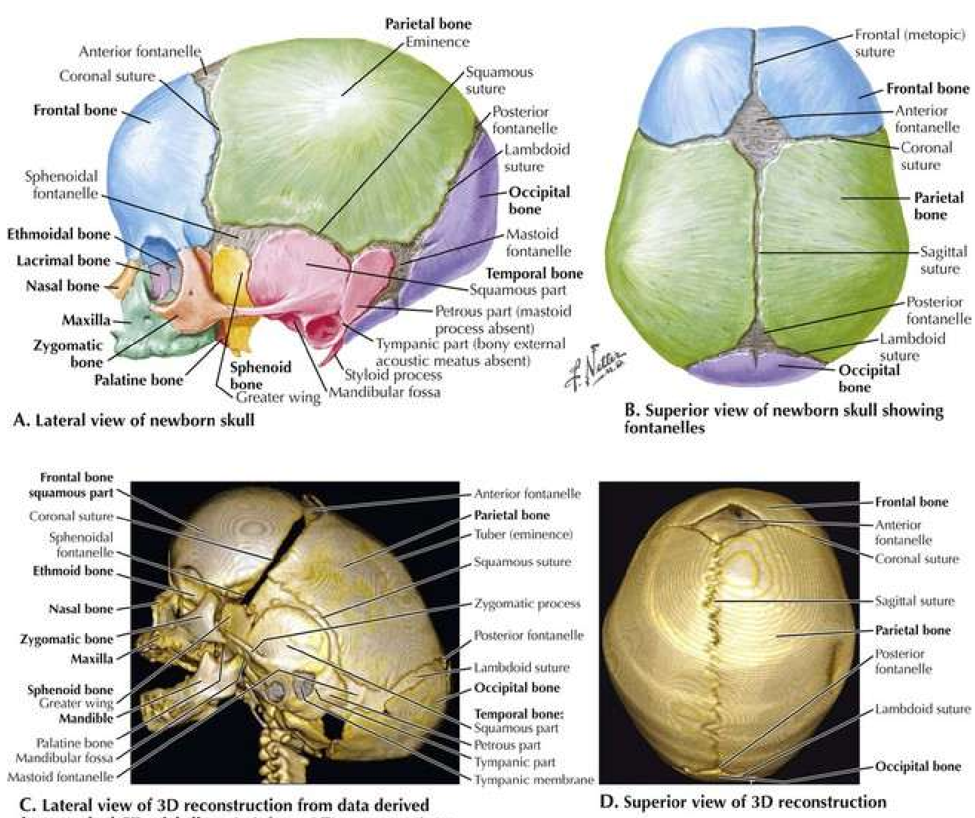

C. Lateral view of 3D reconstruction from data derived from stacked CT axial slices. In infants, 3D reconstructions are used frequently for evaluating patients with craniosynostoses in which there is premature sutural closure that results in abnormal skull shape.

8.10 Skull of the Newborn

A newborn skull has a relatively large neurocranium and a relatively small viscerocranium. The bones of the cranial base develop via endochondral ossification. The flat bones of the neurocranium and the bones of the viscerocranium develop via intramembranous ossification. Unossified portions of the membranes called *fontanelles* are present anterior and posterior to the sagittal suture to facilitate deformation of the skull passing through the birth canal. The tympanic part of the temporal bone is a ring around the tympanic membrane at birth; there is no external acoustic meatus.

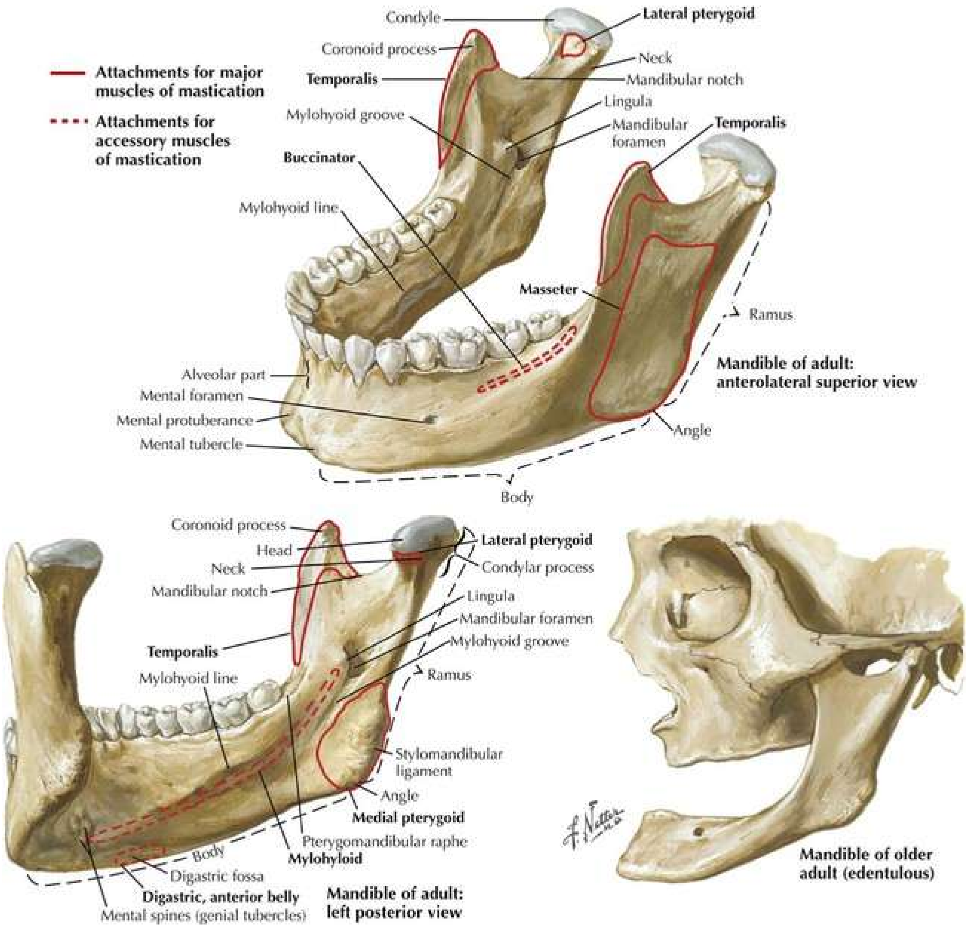

8.11 Mandible

A mandible has a body with dense compact bone, an alveolar part containing the roots of the teeth, and a ramus. Parts of the latter include the angle, condyles for articulation with the temporal bones, and a coronoid process for attachment of the temporalis muscles. With the loss of teeth, the alveolar part of the mandible (and maxilla) is resorbed as a person grows older.

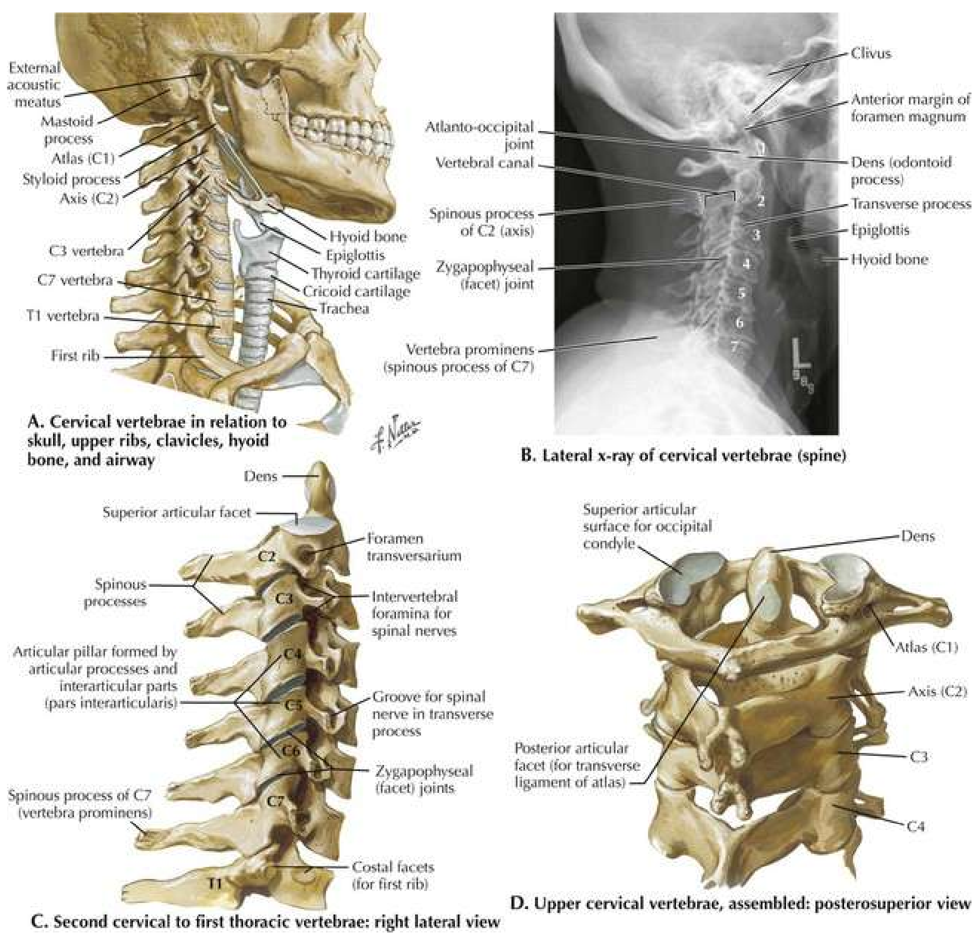

8.12 Cervical Vertebrae and Lateral X-Ray

The seven cervical vertebrae are characterized by transverse foramina in the transverse processes. The first six are for passage of the vertebral arteries; the seventh is vestigial. The articulations between superior and inferior articular processes of adjacent vertebrae (facet joints) are flat and relatively horizontal. In the x-ray note the vertebral canal posterior to the vertebral bodies and the overlap of the dens (odontoid process) of C2 with the occipital condyles of the atlanto-occipital joint. The foramen magnum in this x-ray is obscured by the temporal bones. Its anterior margin can be located by extrapolating the lines of the clivus and the anterior wall of the vertebral canal. The projections of these lines converge on the anterior lip of the foramen magnum.

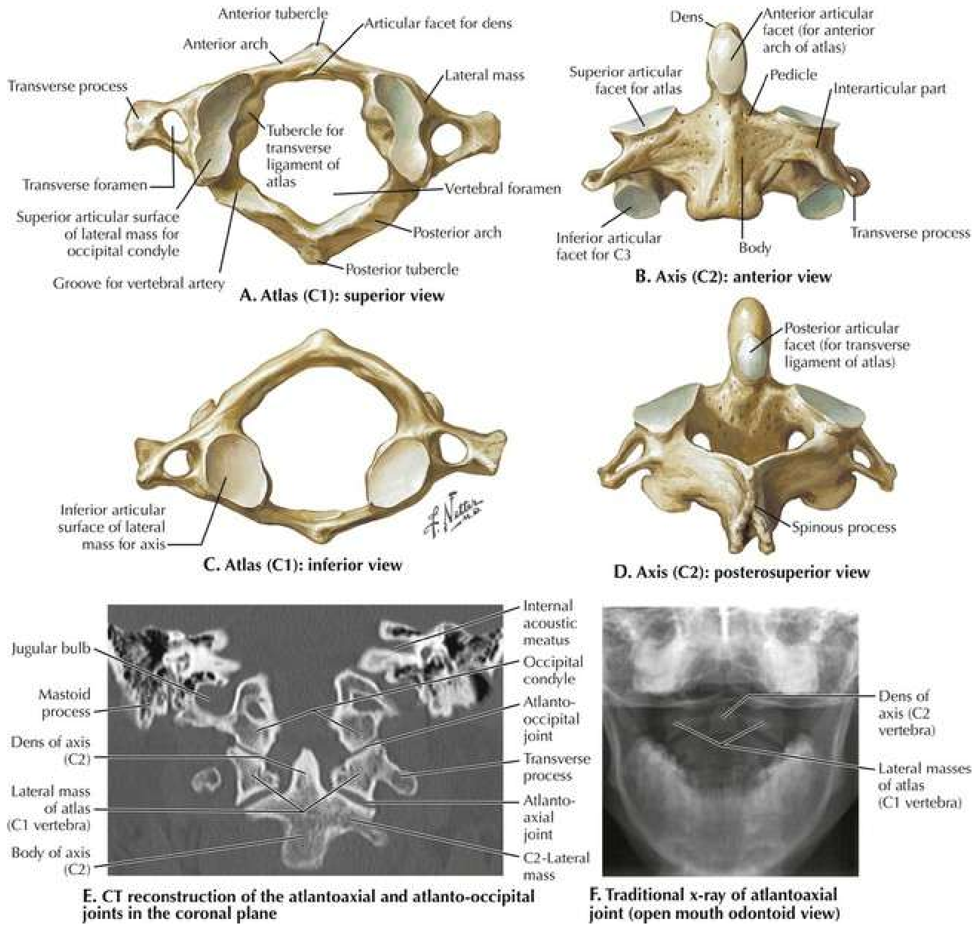

8.13 Atlas and Axis

With the ability to reconstruct different planes, computed tomography (CT) has largely replaced the open mouth C1/C2 x-rays. The atlas is the widest cervical vertebra, and it lacks a body (centrum). It articulates superiorly with the occipital condyles in a hinge joint for flexion and extension. Together with the skull, it pivots on the dens (odontoid process) of the axis (C2). The dens is the body of C1 that fuses to the axis during development.

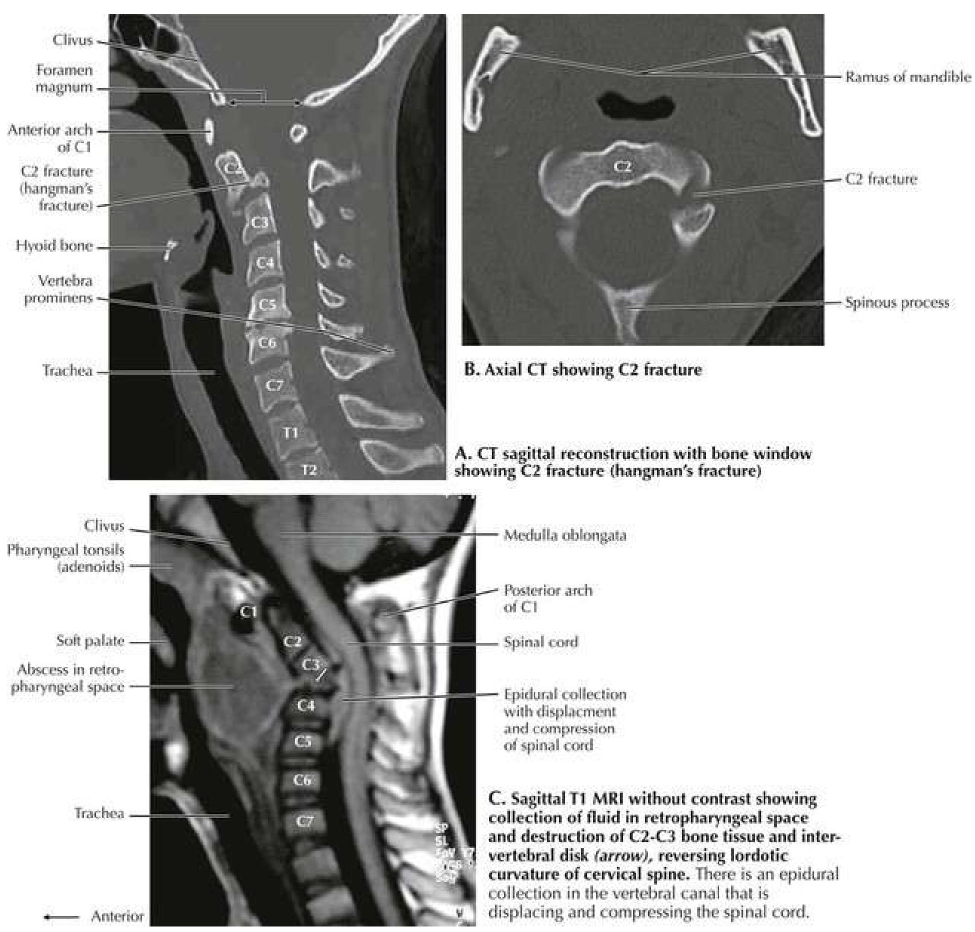

8.14 Imaging of Cervical Trauma and Pathology

Part of the systematic search strategy for the study of any image of the spine includes a close inspection of the size, shape, and alignment of the vertebral bodies. The anterior and posterior walls of the vertebral bodies and the posterior wall vertebral canal are known as the anterior spinal line, posterior spinal line, and spinolaminar line, respectively. The patient in **A** and **B** was in an automobile accident and has a fracture of the C2 body (hangman's fracture) and dislocation of the atlantoaxial joint (C1/C2). The dens is below the arch of the atlas, and the vertebral canal and spinal cord are displaced posteriorly below C1. There are also compression fractures of the C5 and C6 vertebral bodies. Note the increased density of bone, the narrow intervertebral space, and the posterior protrusion of bone into the vertebral canal. Other components of a search strategy include the evaluation of vertebral bodies for metastases and lesions (see Chapter 2, p. 27), other components of the vertebrae, plus the soft tissues anterior to the vertebral column **(C** [a different patient than in **A** and **B**]).

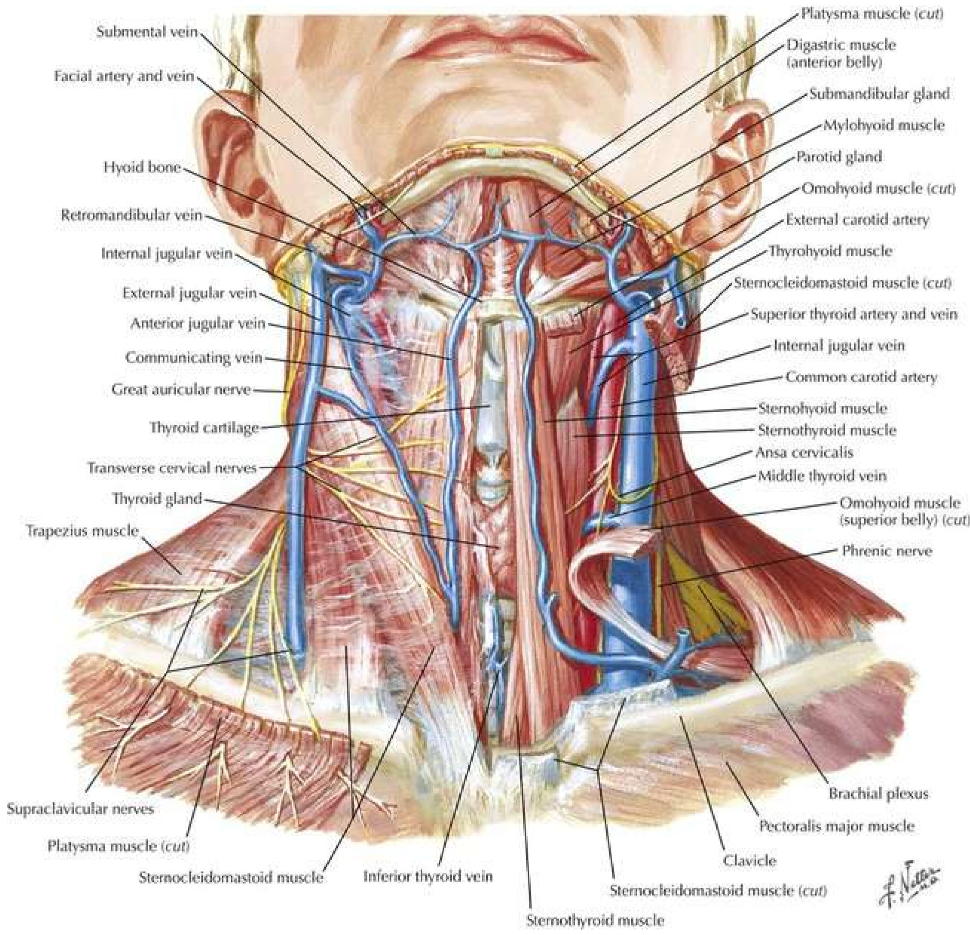

8.15 Superficial Vessels, Nerves, and Muscles of the Neck

The large, superficial sternocleidomastoid and trapezius muscles define the contours of the neck. Deep and anterior to the sternocleidomastoid muscle are the thin, infrahyoid "strap" muscles that are named by their attachments: omohyoid (reflected on one side); sternohyoid; and deep to these, the sternothyroid and thyrohyoid muscles. The hyoid bone is at vertebral level C3. At C5 is the thyroid cartilage of the larynx, and at C7 is the thyroid gland anterior to the trachea. The external jugular vein courses superficial to the sternocleidomastoid muscle. Deep to the muscle is the carotid sheath containing the internal jugular vein, common carotid artery, and vagus nerve.

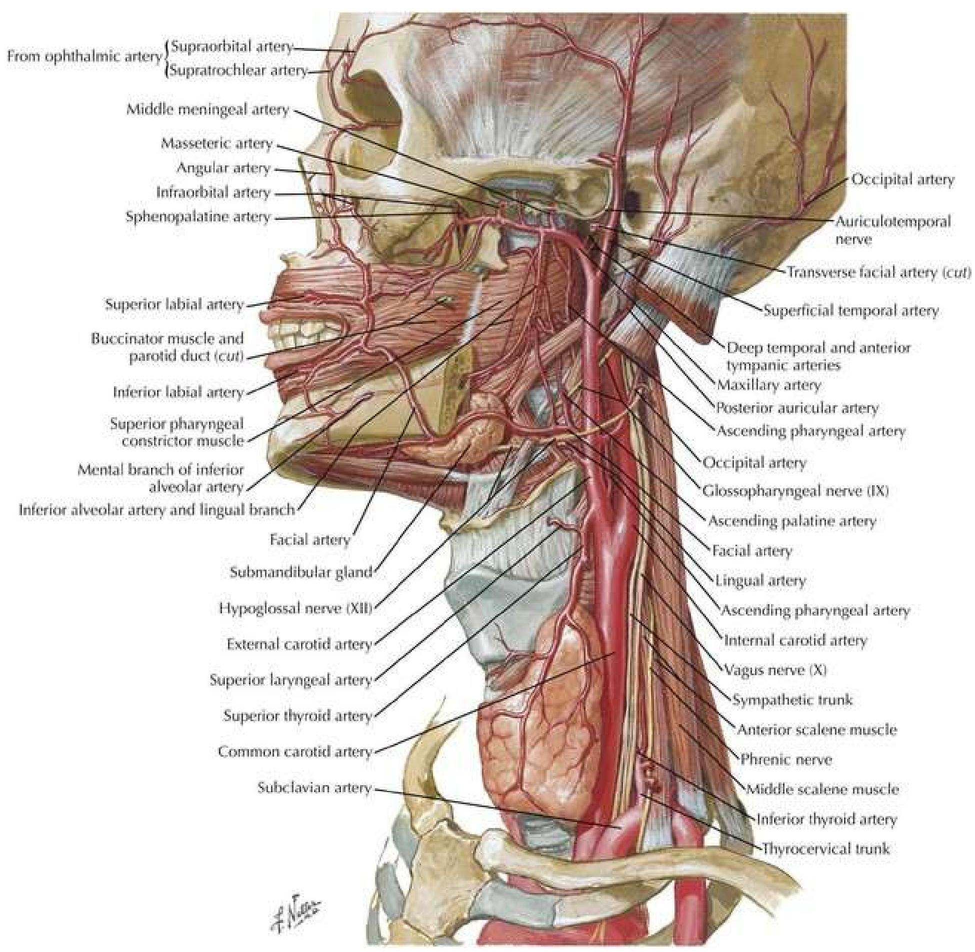

8.16 Arteries of Oral and Pharyngeal Regions

The deeper muscles of the neck are the three scalene muscles (anterior, middle, and posterior) that attach to the first and second ribs and the constrictors of the pharynx. The inferior constrictor muscle attaches anteriorly to the thyroid cartilage of the larynx, the middle constrictor muscle to the hyoid bone (not seen clearly here), and the superior constrictor muscle to the buccinator muscle. The common carotid artery bifurcates in the carotid sheath into the external and internal carotid arteries around the level of C4.

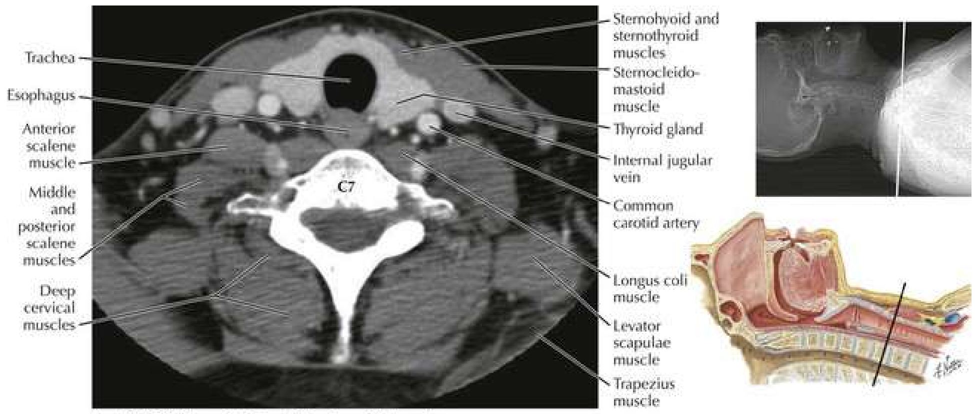

A. Axial CT through C7 and the thyroid gland

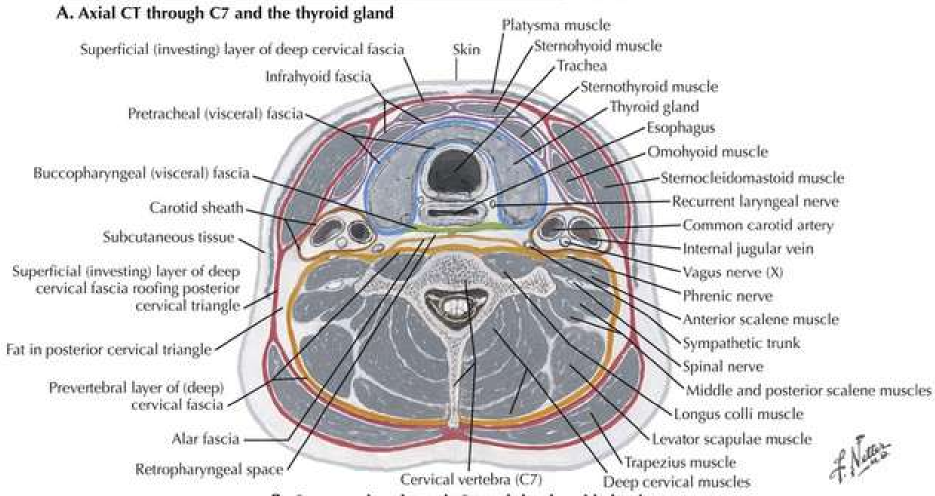

B. Cross section through C7 and the thyroid gland

8.17 Axial CT and Cross Section of the Neck through C7 and the Thyroid Gland

The fascias of the neck envelop a visceral unit that includes the trachea/larynx, esophagus, and thyroid gland and a vertebral unit consisting of the vertebral column and surrounding muscles. The carotid sheath contains the common carotid artery, internal jugular vein, and vagus nerve. An axial (transverse) section of the neck at the level of the seventh cervical vertebra (C7) is through the thyroid gland (**A** and **B**). CT **(A)** is used for evaluation of the neck because of rapid scanning that can be obtained during a breath hold. Magnetic resonance imaging (MRI) can be used as well but is often less well tolerated by patients with significant pathologies. In addition, artifact from motion such as breathing and swallowing can degrade images.

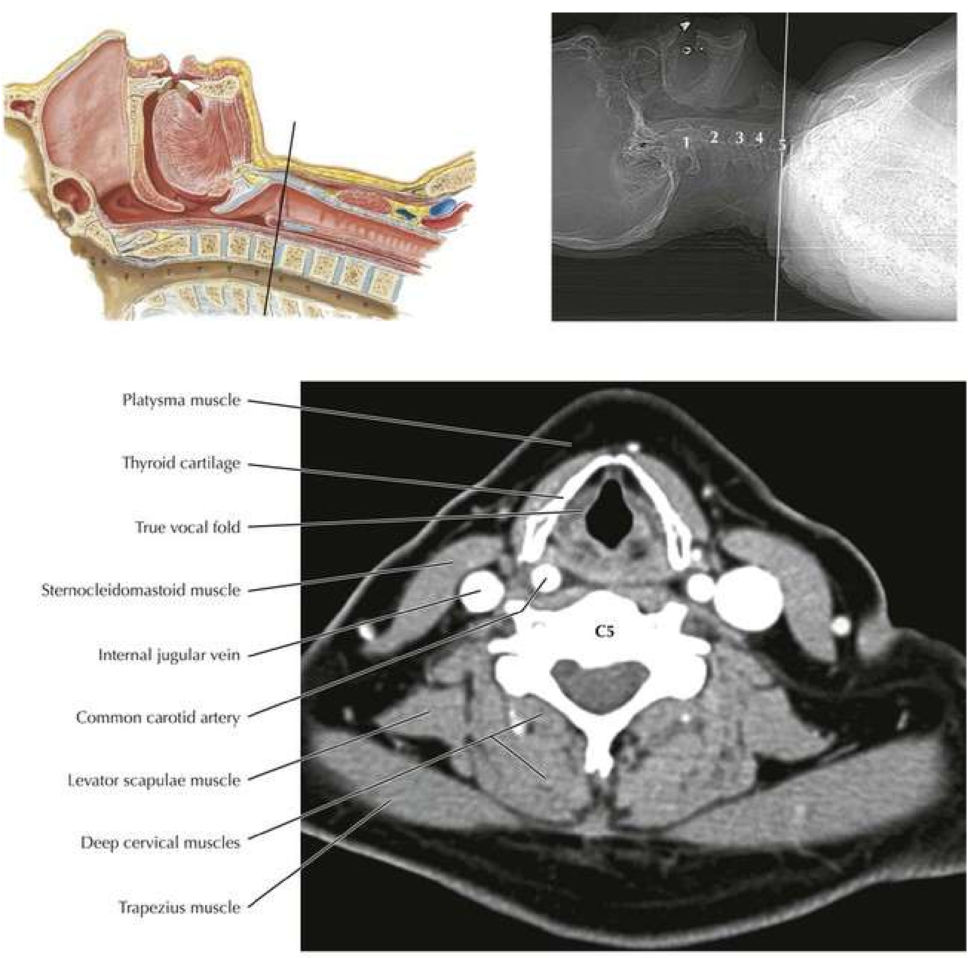

Axial CT through C5 and the thyroid cartilage

8.18 Axial CT Through C5 and the Larynx

The larynx is the most prominent structure at the level of C5. In this axial CT, the section is through the true vocal folds and thyroid cartilage of the larynx. It is above the level of the cricoid cartilage. Between the larynx and C5 vertebra is the carotid sheath containing the internal jugular vein and common carotid artery. Note that the left internal jugular vein is much larger than the right. The sternocleidomastoid and trapezius muscles define the contour of the neck at all levels.

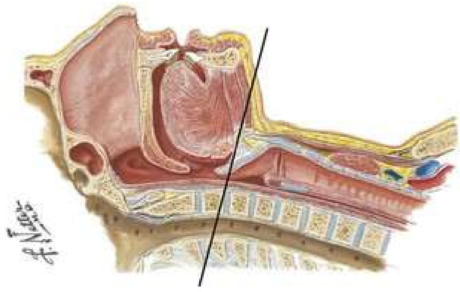

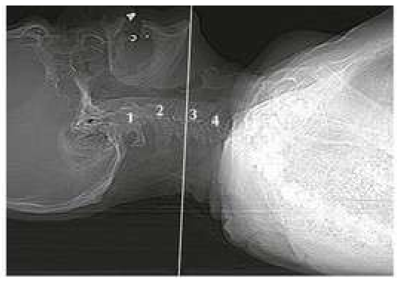

Axial CT through C3 and the hyoid bone

8.19 Axial CT through C3 and the Hyoid Bone

A section at C3 passes through the hyoid bone and epiglottis, just below the mandible in this individual. The projecting contour anteriorly indicates that the plane is close to the mandible, and the mylohyoid and anterior belly of the digastric muscles and the submandibular glands are visible. This is also at the level of the division of the common carotid artery into its internal and external branches.

A. Axial CT of a laryngeal mass at the level of C5. The laryngeal cartilages appear bright because they are probably calcified, a process that can occur with aging.

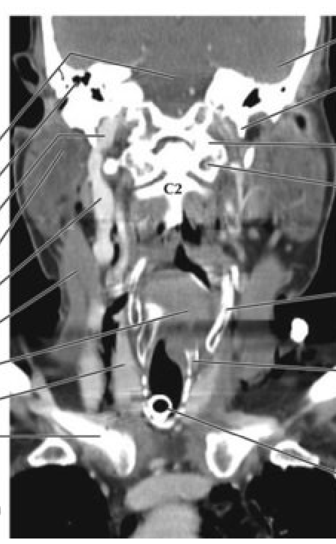

B. CT coronal reconstruction through the laryngeal mass

8.20 Search Strategy: Neck Imaging of Laryngeal Tumor

In addition to an analysis of the vertebral compartment (p. 199), a search strategy for the interpretation of neck images includes careful, systematic study of spaces, blood vessels, lymph nodes, organs of the visceral compartment, and other structures and layers visible in the image. **A** and **B** are views of a mass in the larynx on the left. In the axial image **(A)**, the thyroid cartilage of the larynx is pushed laterally on the left. The mass is eroding and displacing inferiorly the cricoid cartilage on the left and compromising the air space in the larynx. The coronal view **(B)** shows an airway tube in the trachea and the mass filling much of the interior of the larynx.

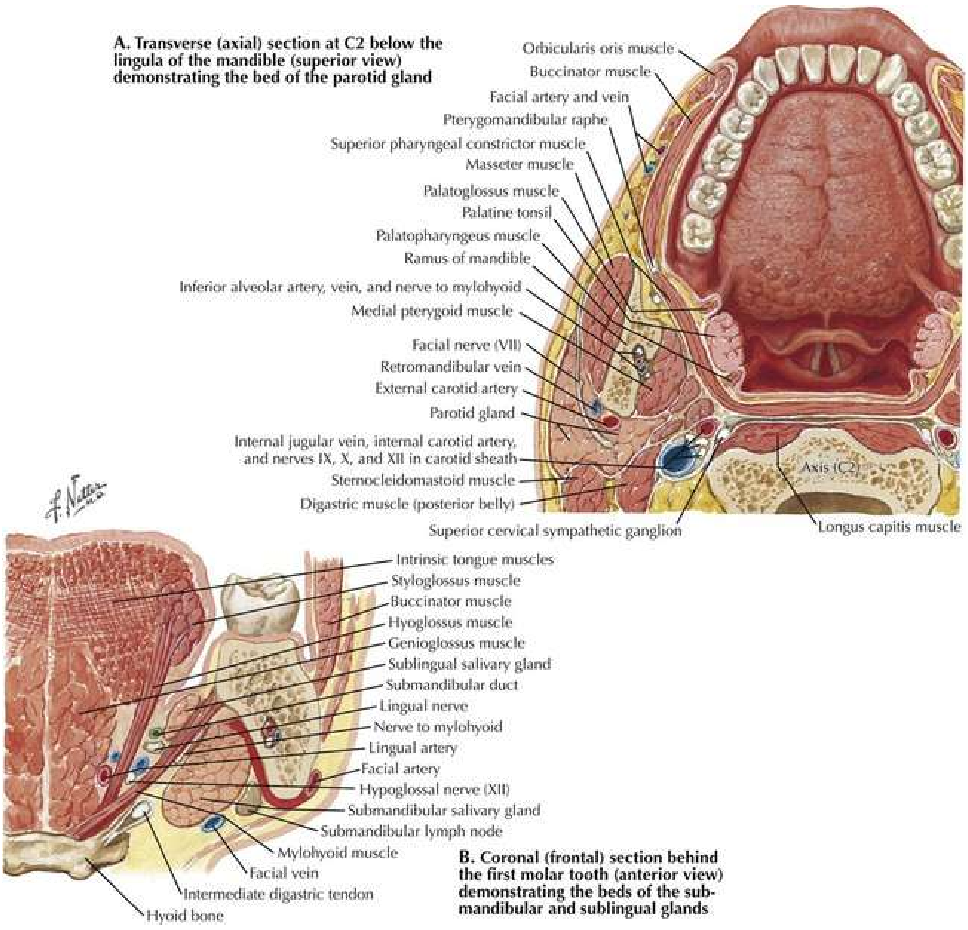

8.21 Cross and Coronal Sections of the Tongue and Salivary Glands

A is a horizontal (axial) section. The buccinator muscle lining the oral cavity is continuous with the superior constrictor muscle of the pharynx. The masseter muscle is superficial to the ramus of the mandible; the medial pterygoid muscle is deep to it. The parotid gland extends deep to the mandibular ramus, and it is traversed in part by the external carotid artery and the facial nerve. **B** is a coronal section. The mylohyoid muscle is the floor of the oral cavity. The sublingual gland on each side is superior to it, and the submandibular gland is inferior to it, although it hooks around the muscle posteriorly to extend into the oral cavity, where its duct passes anteriorly to the lingual frenulum. The inferior half of the tongue is the genioglossus muscle, the fibers of which blend with the intrinsic tongue muscles in the superior half of the tongue.

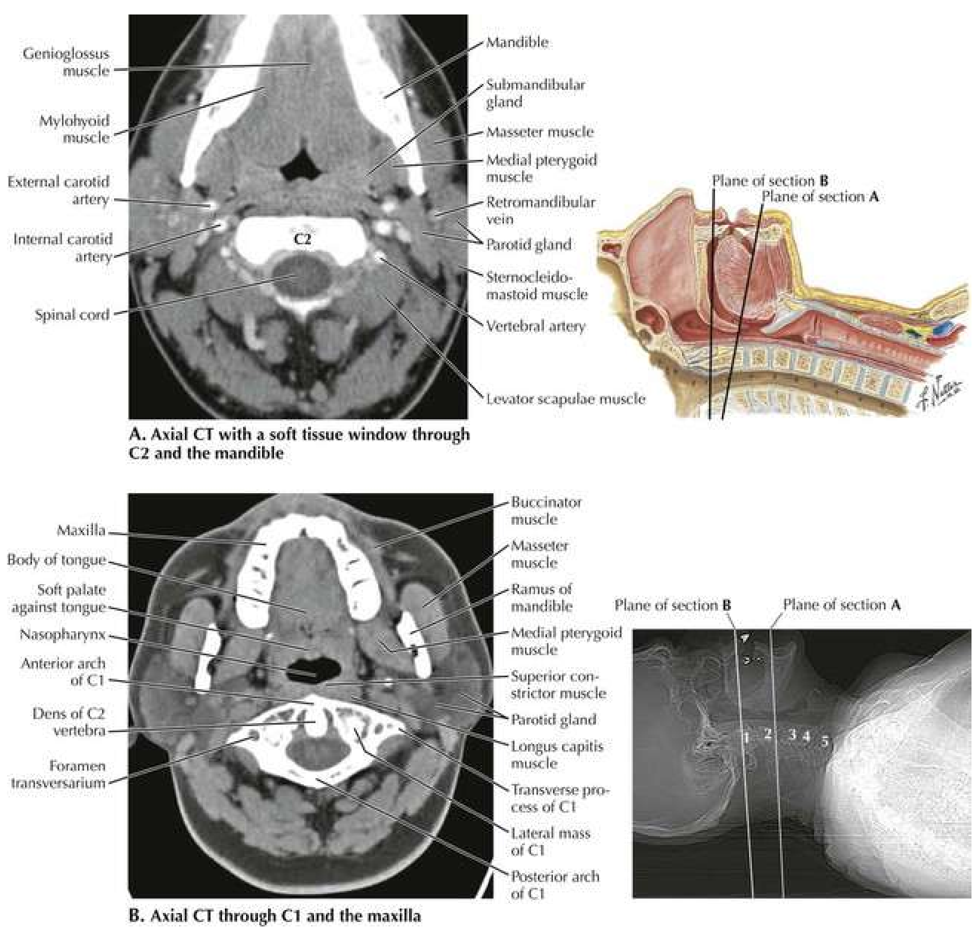

8.22 Axial CT at C2 and C1

A plane at the level of C2 **(A)** includes the mandible and genioglossus and mylohyoid muscles. The plane in this patient is low on the mandibular ramus at the most inferior attachment of the medial pterygoid muscle, and the submandibular gland is visible. The masseter muscle is superficial to the ramus, and the parotid gland wraps around the posterior margin of the ramus. The common carotid artery has just divided into its external and internal branches. At C1 **(B),** the plane is through the maxilla, intrinsic tongue muscles, and nasopharynx. The patient is breathing through the nose, and the soft palate compresses the oropharynx against the tongue. The medial pterygoid and masseter muscles are prominent in their attachments to the mandibular ramus.

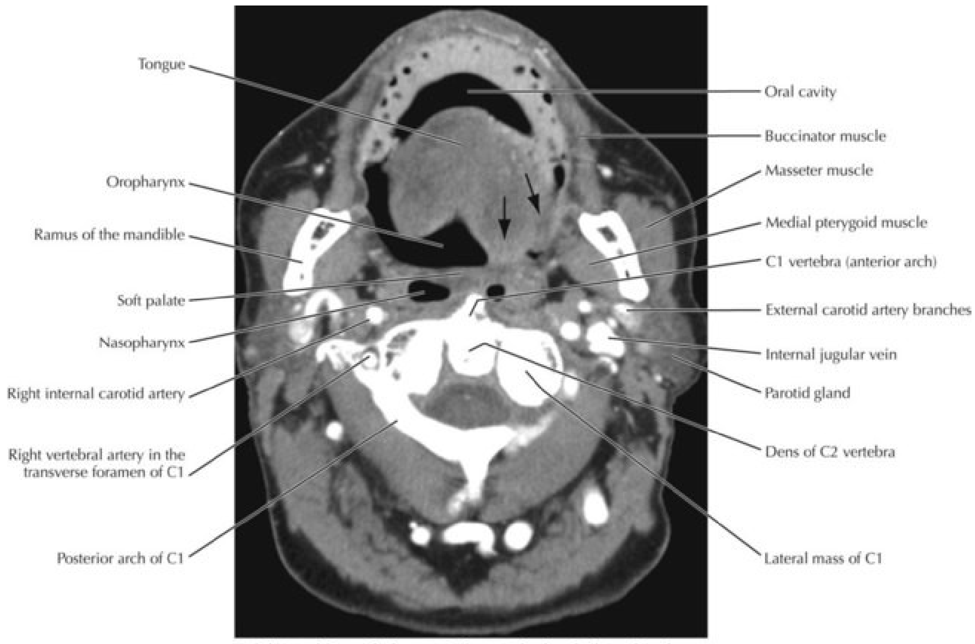

Axial CT with a soft tissue window at the level of C1 showing a mass in the tongue *(arrows)*

8.23 Imaging Pathology of the Oral Cavity

A mass in the tongue projecting into the oropharynx on the left is visible in this image. The patient is breathing through the mouth, with the soft palate elevated against the posterior wall of the pharynx.

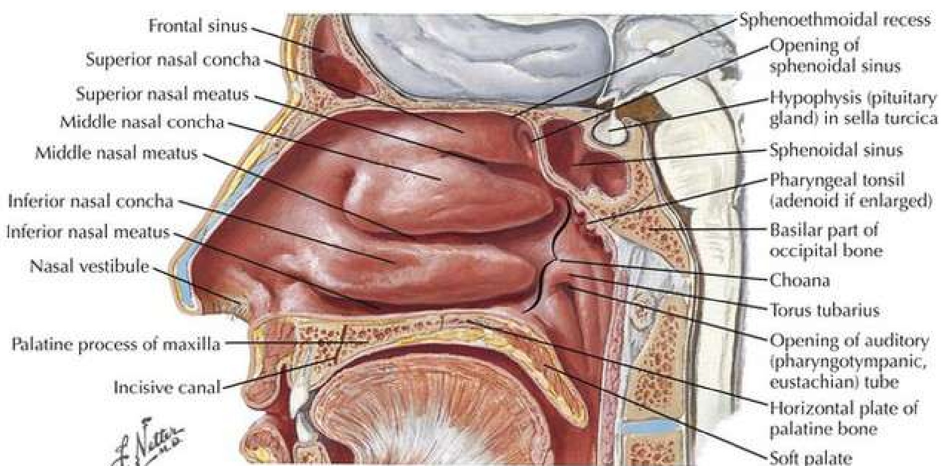

A. Sagittal section through the right nasal cavity, nasopharynx, palate, and oral cavity

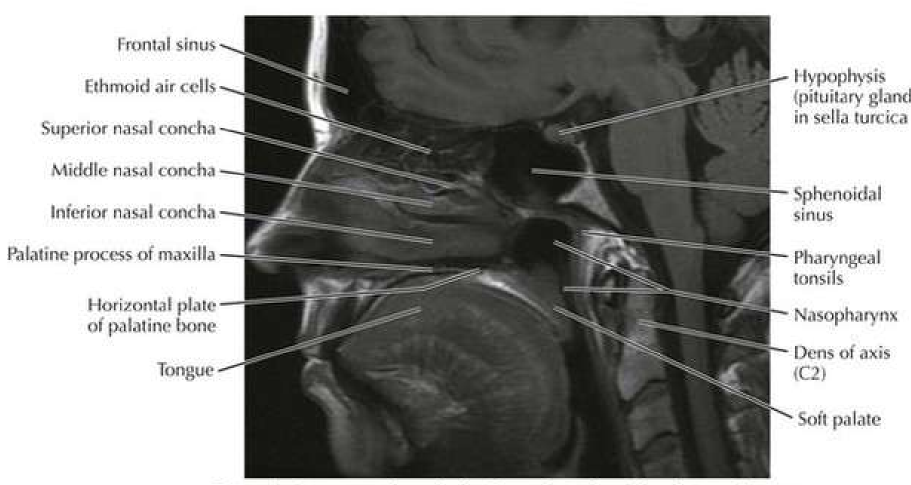

B. Sagittal T1 MRI through the lateral nasal wall and nasopharynx

8.24 Lateral Wall of the Nasal Cavity

Scroll-like superior, middle, and inferior nasal conchae occupy the lateral wall of each nasal cavity **(A).** The spaces below conchae are called meati. The bony palate consisting of the maxilla and palatine bones separates the nasal and oral cavities. The soft palate separates the nasopharynx from the oropharynx. The nasolacrimal duct drains tears into the inferior meatus. Mucus from the frontal sinus, maxillary sinus, and anterior ethmoid air cells drains into the hiatus semilunaris of the middle meatus. Posterior ethmoid air cells drain into the superior meatus. The sphenoid sinus drains into the highest space in the nasal cavity above the superior concha, the sphenoethmoidal recess. The auditory tube from the middle ear cavity opens in the nasopharynx to balance pressure on both sides of the tympanic membrane (eardrum).

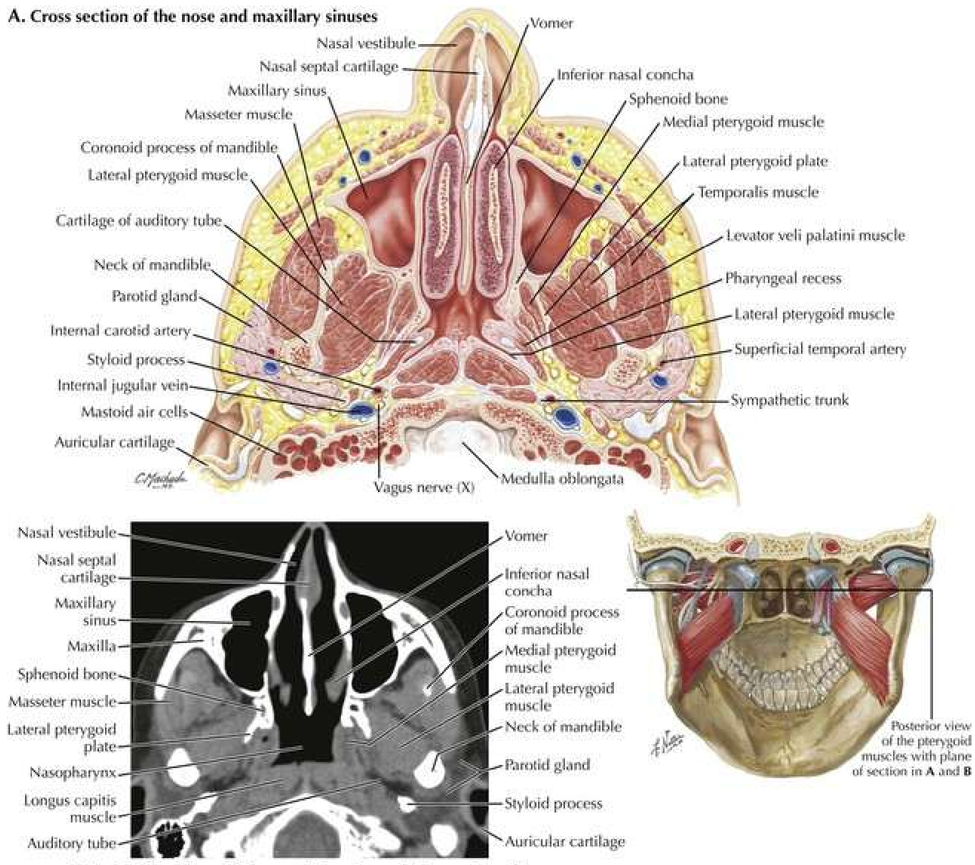

B. Axial CT with a soft tissue window through the nasal cavity, maxillary sinuses, and nasopharynx. The opening of the auditory tube in the nasopharynx is just above the plane of section.

8.25 The Nose, Nasal Cavity, and Maxillary Sinuses in the Transverse Plane

The section is through the maxillary sinuses, inferior nasal conchae, nasopharynx, and mastoid air cells. Note the opening of the auditory tube (which is just above the level of section in the CT). The plane is near the top of the mandible through the coronoid process and neck above most of the medial pterygoid muscle. At this level the lateral pterygoid muscle extends from the lateral pterygoid plate to the neck of the condyle and articular disk. The soft tissue window in the axial CT **(B)** is useful for the identification of masses and other soft tissue pathology that might extend into the air spaces of nose, nasal cavity, nasopharynx, and maxillary sinuses.

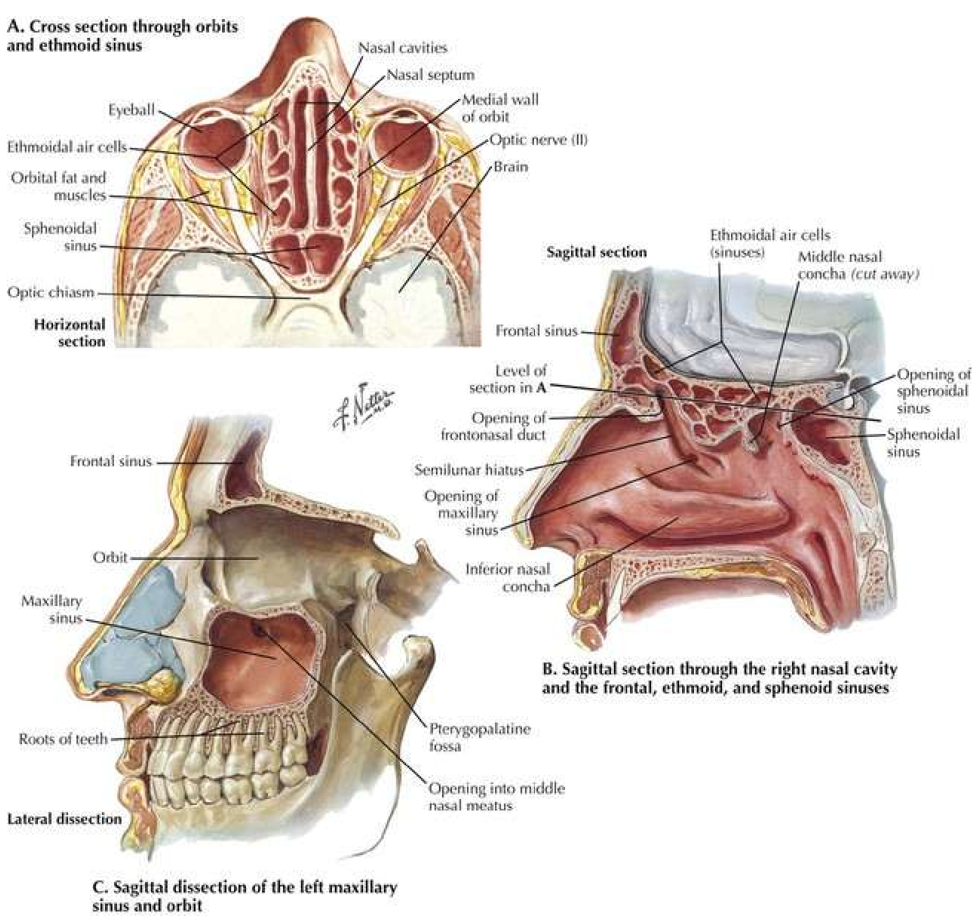

8.26 Paranasal Air Sinuses

The orbits are bounded by paranasal air sinuses. Between the orbits is the ethmoid bone with its ethmoid air cells (ethmoid sinus); the large chamber of each maxillary sinus is below the orbit. Continuous with the ethmoid air cells anteriorly and superiorly is the frontal sinus, and posterior to the ethmoid air cells is the sphenoid sinus in the body of the sphenoid bone.

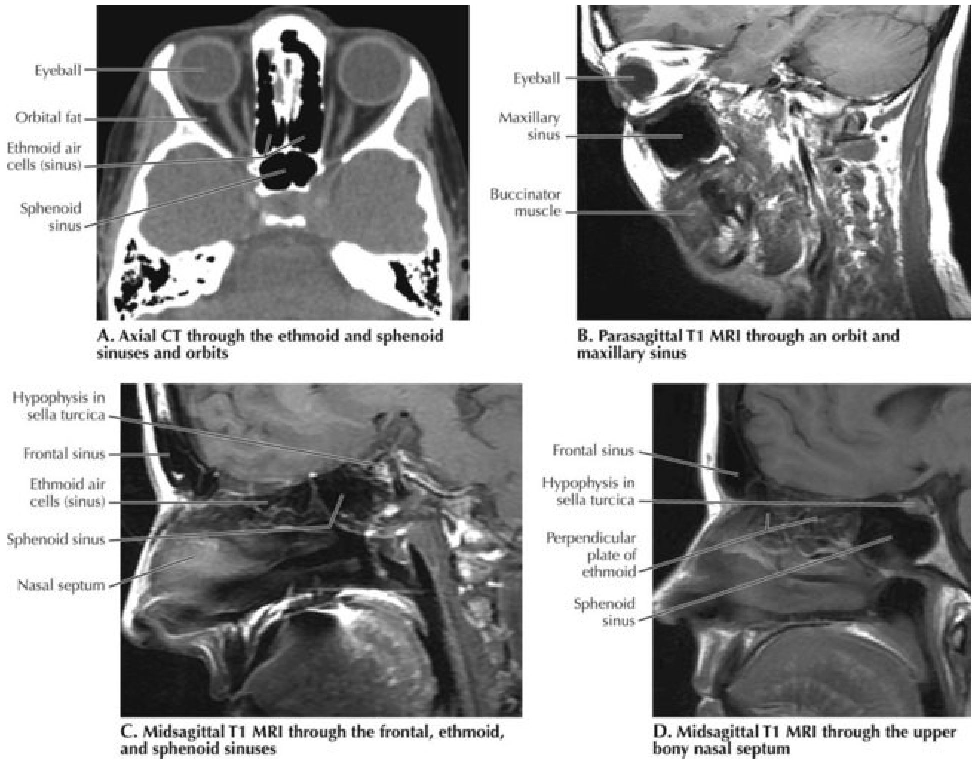

8.27 Imaging of the Paranasal Sinuses

A through **D** are axial and sagittal sections that show the paranasal sinuses. The sections in **A** and **B** also capture the orbit. The air in the sinuses appears black in both CT and MRI, which makes them prominent features in any image. The section in **D** is close to the perpendicular plate of the ethmoid bone, the upper part of the nasal septum. Large ethmoid air cells are not seen. CT is excellent for evaluating bones of the orbits and paranasal sinuses and aeration status of the paranasal sinuses. MRI is better at evaluating the nature of soft tissues, especially if masses are present. MRI is also excellent for evaluating intraorbital pathology.

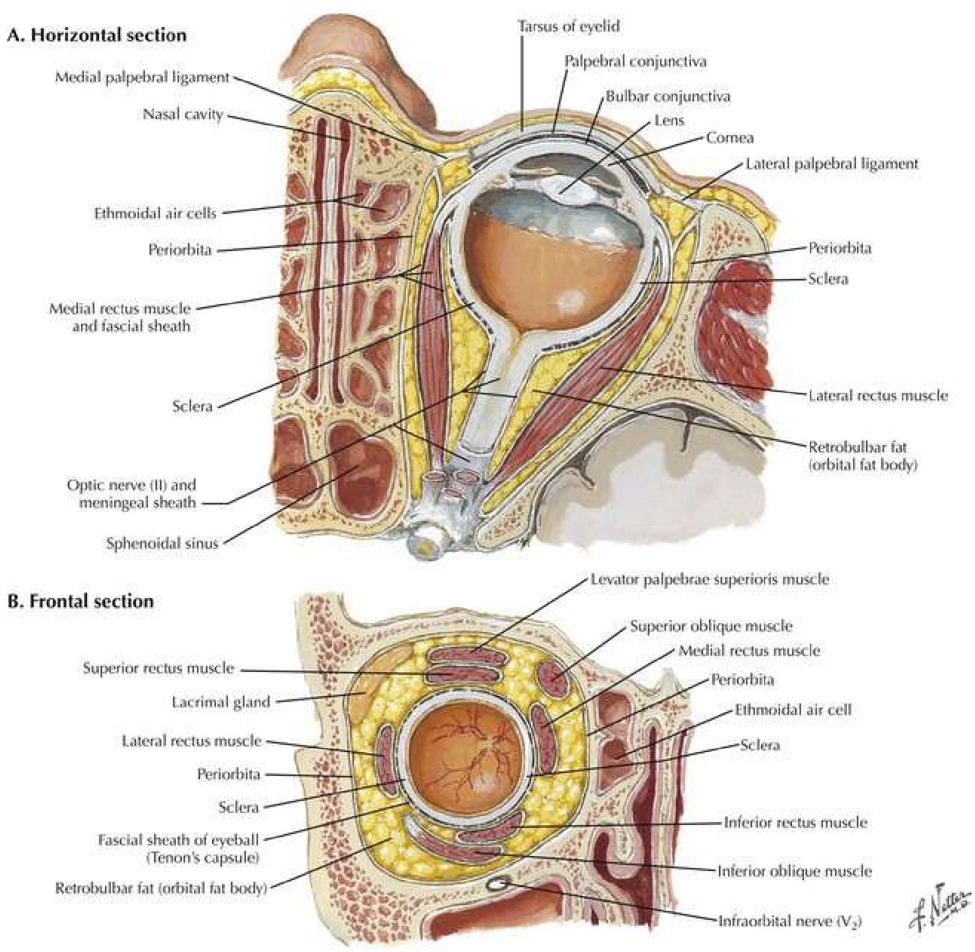

8.28 Cross and Coronal Sections of the Orbit

Six extraocular eye muscles attach to each eyeball (oculus) in the orbit: four rectus muscles (superior, inferior, medial, and lateral) and two oblique muscles (superior and inferior). The levator palpebrae superiorus runs above superior rectus into the upper eyelid. The lacrimal gland produces tears in the upper lateral aspect of the orbit. The optic nerve is surrounded by meninges, and the dura mater is continuous anteriorly with the sclera, the thick, connective tissue framework of the eye. The visual axes of the eyes are AP, but the axes of the orbits and optic nerves diverge laterally.

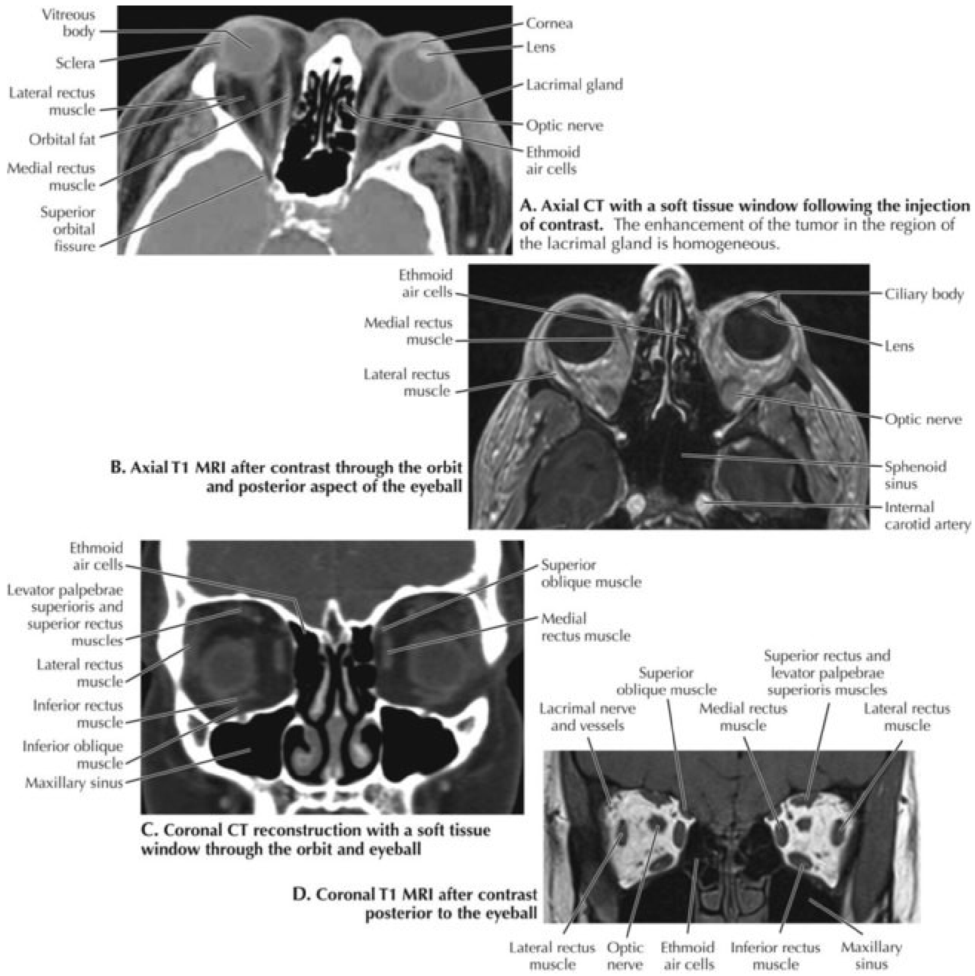

A. Axial CT with a soft tissue window following the injection of contrast. The enhancement of the tumor in the region of the lacrimal gland is homogeneous.

B. Axial T1 MRI after contrast through the orbit and posterior aspect of the eyeball

C. Coronal CT reconstruction with a soft tissue window through the orbit and eyeball

D. Coronal T1 MRI after contrast posterior to the eyeball

8.29 Imaging of the Orbit

The coronal section in **C** is posterior to the midline of the eyeball, and there is space between the extraocular muscles and the sclera. The inferior oblique muscle is not seen in **D** because the section is at the back of the orbit posterior to the eye; the muscle originates near the anterior margin of maxilla. CT is useful for evaluating the bony orbit, for hematomas as a result of trauma, and for foreign bodies. MRI is more sensitive for the detection of masses and inflammatory lesions.

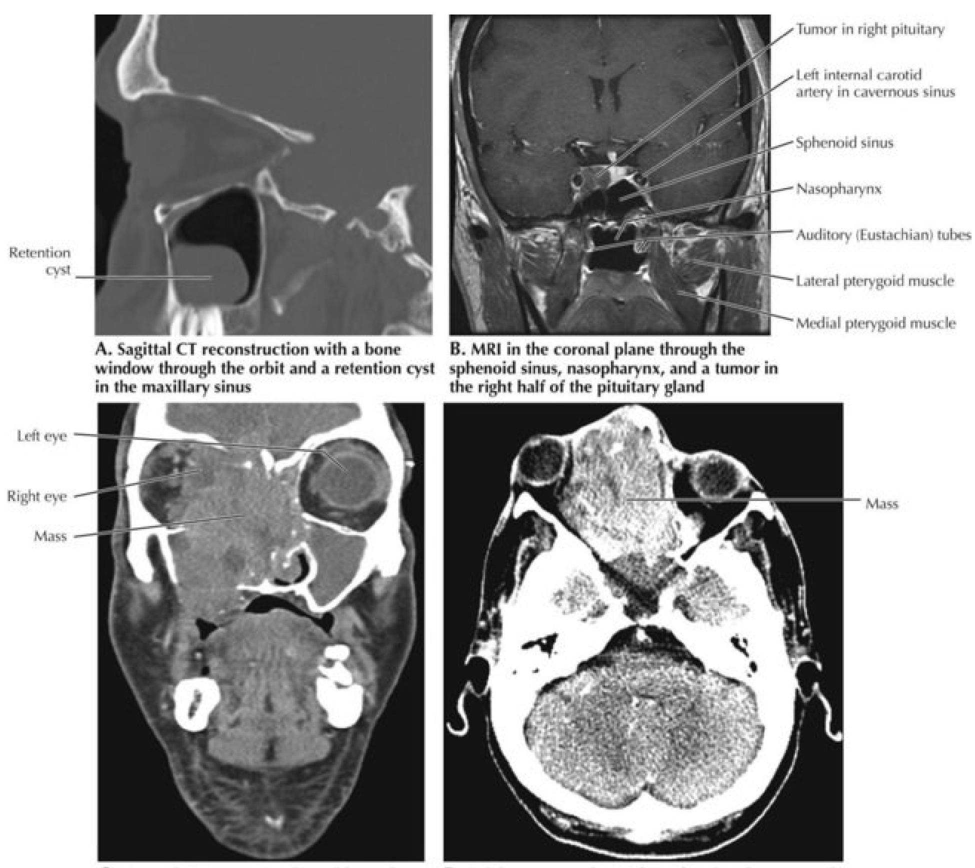

A. Sagittal CT reconstruction with a bone window through the orbit and a retention cyst in the maxillary sinus

B. MRI in the coronal plane through the sphenoid sinus, nasopharynx, and a tumor in the right half of the pituitary gland

C. Coronal CT reconstruction with a soft tissue window showing a large mass in the right side of the face

D. Axial contrast-enhanced CT showing the extent of the mass in the transverse plane

8.30 Imaging of Sinus and Orbit Pathology

The paranasal sinuses are air-filled, mucus-lined spaces in the bones that appear black in imaging studies. It is easy to see if they contain blood, mucus, fluid, masses, or other pathology. Compare one side with the other. **A** shows a mucus retention cyst in the maxillary sinus. **B** shows asymmetry of the sphenoid sinus in the coronal plane from a small tumor (microadenoma) of the pituitary gland that is projecting into the sphenoid sinus on the right side. **C** and **D** are coronal and axial CTs showing the extent of a large mass in the right side of the face. It has filled the ethmoid sinus, right maxillary sinus, and most of the nasal cavity. It has invaded the oral cavity and right orbit, obliterating the medial orbital wall and protruding the right eyeball. Note how the left maxillary sinus is filled with mucus or fluid from obstruction of its outflow into the nasal cavity.

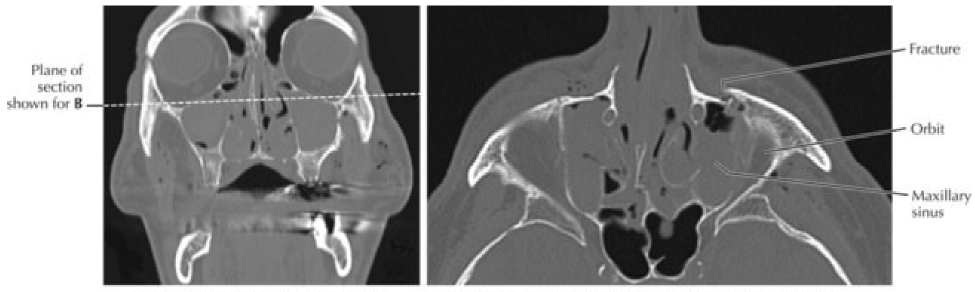

A. Coronal CT reconstruction showing soft tissue density, most likely blood, in the maxillary and ethmoid sinuses and nasal cavity

B. Axial CT of the same patient as in A (plane of section indicated in A) showing fracture of the roof of the left maxillary sinus (floor of the orbit) and multiple fractures of the ethmoid bone. The sphenoid sinus is mostly clear.

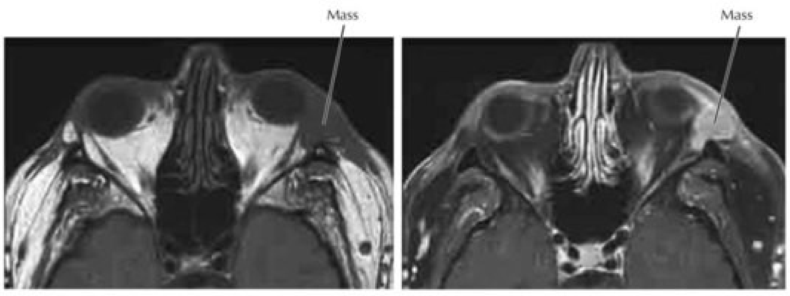

C. Axial T1 MRI through the orbits before vascular contrast showing a mass in the lacrimal region of the left orbit

D. Axial T1 MRI with a fat saturation sequence of the same patient in C after the administration of contrast

8.31 Imaging of Sinus and Orbit Pathology (cont'd)

The CT images in **A** and **B** show fractures of the relatively thin bone of the floor and medial walls of the orbits with filling of the ethmoid and maxillary sinuses and nasal cavity with blood. The mass in the lacrimal region of the orbit in **C** and **D** is visualized with MRI before vascular contrast **(C)** and after vascular contrast **(D).** Its homogeneous appearance after contrast indicates that it is not a fluid-filled cyst or other nonvascular mass.

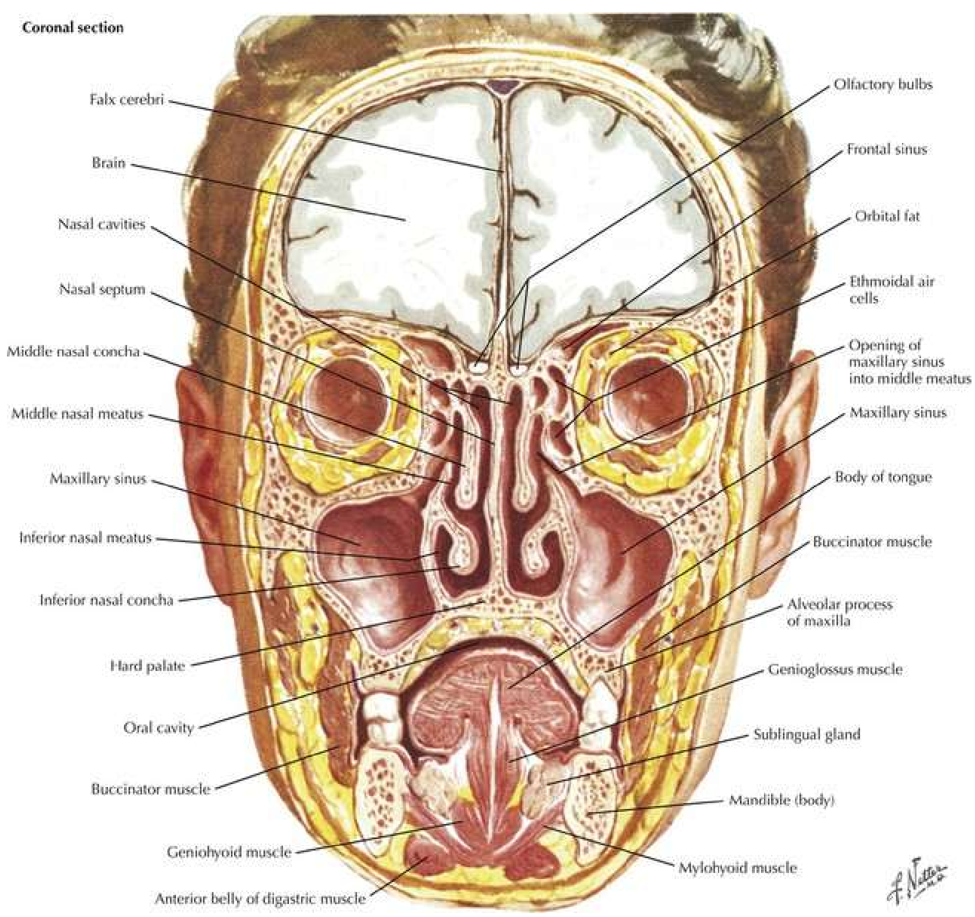

8.32 Coronal Section of the Head through the Orbit, Sinuses, and Oral Cavity: Overview

Review in this coronal section of the head the relationships of the orbit, nasal cavity, oral cavity, maxillary sinus, frontal and ethmoid sinuses, and frontal lobes of the brain. Captured in this plane are the openings of the maxillary sinuses in the middle meati. Bounding the oral cavity are the bony (hard) palate above, the buccinator muscles laterally, and the mylohyoid muscle comprising the floor. In the anterior cranial fossa of the skull with the brain are sections through the superior sagittal sinus, the falx cerebri (originating from the crista galli of the ethmoid bone), and olfactory bulbs on the cribriform plate of the ethmoid bone.

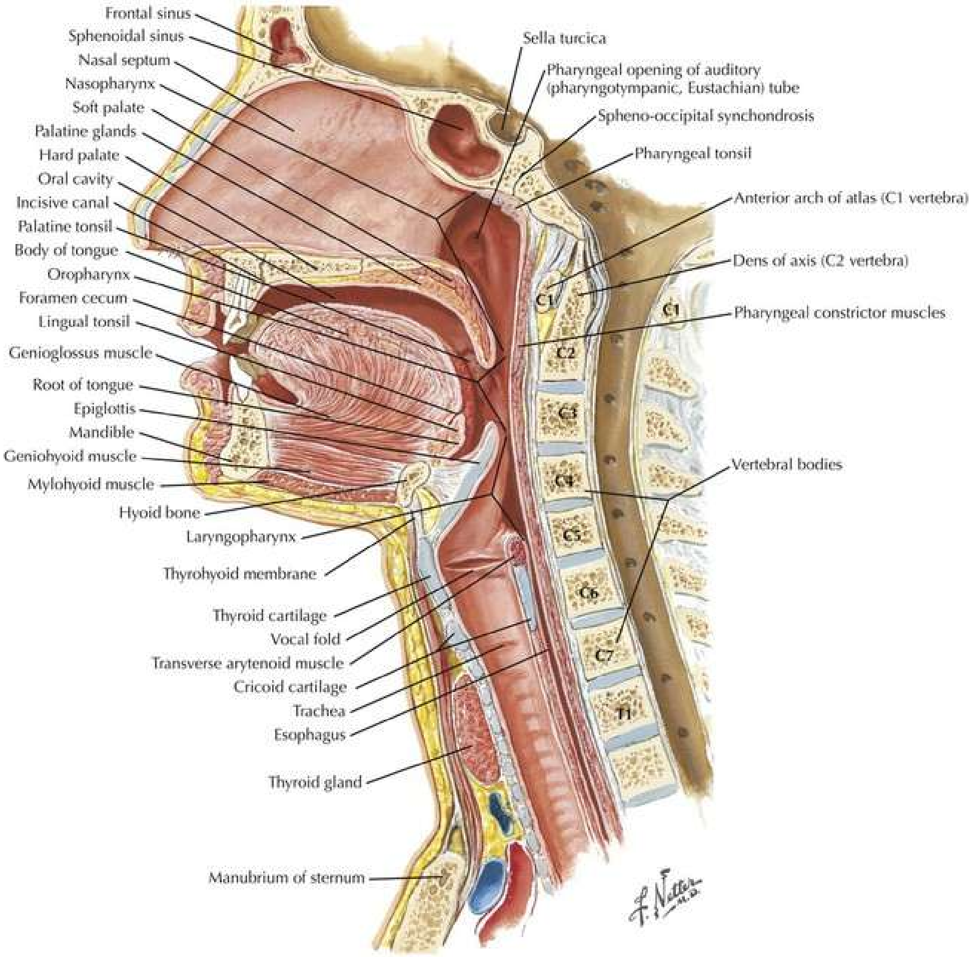

8.33 Midsagittal Section of the Nasal Cavity, Pharynx, Oral Cavity, and Neck: Overview

Review in this median (midsagittal) section the anatomical relationships between structures in the face and neck. Included are the frontal and sphenoid sinuses; nasal cavity; oral cavity; and subdivisions of the pharynx, larynx, trachea, esophagus, cranial base, and cervical vertebrae. Also note the sella turcica, auditory tube, tonsils (pharyngeal, palatine, and lingual), genioglossus muscle, hyoid bone, vocal fold, and thyroid gland anterior to tracheal rings. Compare these structures with their appearance in MRI on the following page.

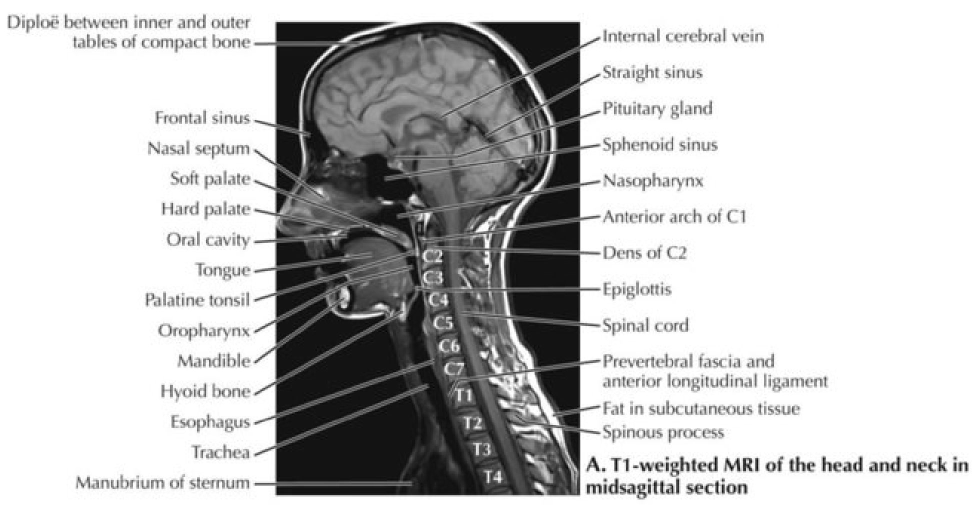

A. T1-weighted MRI of the head and neck in midsagittal section

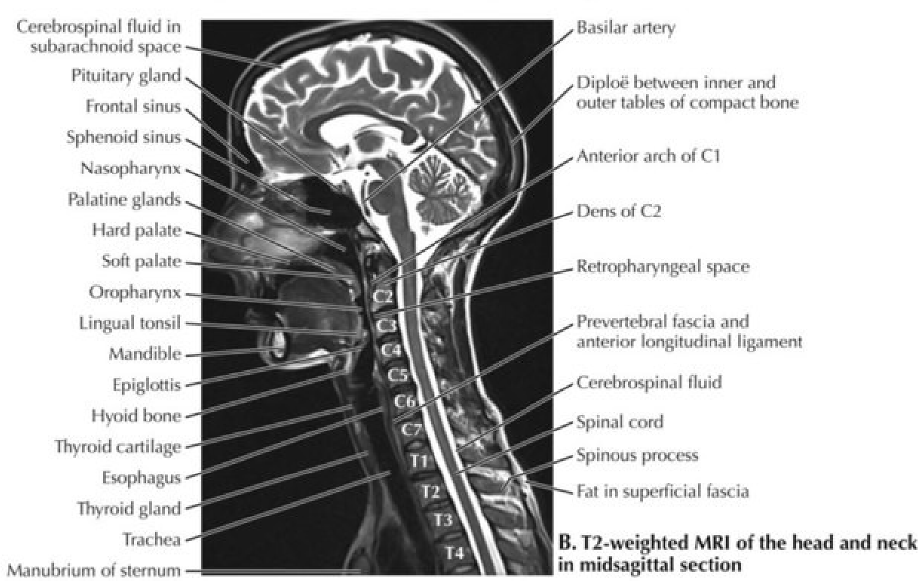

B. T2-weighted MRI of the head and neck in midsagittal section

8.34 T1 and T2 MRI of the Head and Neck in Midsagittal Section

A review of the entire head and neck provides a good overview of the differences in tissue densities seen in T1-weighted compared to T2-weighted MRI. In a T1 MRI **(A),** air and compact bone appear black, and fat white. Fluid and blood are also dark, whereas spongy bone and most soft tissues have an intermediate density. The most prominent difference in a T2 MRI **(B)** is that fluid appears bright white in addition to fat. Note the bright CSF around the brain and spinal cord. The signals for fat, bone, and soft tissues are similar in T1 and T2. Note how compact bone appears as a black rim around vertebral bodies, manubrium, and mandible in both figures. As we proceed to the study of meninges and dural sinuses, note the relationship between the appearance of CSF in the subarachnoid space and the inner and outer tables of compact bone in the neurocranium.

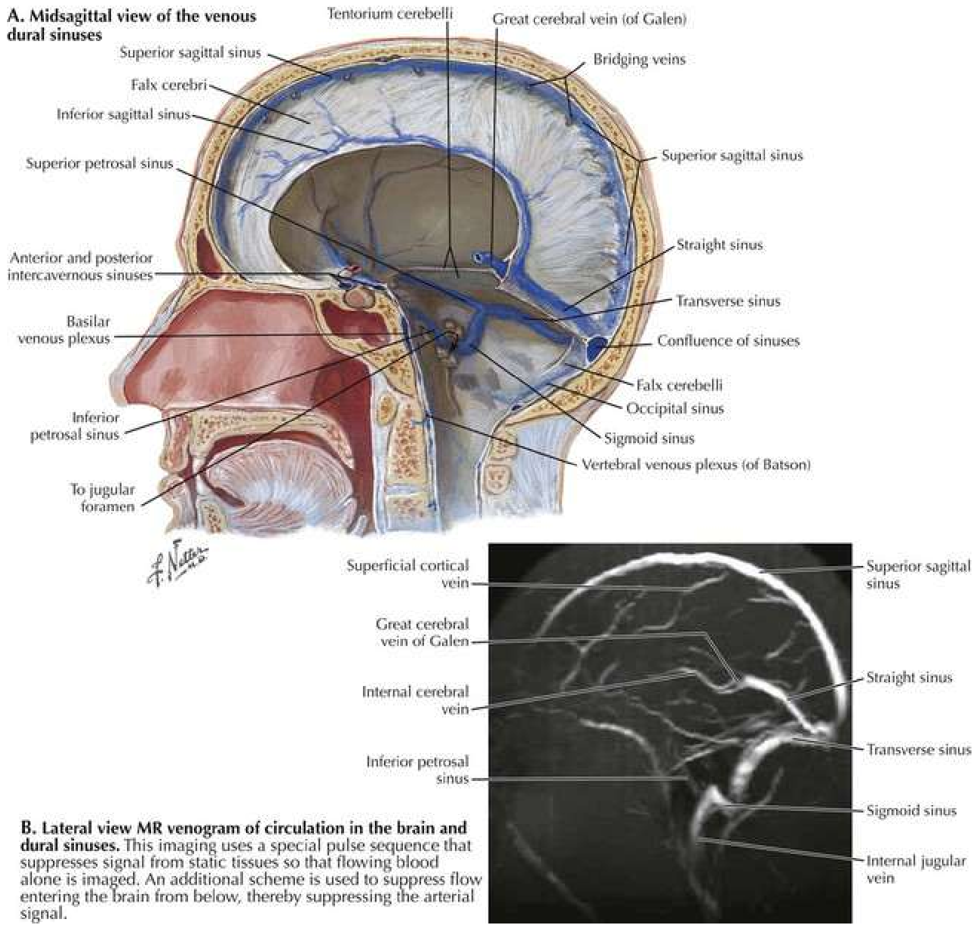

A. Midsagittal view of the venous dural sinuses

B. Lateral view MR venogram of circulation in the brain and dural sinuses. This imaging uses a special pulse sequence that suppresses signal from static tissues so that flowing blood alone is imaged. An additional scheme is used to suppress flow entering the brain from below, thereby suppressing the arterial signal.

8.35 Dural Venous Sinuses

Dural sinuses are venous channels in the dura mater that receive blood from the orbits, brain, and neurocranial bones and carry it to the internal jugular veins. The superior sagittal sinus and straight sinus in the falx cerebri converge on the transverse sinuses that course in the back edge of the tentorium cerebelli. Internal cerebral veins converge on the great cerebral vein of Galen, which joins the inferior sagittal sinus to form the straight sinus. The transverse sinuses continue as the sigmoid sinuses, which in turn exit the skull as the internal jugular veins. Blood from the orbits and deep brain enter the cavernous sinus that surrounds the body of the sphenoid bone. From there, blood passes into the sigmoid sinuses via the superior and inferior petrosal sinuses.

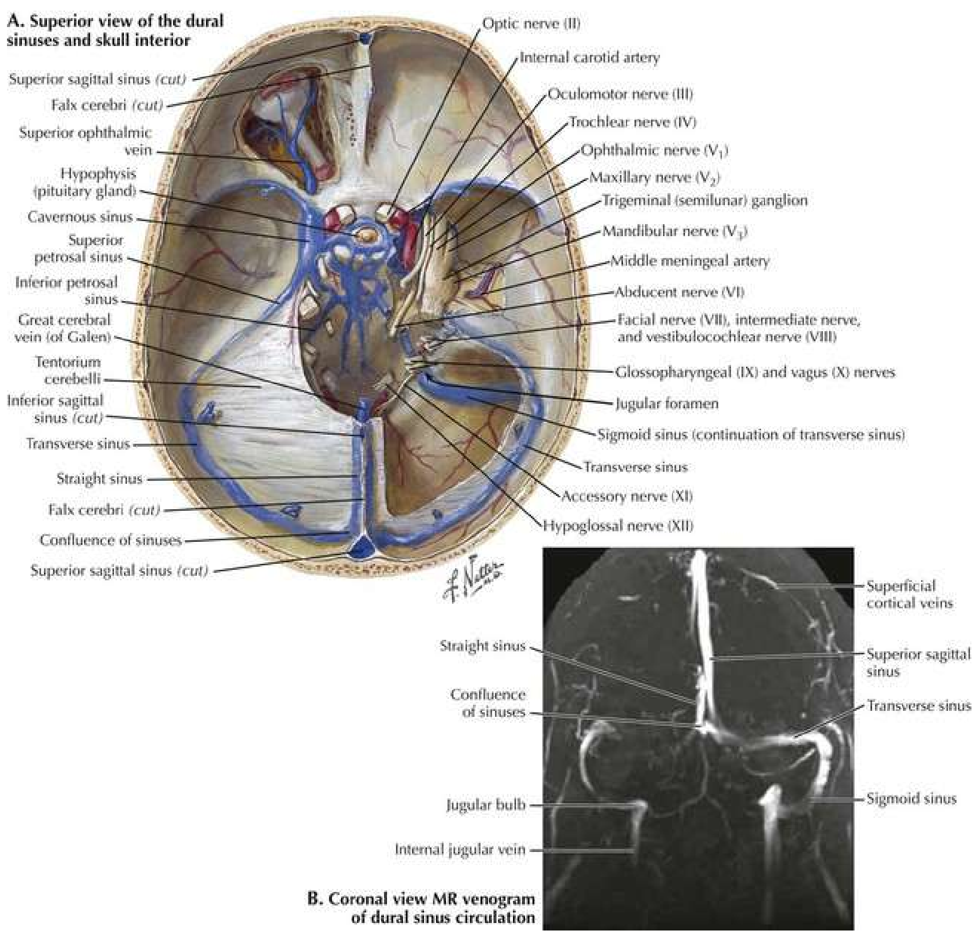

A. Superior view of the dural sinuses and skull interior

B. Coronal view MR venogram of dural sinus circulation

8.36 Dural Venous Sinuses (cont'd)

In superior and coronal views it is easier to appreciate the junction of the superior sagittal and straight sinuses at the confluence of sinuses and the left and right transverse sinuses continuing as the sigmoid sinuses. Most of the blood in the superior sagittal sinus typically flows into the left transverse sinus, and most of the blood in the straight sinus usually goes to the right transverse sinus. The patient in **B** has aplasia (congenital underdevelopment) of the right transverse sinus. The blood from both the superior sagittal sinus and straight sinus flows to the left side, where the transverse sinus, sigmoid sinus, and internal jugular vein are enlarged to accommodate the increased volume of flow.

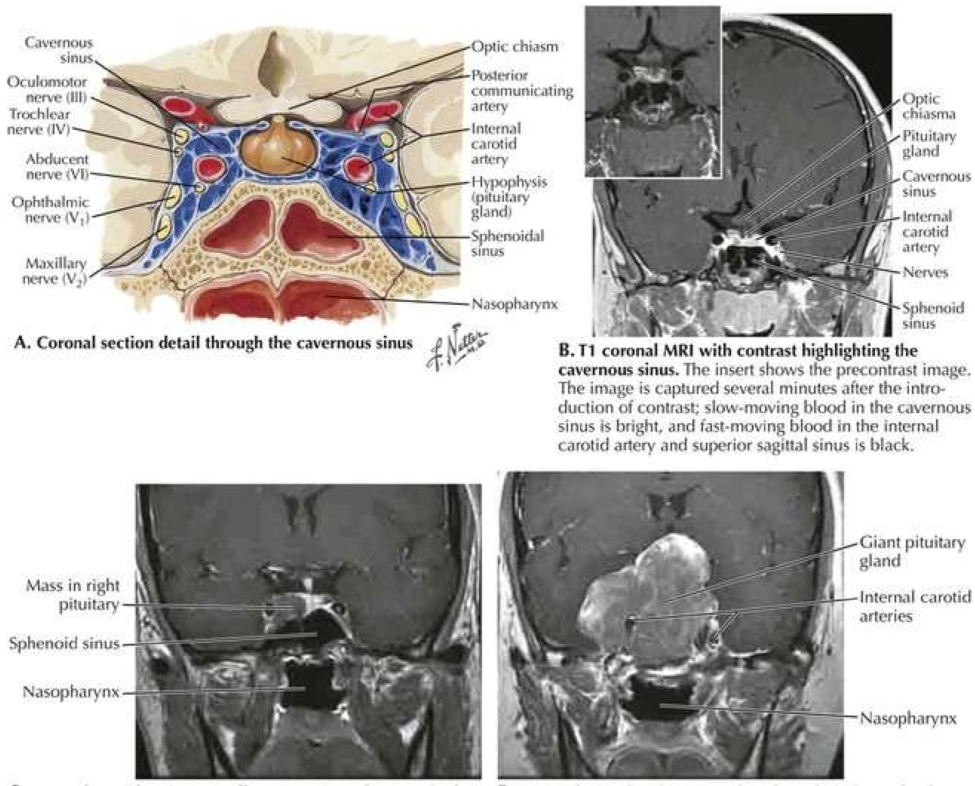

A. Coronal section detail through the cavernous sinus

B. T1 coronal MRI with contrast highlighting the cavernous sinus. The insert shows the precontrast image. The image is captured several minutes after the introduction of contrast; slow-moving blood in the cavernous sinus is bright, and fast-moving blood in the internal carotid artery and superior sagittal sinus is black.

C. Coronal MRI showing a small tumor (microadenoma) in the right half of the pituitary gland filling the cavernous sinus on that side

D. Coronal MRI showing a greatly enlarged pituitary gland obliterating the cavernous sinus and sphenoid sinus. The internal carotid arteries are still visible.

8.37 the Cavernous Sinus

The cavernous sinus flanks the body of the sphenoid bone and has anatomical relationships that are clinically significant. Passing through the sinus are the internal carotid artery, the three motor nerves to the orbit, and the ophthalmic and maxillary divisions of the trigeminal nerve. In the middle of the cavernous sinus is the pituitary gland. The cavernous sinus receives blood from the orbits and deeper parts of the brain. Its outflow is to the sigmoid sinus via the petrosal sinuses. Contrast in the cavernous sinus **(B)** makes it easier to see masses that might arise from the pituitary gland (**C** and **D**), meninges, nerves, or other sources and impair the functions of the nerves in the sinus. The internal carotid artery may rupture in the sinus, causing a large arteriovenous shunt that reverses the flow of blood through the ophthalmic veins and deep cerebral veins.

A. Coronal section of the superior sagittal sinus

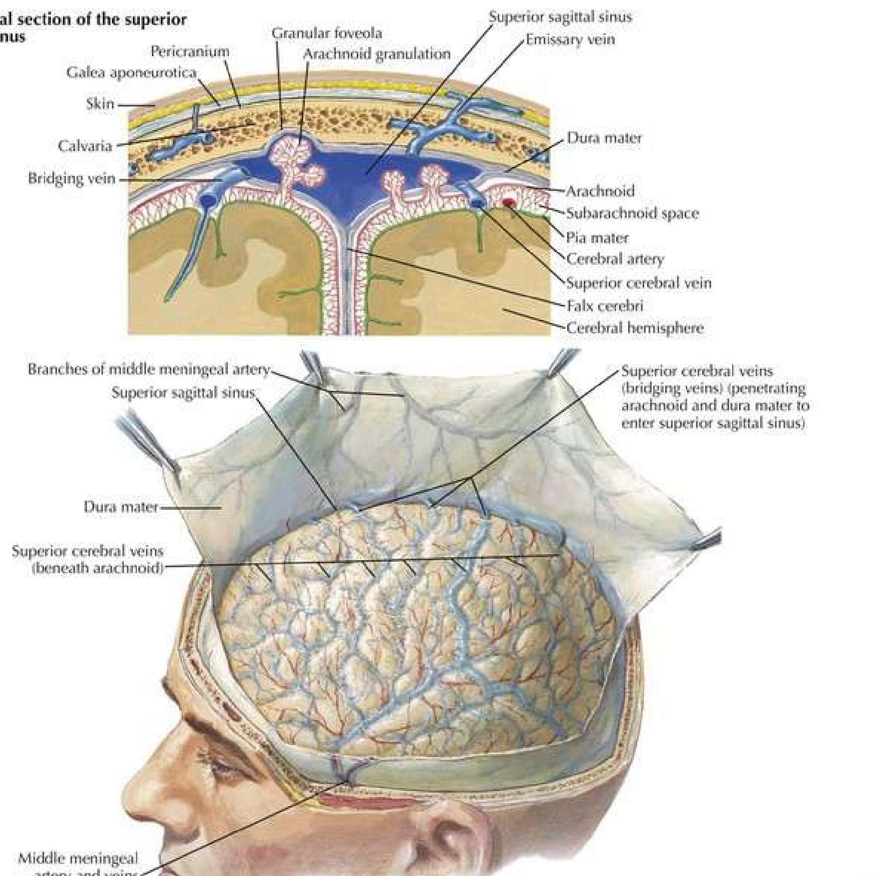

B. Epidural middle meningeal vessels and cerebral veins. Note the veins traversing the subarachnoid space to pierce the arachnoid and dura mater to enter the superior sagittal sinus.

8.38 Superior Sagittal Sinus, Middle Meningeal Artery, and Superficial Cerebral Veins

The superior sagittal sinus, like other dural sinuses, receives venous blood from the brain and neurocranial bones and is connected to veins of the scalp via emissary veins. It is also the only location where CSF enters the venous circulation. Tufts of arachnoid called *arachnoid granulations* pierce the superior sagittal sinus and its lateral extensions (lacunae) to act as simple valves for the diffusion of CSF into the blood. The blood supply to the neurocranial bones and dura is by the middle meningeal branch of the maxillary artery. Rupture of this artery from a blow to the thin bones on the side of the skull results in serious bleeding in an epidural location. Venous bleeding from head trauma is usually subdural. The cerebral veins often tear where they enter the dural sinuses, and blood accumulates between the arachnoid and the dura mater.

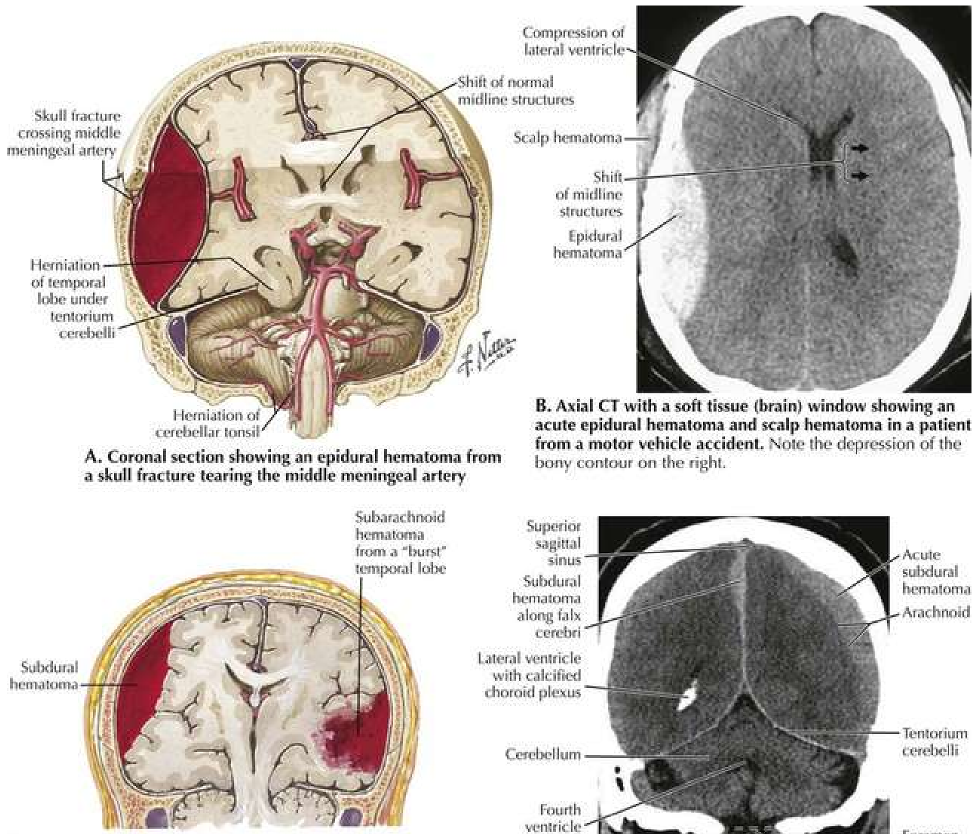

A. Coronal section showing an epidural hematoma from a skull fracture tearing the middle meningeal artery

B. Axial CT with a soft tissue (brain) window showing an acute epidural hematoma and scalp hematoma in a patient from a motor vehicle accident. Note the depression of the bony contour on the right.

C. Coronal section showing an acute, venous, subdural hematoma on the left and a subarachnoid, arterial hematoma on the right originating from a temporal lobe intracerebral hematoma ("burst" temporal lobe) (e.g., from trauma or a ruptured aneurysm)

D. Coronal CT reconstruction showing an acute subdural hematoma on the left and along the right side of the falx cerebri. This patient was also in an automobile accident.

8.39 Imaging of Epidural and Subdural Bleeding

If the middle meningeal artery ruptures, high-pressure arterial blood separates the dura from the bone, producing an epidural accumulation of blood that is convex toward the brain (**A** and **B**). The increased pressure on cranial nerves, vessels, and brain tissue in general is a medical emergency. Subdural bleeding (**C** and **D**) is usually venous blood. A blow to the head puts tension on the cerebral veins, and they typically tear at their attachment to the dural sinuses. The blood extends between the dura and arachnoid, which are only held together by the pressure of the CSF in the subarachnoid space. The profile of the venous accumulation of blood is more irregular and less convex toward the brain compared with epidural bleeding. Subarachnoid bleeding into the CSF **(C)** follows the contours of the surface of the brain and is arterial if it is from an intracerebral hematoma.

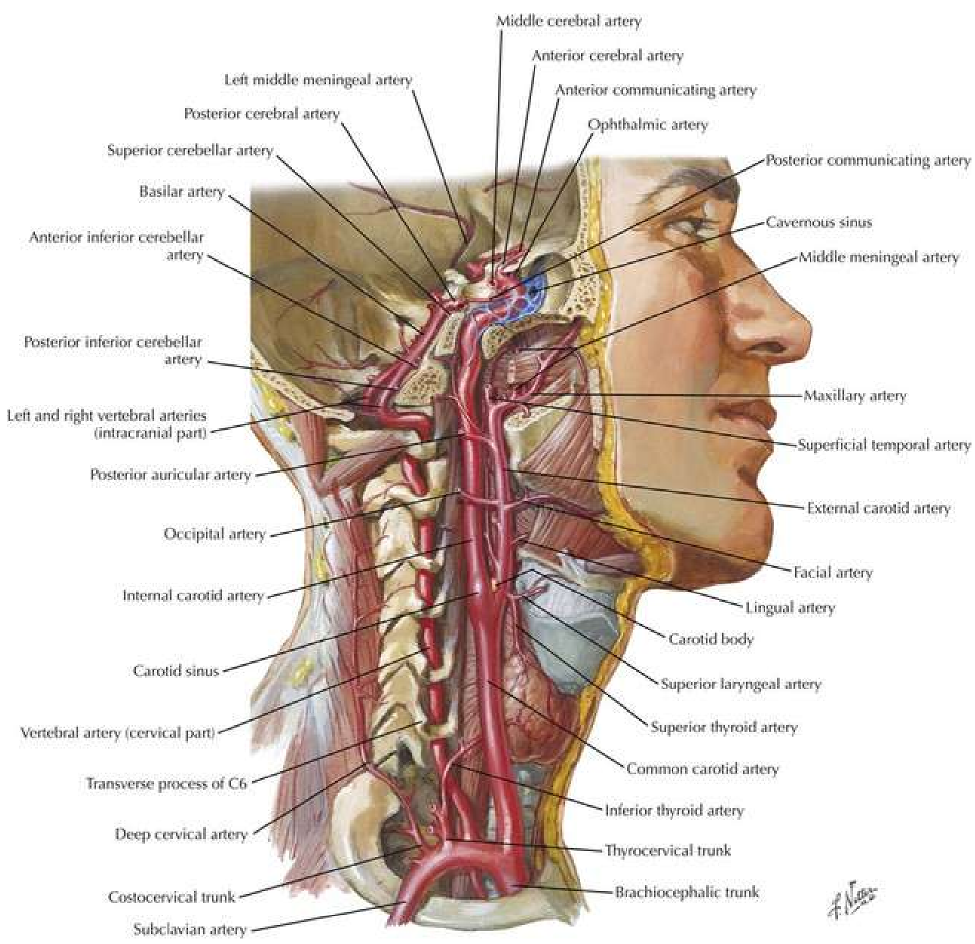

8.40 Arteries from the Neck to the Brain

The brain receives its blood supply from the vertebral and internal carotid arteries. The vertebral arteries form the basilar artery, which divides into the posterior cerebral arteries. The internal carotid arteries continue as the middle cerebral arteries and give off the anterior cerebral arteries. The orbits are also supplied by the internal carotid arteries via their ophthalmic branches. The external carotid arteries supply the nasal cavities, oral cavity, muscles of mastication, structures of the face, and most of the anterior neck down through the upper half of the thyroid gland.

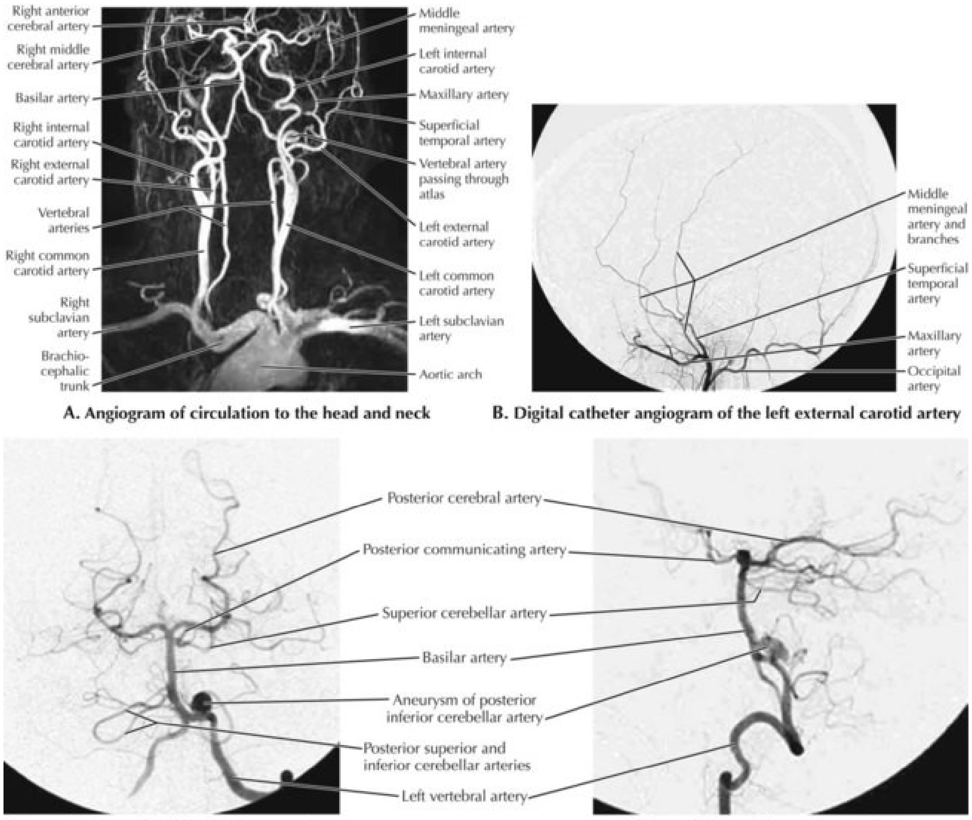

A. Angiogram of circulation to the head and neck

B. Digital catheter angiogram of the left external carotid artery

C. Anterior view of a digital catheter angiogram of the left vertebral artery with retrograde flow into the right vertebral artery

D. Left lateral view of the angiogram in C

8.41 Vascular Studies

Vascular imaging studies of the head and neck detect aneurysms (dilations) (**C** and **D**), arteriovenous malformations, vessels leaking from trauma, and the reduction in blood flow from compression of arteries (e.g., from tumors) or narrowing of the lumen from plaque formation, which occurs often in the common carotid arteries. **A** is an angiogram in which contrast is introduced into the arch of the aorta, filling the common carotid and vertebral arteries and their branches on both sides. **B, C,** and **D** are digital subtraction angiograms. In digital angiography a "mask" image is obtained before administration of contrast. Following injection of the contrast agent into a specific vessel, the mask image is subtracted electronically. This leaves only the image of the contrast in the blood vessels, which can be rotated to view from any angle. Interventions can also be performed through the catheter at the time of the study, such as the placement of stents, balloon dilation of narrow vessels, stripping of the arterial intima, or injection of clot-dissolving agents.

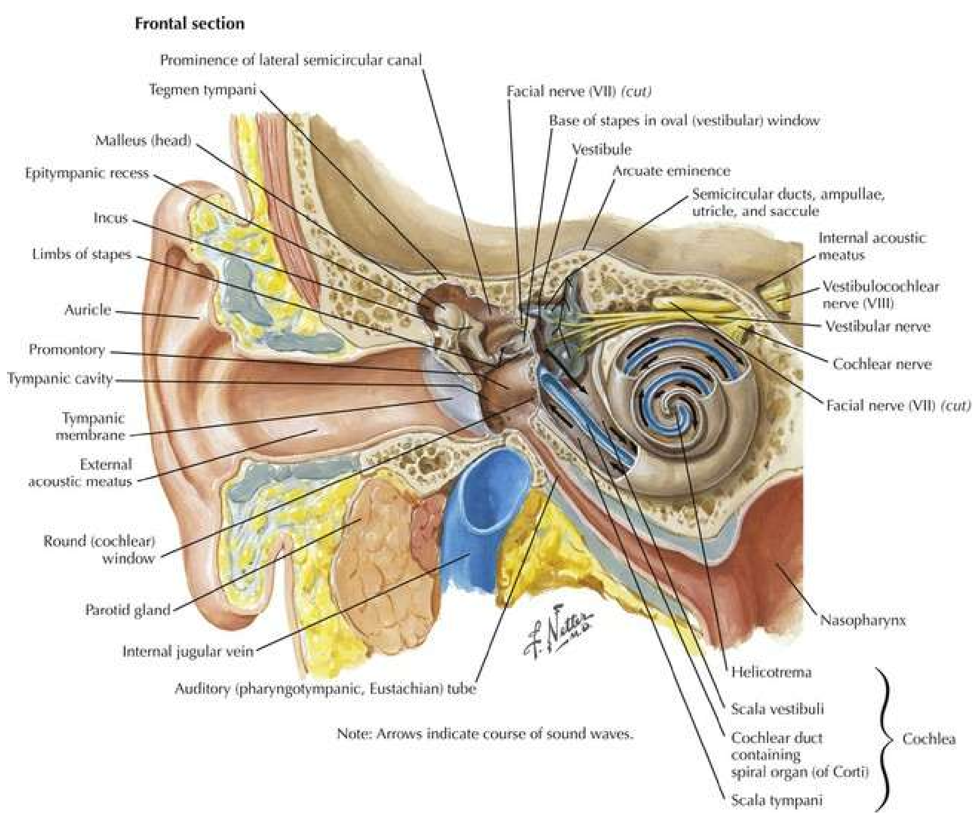

8.42 External, Middle, and Inner Ear

The three compartments of the ear are contained within the temporal bone. The external ear consists of the auricle and the external acoustic meatus, which transmit sound waves to the tympanic membrane (eardrum). The air-filled tympanic cavity (middle ear) has three ear ossicles that carry the sound vibrations from the tympanic membrane to the cochlea of the inner ear, where sound vibrations are converted into electrical impulses in the auditory branch of the vestibulocochlear nerve (cranial nerve VIII). The tympanic cavity is connected to the nasopharynx anteriorly by the auditory (Eustachian) tube to balance pressure on both sides of the eardrum and posteriorly to the mastoid air cells. The inner ear also contains the vestibular apparatus containing the three semicircular canals, utricle, and saccule that register positional sense, balance, rotations, and linear acceleration. This information is conveyed via the vestibular branch of nerve VIII. Inferior to the middle ear cavity is the jugular bulb. The facial nerve (VII) is superior to the tympanic cavity and then passes inferiorly along its posterior wall.

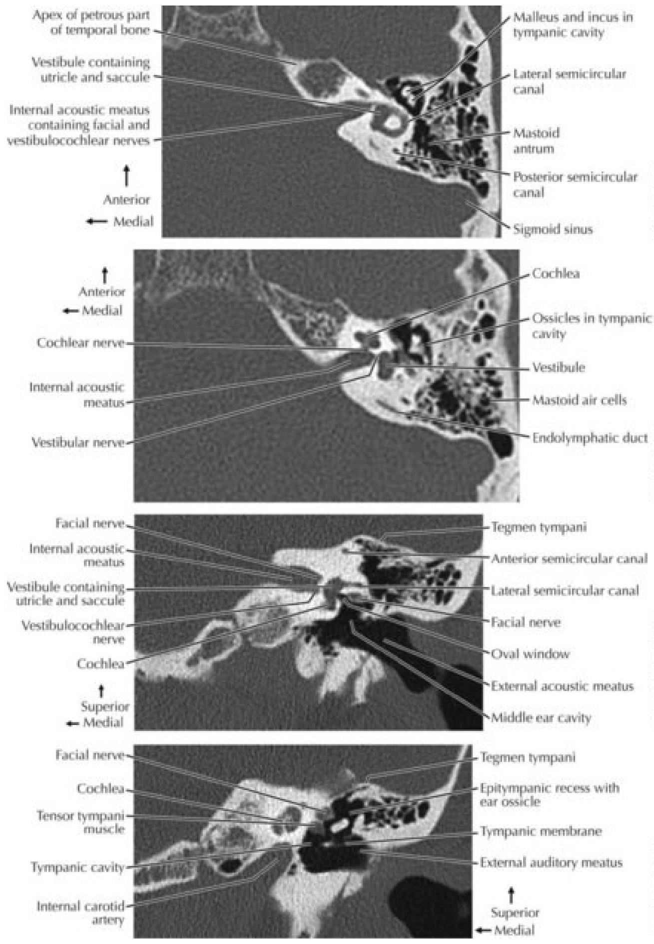

A. Axial CT of the left temporal bone. The plane is through the internal acoustic meatus, vestibular apparatus, and middle ear (tympanic) cavity.

B. Axial CT of the left temporal bone at a lower level than in A. The plane contains the cochlea and division of the vestibulocochlear nerve.

C. Coronal CT reconstruction of the left temporal bone in a plane containing the facial and vestibulocochlear nerves, oval window, and middle ear cavity. The tympanic membrane (eardrum) is not visible.

D. CT reconstruction of the left temporal bone anterior to the plane in C. It contains the cochlea, tensor tympani muscle, and an ear ossicle in the epitympanic recess of the tympanic cavity.

8.43 CT of the Temporal Bone and Ear Compartments

Study of the tiny structures and compartments in the temporal bone with CT bone windows requires thin slice acquisition—0.6 or 1.25 mm rather than the more typical 5 mm—and the slices are overlapped in plane reconstructions to provide greater detail. The inner ear organs are enclosed in dense cortical bone, the bright white signal in the illustrations. The cochlea is anterior and a bit inferior to the vestibular apparatus, and each plane of section predominantly captures one or the other. The facial and vestibulocochlear nerves enter the internal acoustic meatus of the petrous part of the temporal bone **(B).** The vestibulocochlear nerve **(C)** divides into anterior cochlear and posterior vestibular branches **(B).** The cochlear branch then passes inferiorly to the cochlea. Note the continuity of the tympanic cavity (middle ear) with the mastoid air cells **(A).** The tensor tympani muscle **(D)** is in the roof of the auditory tube (not shown). The epitympanic recess is the extension of the middle ear cavity above the level of the tympanic membrane **(D).**

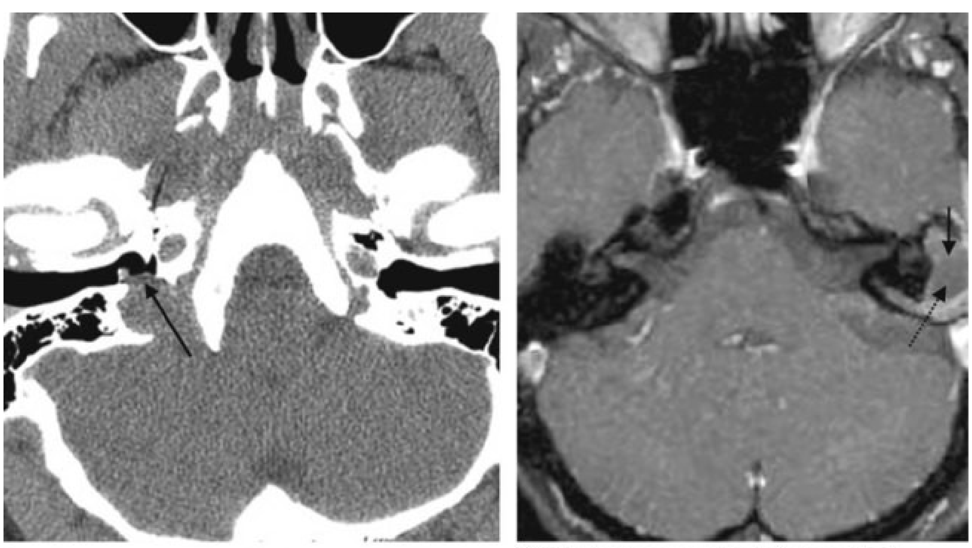

A. Axial CT showing the jugular bulb extending into the middle ear cavity *(arrow)*

B. MRI showing a mass (cholesteatoma) in the epitympanic recess *(solid arrow)* and mastoid antrum *(dashed arrow)*

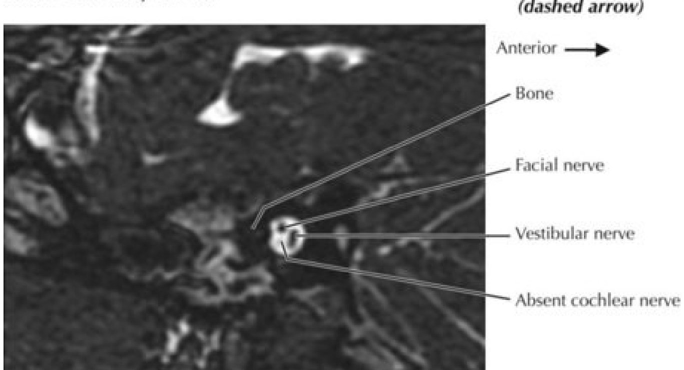

C. T2 MRI in a sagittal plane through the internal acoustic meatus of a deaf patient with congenital absence of the cochlear nerve

8.44 Imaging of Temporal Bone/Ear Pathology

Imaging studies of the temporal bone require careful evaluation of the spaces and the selection of modalities that best highlight soft tissue structures. **A** shows an anatomical variation that impacts function of the middle ear. The sigmoid sinus curves upward under the middle ear cavity as the jugular bulb, the beginning of the internal jugular vein. Here the jugular bulb projects through the bony floor of the tympanic cavity. The MRI in **B** shows a mass in the tympanic cavity extending into the mastoid antrum. It is a congenital cholesteatoma, a cyst with keratinized epithelial debris and cholesterol. It shows the typical lack of enhancement when T1 with vascular contrast is used. In **C,** landmarks are hard to discern; but the T2 MRI clearly shows the congenital lack of the cochlear nerve in the internal acoustic meatus within dense, cortical bone *(black)*.

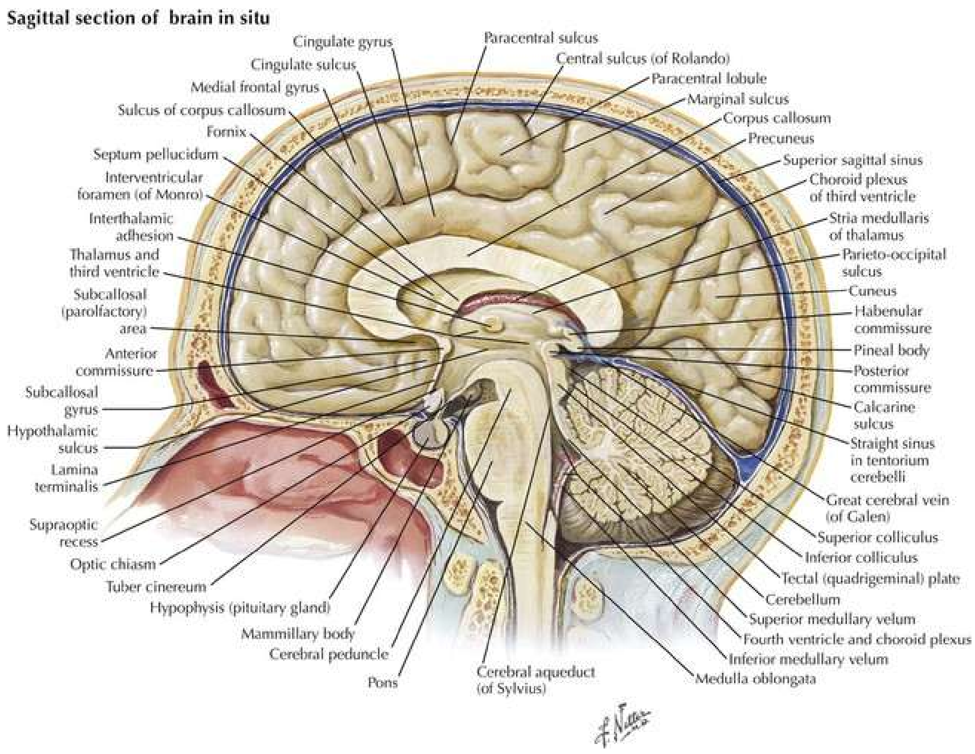

8.45 Midsagittal Section of Brain; Medial View of Cerebrum

The subdivisions of the brain are, from superior to inferior, the large cerebral hemispheres (telencephalon) and the smaller diencephalon (thalamus and related structures) that together make up the cerebrum (prosencephalon), the narrow midbrain (mesencephalon) seen here as the tectal plate and cerebral peduncle, the pons anteriorly and the cerebellum posteriorly (metencephalon), and the tapering medulla oblongata (myelencephalon) that is continuous with the spinal cord at the foramen magnum. Each cerebral hemisphere is divided into four lobes from anterior to posterior: the frontal lobe, the parietal lobe, the occipital lobe and, inferiorly, the temporal lobe (out of the plane of section). The corpus callosum is a large bundle of commissural fibers connecting functionally related areas in the two hemispheres. Inferior to the corpus callosum is the C-shaped fornix, a smaller bundle of fibers that project from the hippocampal formation in the temporal lobe to primarily the mammillary body of the hypothalamus.

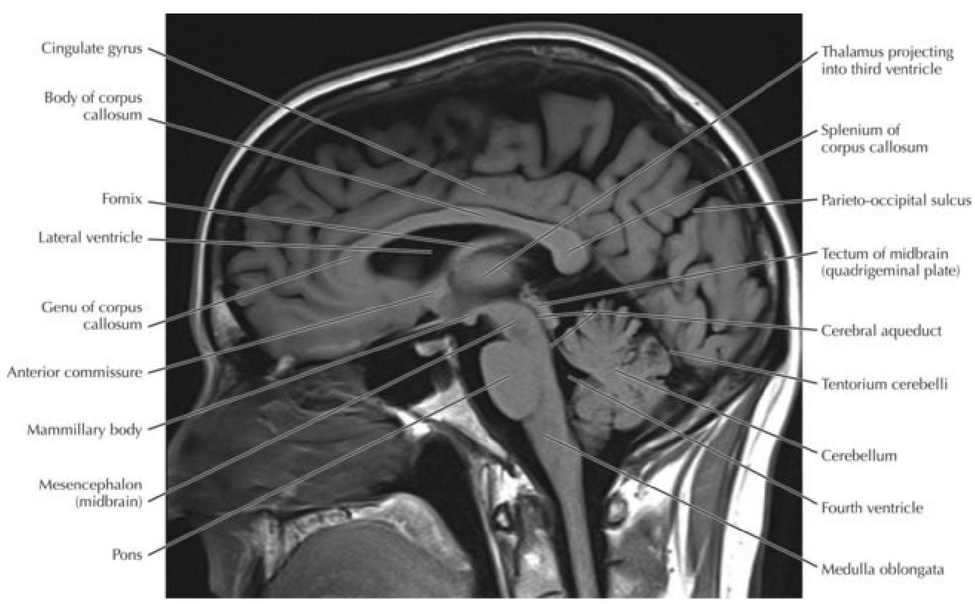

8.46 Midsagittal T1 MRI

In general, when the neuroradiologist reviews a series of MR images, the anatomy is scrutinized for normalcy rather than searching for specific abnormal findings first. For example, the junction of the gray and white matter is evaluated; if it is normal, the next structure is evaluated. If it is abnormal, a differential diagnosis of pathologies that could blur that interface is constructed within the context of the patient's history. This search strategy is more comprehensive than a search for particular pathologies, most of which are unlikely to be found. This midsagittal MRI is T1-weighted, in which fluid, compact bone, and air have dark signal and subcutaneous fat and bone marrow have bright signal. Brain tissue is gray, with white matter being a bit lighter than gray matter. Very evident in the section is CSF in the ventricles and surrounding the brain and spinal cord. Although close to the midline, the falx cerebri is out of the plane, and a mammillary body and part of a lateral ventricle are seen. The midsagittal T1-weighted MR image of the brain is where many neuroradiologists begin when evaluating a series of images for pathology. Abnormalities that are usually first recognized sagittally include pituitary tumors, abnormally sized CSF spaces (ventricles, cisterns, and subarachnoid space), and pathology within the corpus callosum.

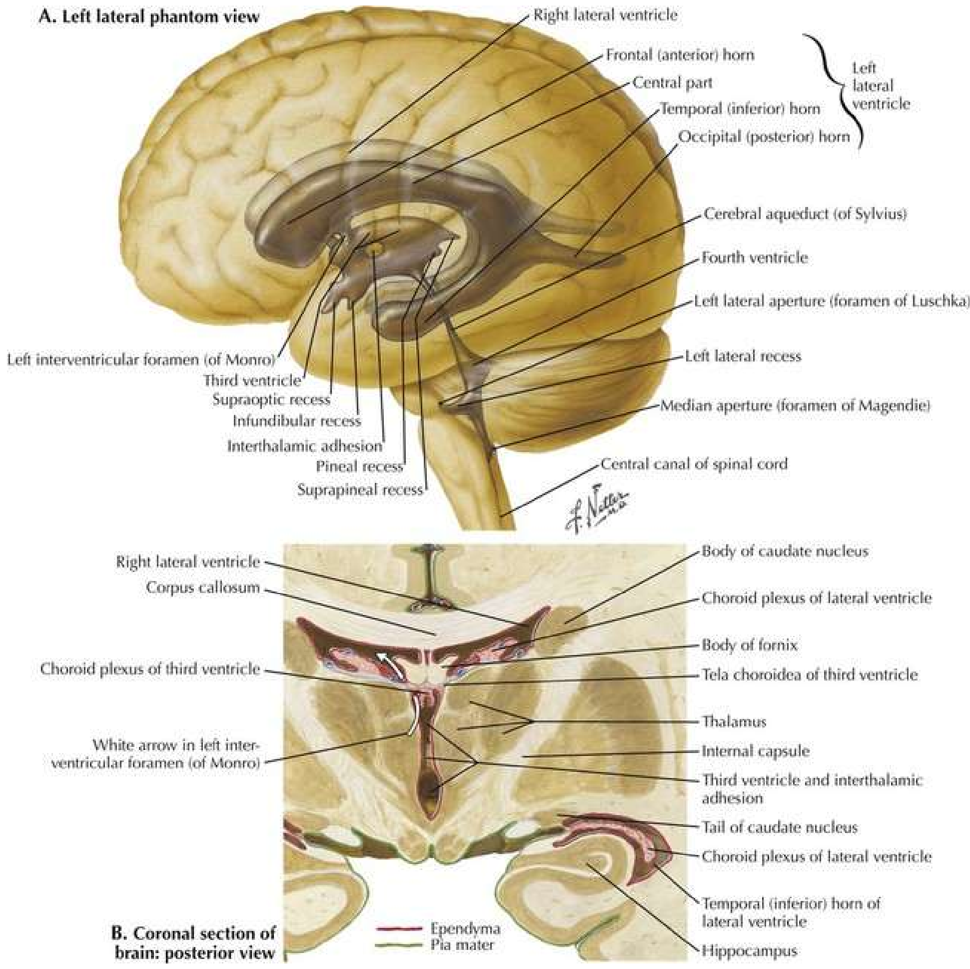

8.47 Ventricles of the Brain

CSF is produced as an ultrafiltrate of blood in the choroid plexus of vessels in the ventricles of the brain, an interconnected series of chambers that develop from the lumen (central canal) of the neural tube. C-shaped left and right lateral ventricles connect via the interventricular foramina (of Monro) to a midline third ventricle in the middle of the thalamus. The third ventricle connects with the fourth ventricle via the cerebral aqueduct of Sylvius. CSF enters the subarachnoid space around the brain through a median foramen in the fourth ventricle, the foramen of Magendie, and bilateral foramina of Luschka.

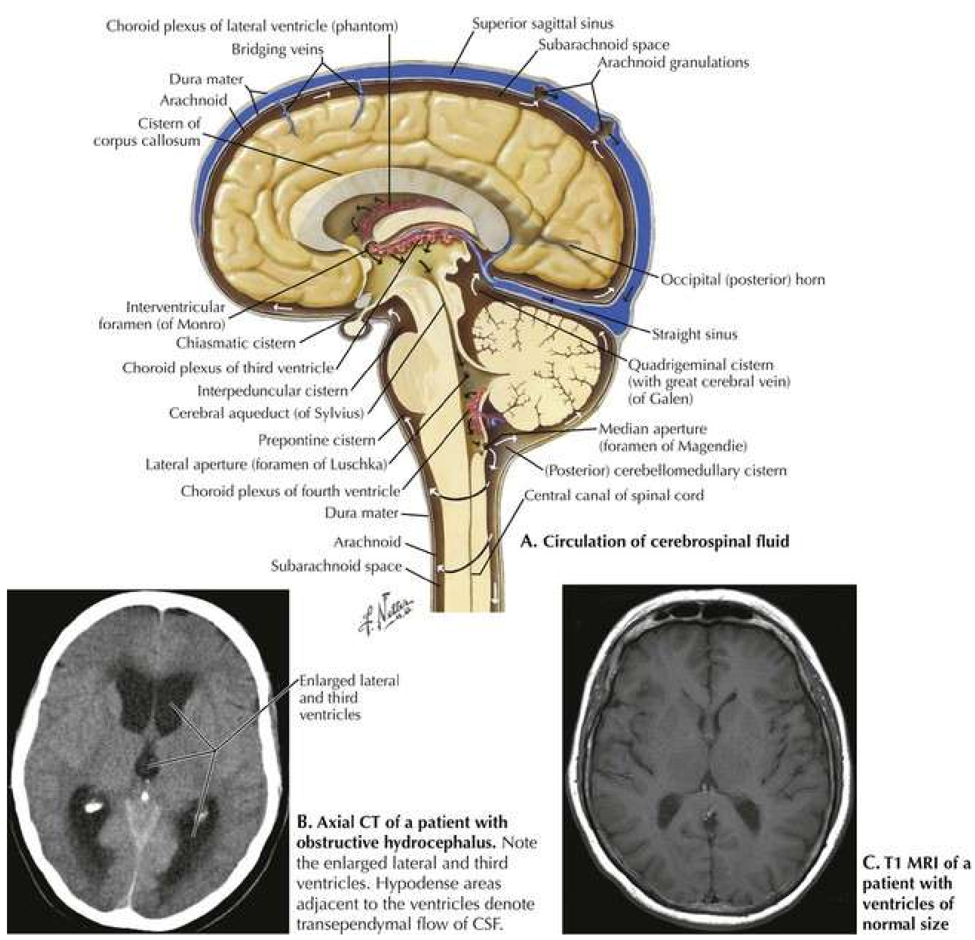

8.48 Circulation of Cerebrospinal Fluid and Hydrocephalus

CSF passes sequentially from the lateral ventricles to the third ventricle to the fourth ventricle. From the fourth ventricle it enters the subarachnoid space around the brain and spinal cord through the median foramen of Magendie and lateral foramina of Luschka. CSF from the brain and spinal cord reenters the bloodstream by passing through tufts of arachnoid (granulations) that project into the dural venous sinuses. Obstructive, also known as *noncommunicating*, hydrocephalus is the accumulation of CSF within the ventricles caused by blockage of the foramina or cerebral aqueduct.

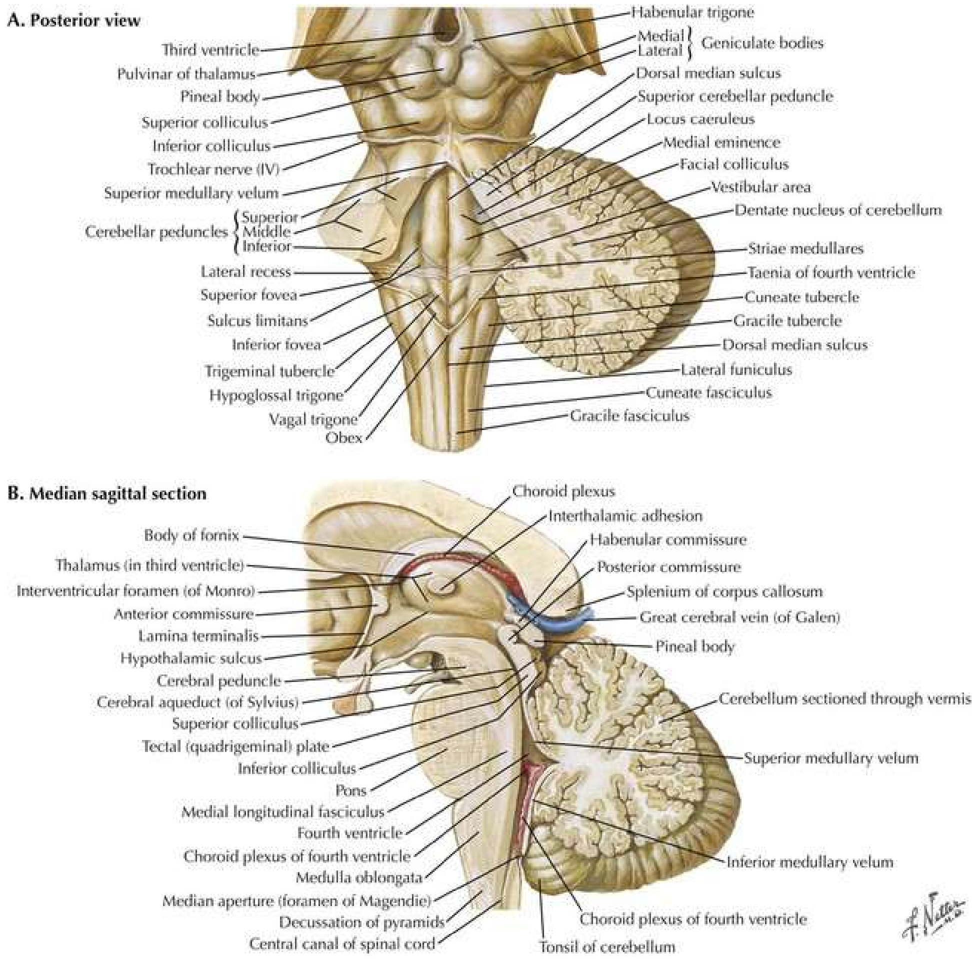

8.49 Fourth ventricle and Sections of the Cerebellum

In **A,** the right half of the cerebellum is cut in a coronal section. The left half of the cerebellum has been removed by cutting the cerebellar peduncles, opening up the fourth ventricle. The brainstem here is divided into left and right halves by the dorsal median sulcus. Each half is subdivided by the sulcus limitans into a medial eminence and hypoglossal and vagal trigones containing the motor nuclei of cranial nerves and a lateral vestibular area containing the sensory nuclei of cranial nerves. In **B,** the diencephalon, brainstem, cerebellum, and ventricular system are cut in a midsagittal section. The slitlike third ventricle separates the two halves of the diencephalon. It is continuous with the narrow cerebral aqueduct of Sylvius in the midbrain and the triangular fourth ventricle between the pons and rostral medulla anteriorly and the cerebellum posteriorly.

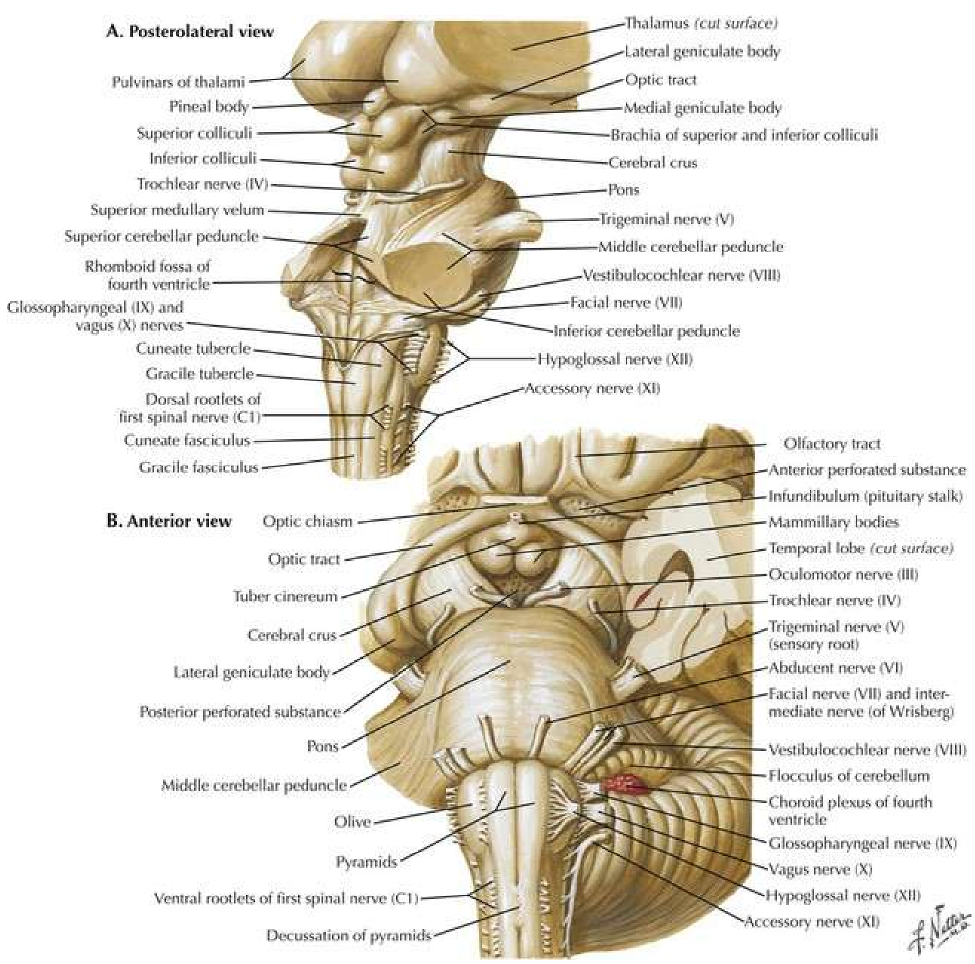

8.50 Brainstem

In **A**, the cerebellum has been removed by cutting the cerebellar peduncles, opening up the rhomboid fossa of the fourth ventricle that overlies the posterior surface of the pons and the rostral medulla. The brainstem consists of, from inferior to superior, the medulla oblongata, pons, and midbrain. The tapering medulla is characterized by the pyramids and olive anteriorly and the gracile and cuneate fasciculi and tubercles posteriorly. The pyramidal decussation is the boundary between the medulla and the cervical spinal cord. The wide pons consists of a large anterior basal portion and a smaller posterior tegmentum in the floor of the rhomboid fossa. The short midbrain has the paired superior and inferior colliculi and their brachia posteriorly and the cerebral crus anteriorly. Cranial nerves III to XII arise from the brainstem. The trochlear (IV) nerve is the only one to leave the dorsal surface of the brainstem.

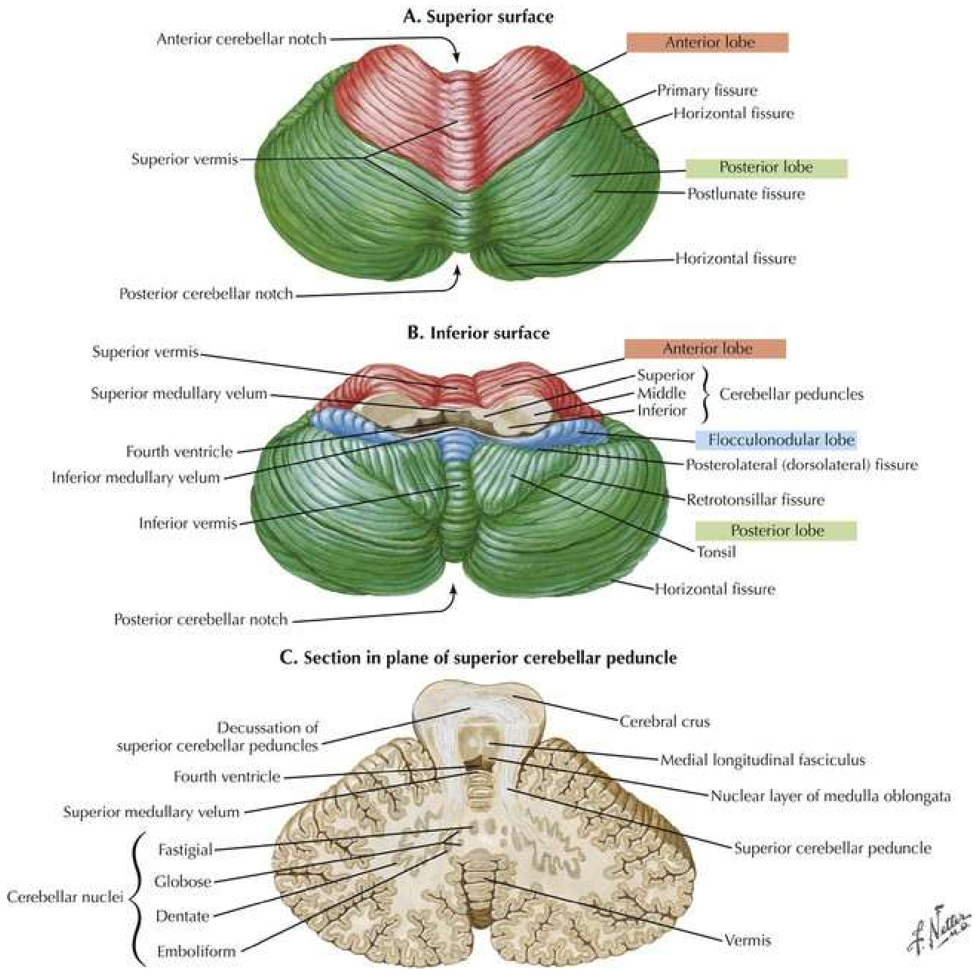

8.51 Cerebellum

In these figures the cerebellum has been removed from the brainstem by cutting the superior, middle, and inferior cerebellar peduncles. The nerve fibers that make up the peduncles connect the cerebellum to the brainstem and thalamus. The cerebellum consists of a cortex or thin surface layer of gray matter that is extensively folded into thin, transverse, leaflike folia. White matter deep to the cortex is composed mostly of fibers going to or coming from the cortex. Four pairs of deep nuclei embedded in the white matter consist of neurons that project the cerebellar output to other portions of the brain. The dentate is the largest and most prominent. The cerebellum is divided into a narrow median vermis and large bilateral hemispheres. Two deep fissures divide the vermis and hemispheres into three lobes. The vermis and hemispheres can be further subdivided into lobules.

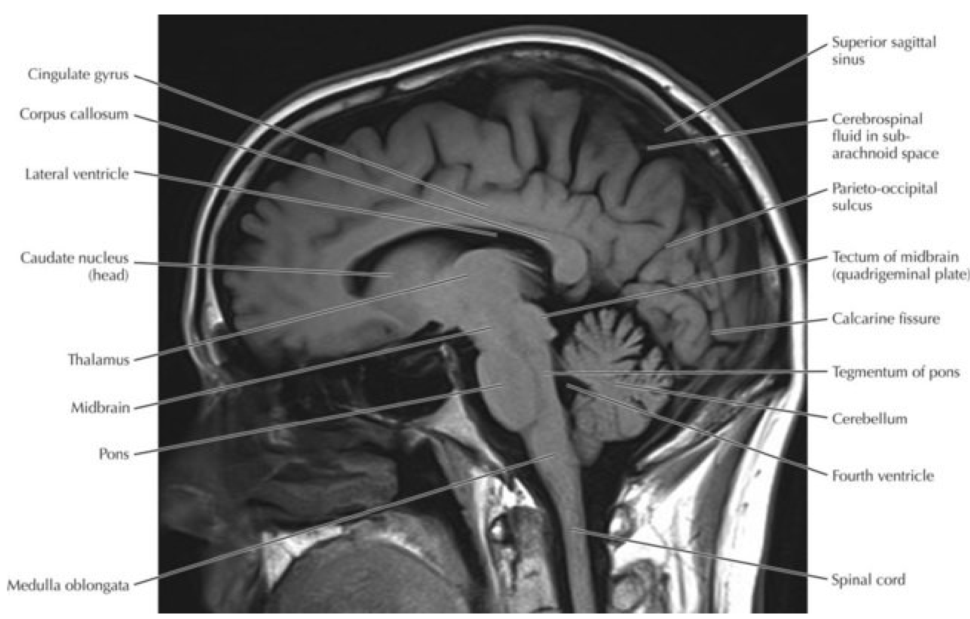

8.52 T1 Sagittal MRI near the midline

This section is just off the midline lateral to the falx cerebri. More of the thalamus and a lateral ventricle are seen. The strategy for looking for pathology just lateral to the midline usually stems from the pathology that is also commonly seen in the midline, which may stretch laterally. For example, abnormalities in the corpus callosum, as can be seen in multiple sclerosis, may be off the midline. Sometimes pituitary or optic nerve abnormalities may also be seen off the midline. The basal ganglia and thalami are seen in the parasagittal plane, which allows the neuroradiologist to assess for changes to the brain as a result of hypertension affecting the small arteries that penetrate these structures.

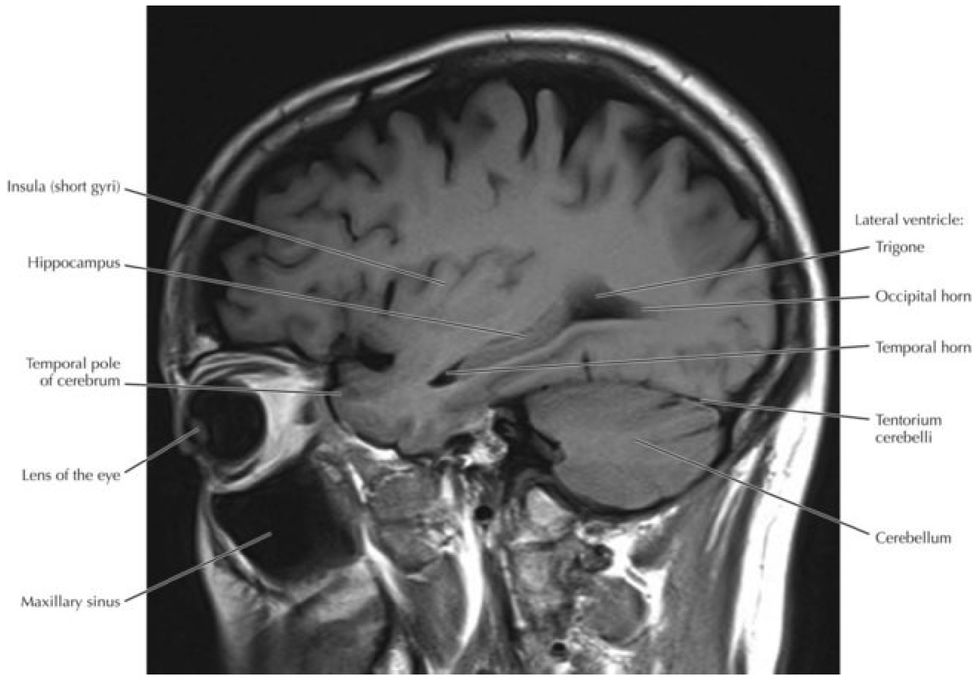

8.53 T1 sagittal MRI through the Temporal Lobe

This is a parasagittal plane through the middle of the orbit, maxillary sinus, and cerebral hemisphere. The optic nerve and apex of the orbit are medial to the plane. The section is through the trigone of a lateral ventricle, including the occipital horn and full extent of the temporal horn in the middle of the temporal lobe of the cerebrum. The contours of the anterior, middle, and posterior cranial fossae are seen containing the frontal lobe of the cerebrum, temporal lobe, and cerebellum, respectively. The trigeminal (semilunar) ganglion and three divisions of the trigeminal nerve are medial to the plane of section. The dura mater of the tentorium cerebelli separates the cerebellum from the overlying occipital lobe of the cerebrum.

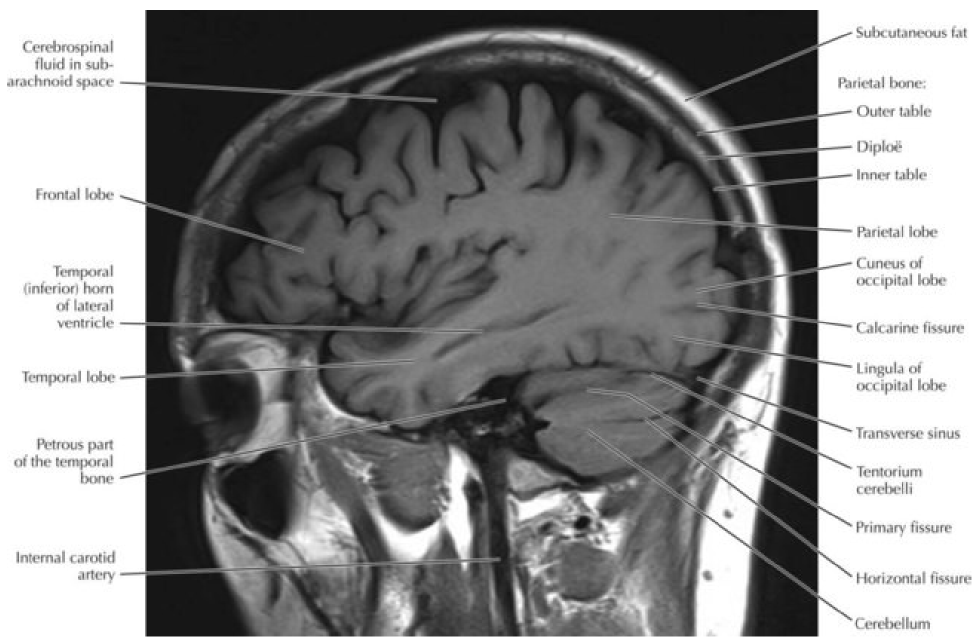

8.54 T1 Sagittal MRI through the Temporal Lobe (cont'd)

This section captures the internal carotid artery entering the carotid canal in the petrous part of the temporal bone inferior to the temporal lobe of the cerebrum. Recall that, with a T1-weighted MRI pulse sequence, fluid (including blood), bone, and air all appear dark. Attaching to the petrous posteriorly is the tentorium cerebelli between the cerebellum and occipital lobe. The transverse sinus is at the intersection of the tentorium cerebelli and the occipital bone on either side of the midline. Labeled in this section are the layers of the parietal bone—inner and outer tables of compact bone surrounding the more intense signal from the fatty diploë. It is hard to distinguish the inner table of bone from the underlying cerebrospinal fluid in the subarachnoid space.

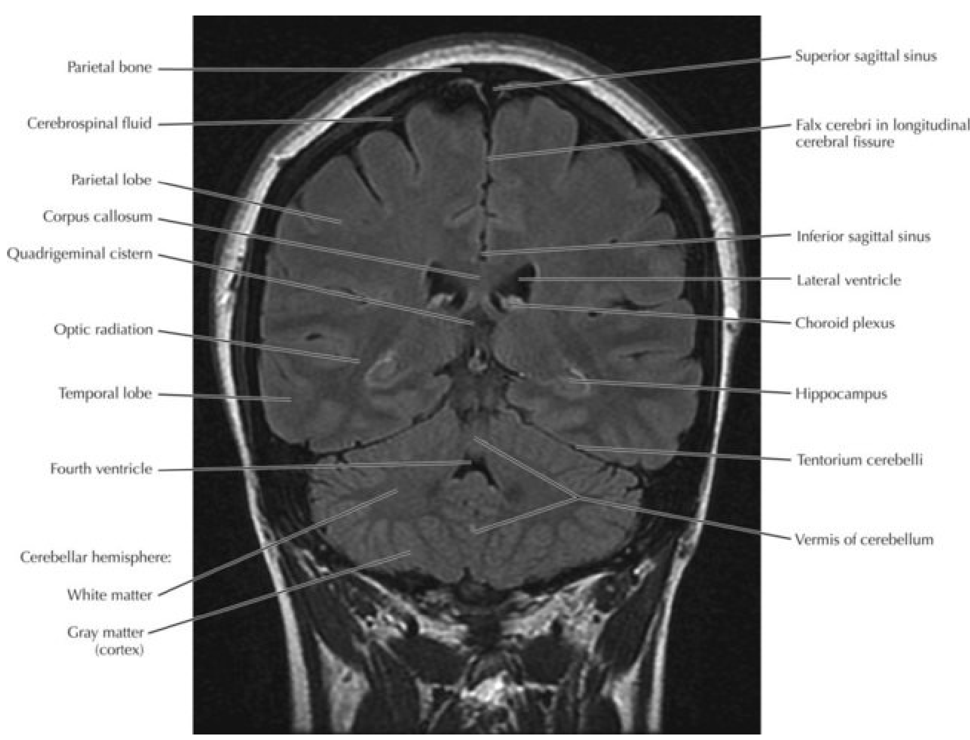

8.55 T2 Flair Coronal MRI through the Cerebellum

The brain must be visualized in all three planes to evaluate the extent of a pathological process. This T2 fluid attenuation inversion recovery (FLAIR) MRI is a coronal section through the cerebellum, parietal lobes, and posterior aspect of the temporal lobes. This FLAIR pulse sequence on MRI is T2 based, but the normally T2 bright signal of fluid is suppressed on FLAIR imaging because of the application of an inversion pulse, which nulls the MRI signal from fluid. This is the reason that CSF appears dark on FLAIR imaging. In addition, white matter appears darker than gray matter. Also seen in this section are the lateral ventricles, fourth ventricle, and quadrigeminal cistern behind the third ventricle. The superior and inferior sagittal sinuses are seen in the superior and inferior margins of the falx cerebri.

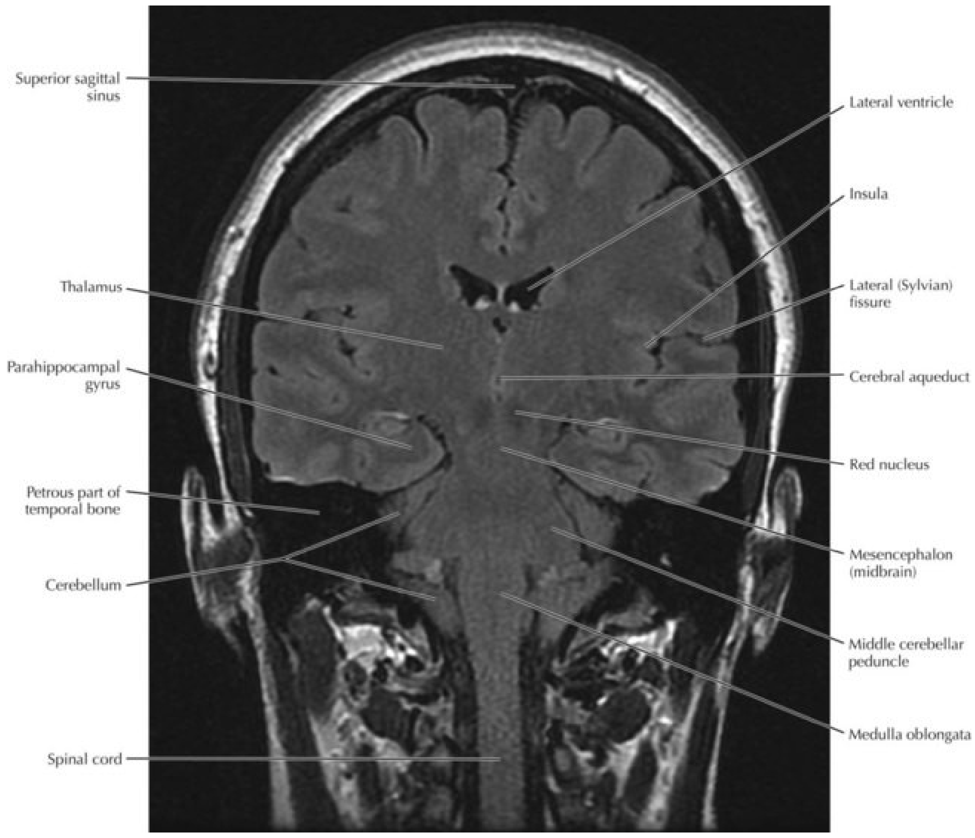

8.56 T2 Flair Coronal MRI through the Brainstem

FLAIR is a standard sequence that is obtained with most neurological MRIs. It is not requested for a particular suspected pathology because it is always done. It is most helpful because it highlights pathology with associated edema. The FLAIR sequence suppresses the fluid signal from CSF but not from edematous pathology such as edema surrounding a tumor or abscess. T1 images have black CSF but do not show edema with the same sensitivity as FLAIR images would. This section is just anterior to the cerebellum through the midbrain, medulla oblongata, and spinal cord. It is in between the third and fourth ventricles and through the cerebral aqueduct that connects them. The petrous part of the temporal bone is black; it contributes to the floor of the middle cranial fossa containing the temporal lobe.

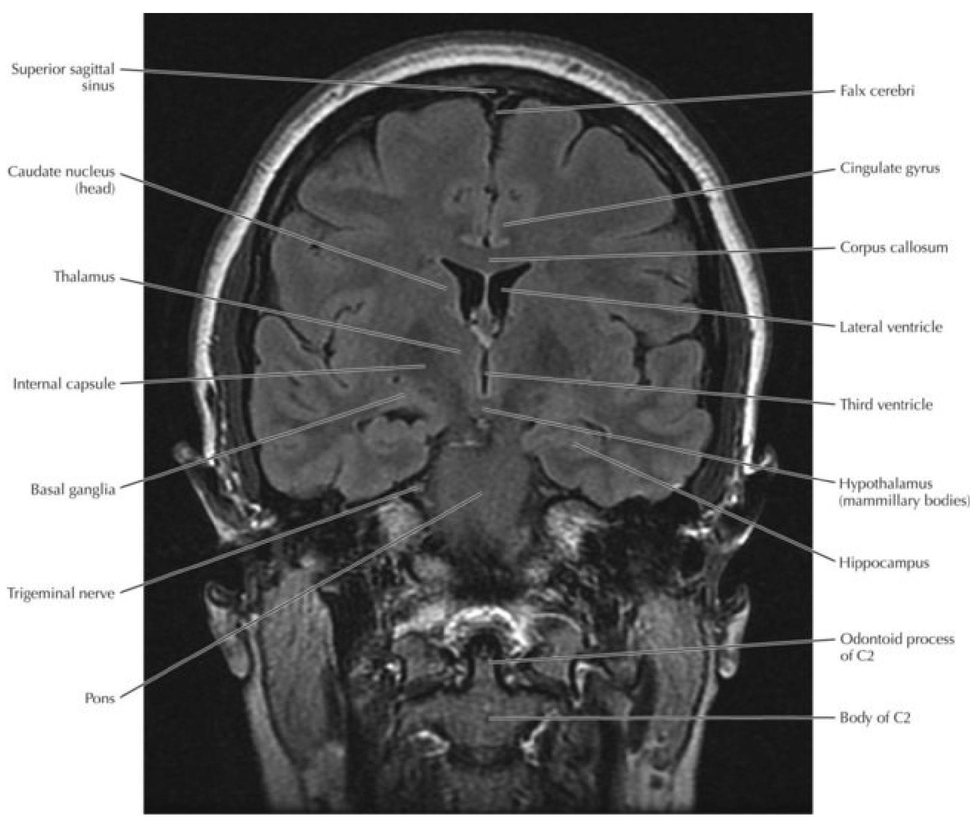

8.57 T2 Flair Coronal MRI through the Pons and Third Ventricle

The body and odontoid process of the second cervical vertebra indicate that this section is just anterior to the foramen magnum and vertebral canal. The temporal lobe of the cerebrum connects with the parietal lobe above. The section is through the middle of the third ventricle with the thalamus and basal ganglia on either side. It is also through the pons at the level of cranial nerves exiting the brainstem. Here, the cisternal segment of the trigeminal (V) nerve is seen passing toward Meckel's cave in the middle cranial fossa. All of the coronal sections contain the corpus callosum connecting the left and right cerebral hemispheres just superior to the lateral ventricles. They also show the internal capsule of white matter sending information to and from the cerebral hemispheres.

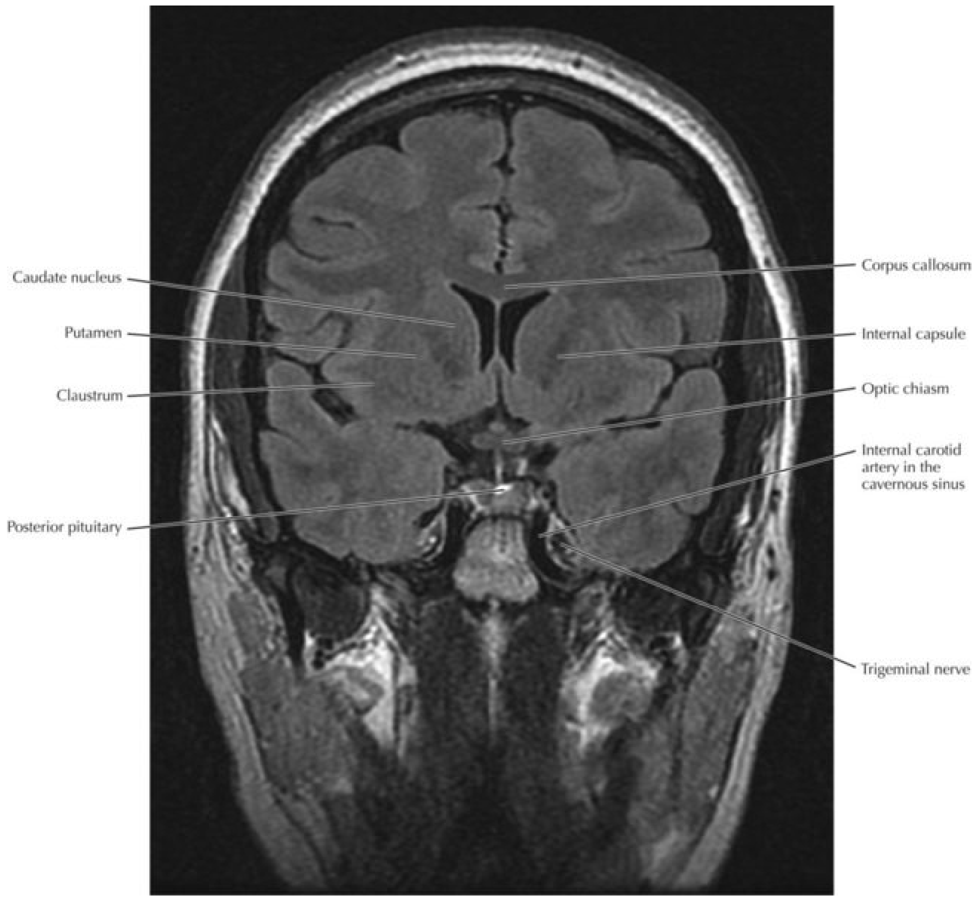

8.58 T2 Flair Coronal MRI through the Optic Chiasm

Continuing anteriorly, this section is through the posterior lobe of the pituitary gland (neurohypophysis) near the junction of the occipital and sphenoid bones in the midline. The continuity between the temporal and parietal lobes diminishes. The internal carotid artery enters the cavernous sinus from the carotid canal at the apex of the petrous part of the temporal bone on either side, just medial to the trigeminal nerve. Superior to the pituitary gland is the optic chiasm. The internal capsule courses between the caudate nucleus and putamen.

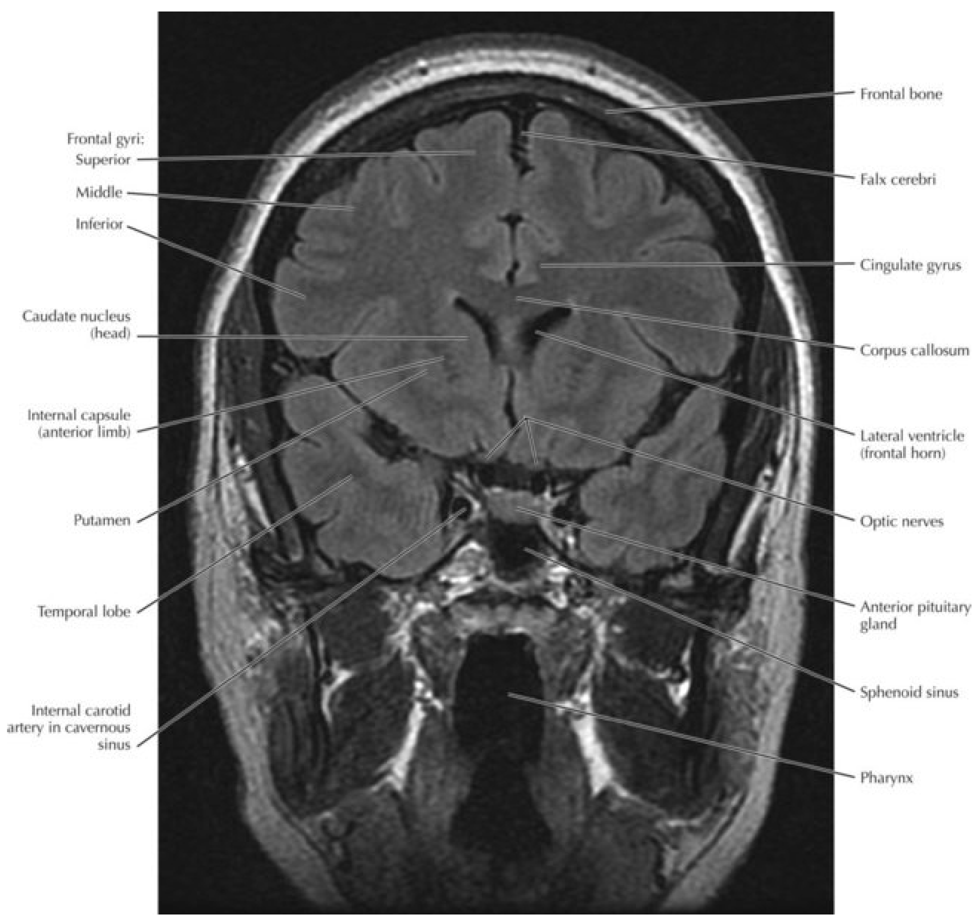

8.59 T2 Flair Coronal MRI through the Temporal Lobes

In this section the temporal lobes are now discrete and closer to the temporal poles. The section is through the anterior lobe of the pituitary gland (adenohypophysis), sphenoid sinus, and pharynx. Many important structures surround the body of the sphenoid bone. On either side of the sphenoid bone the internal carotid artery continues anteriorly through the cavernous sinus, a dural sinus that receives blood from the ophthalmic veins of the orbits and veins from deep in the brain. Also passing through the sinus with the internal carotid artery are cranial nerves III, IV, VI, and the first two divisions of the trigeminal nerve (V). The optic nerves are visible in this section, which is just anterior to the optic chiasm. The heads of the caudate nuclei are seen indenting the lateral ventricles.

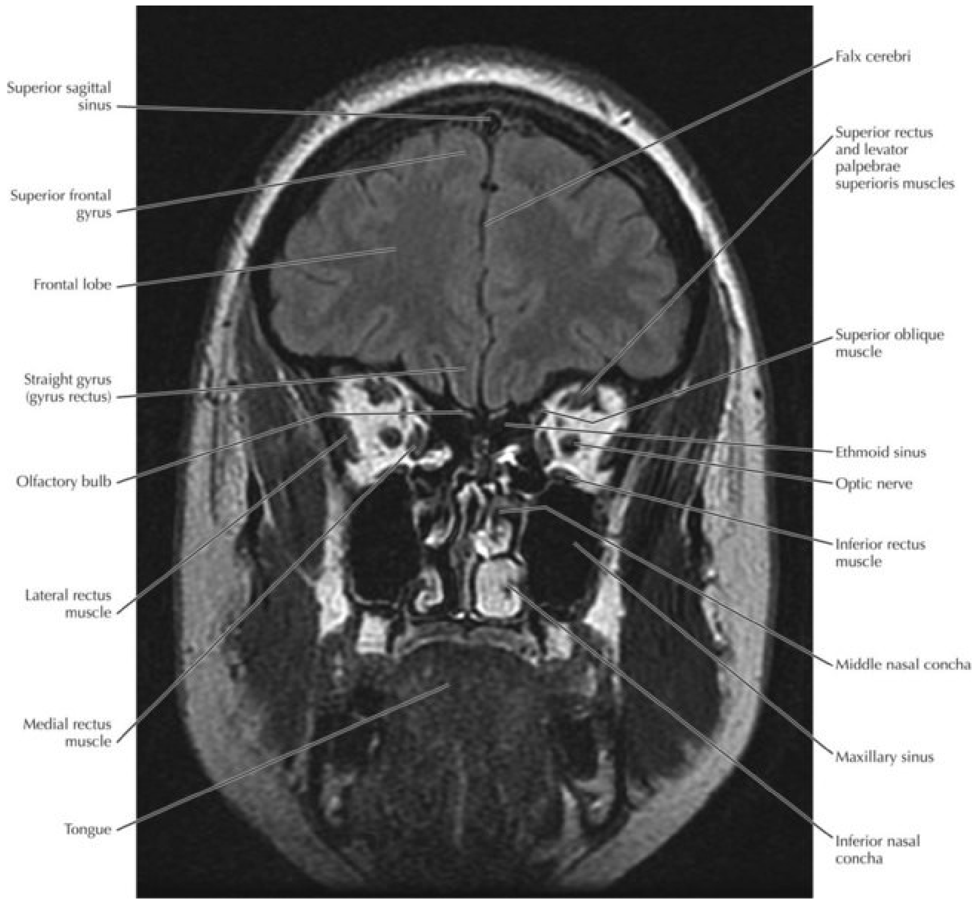

8.60 T2 Flair Coronal MRI through the Frontal Lobes

The posterior aspects of the orbits and maxillary sinuses indicate that the plane of section is anterior to the temporal lobes; only the frontal lobes of the brain are visible. They are separated by the falx cerebri that is visible in all of the coronal sections of the brain. Just inferior to the frontal lobes near the midline are the olfactory bulbs resting on the cribriform plate of the ethmoid bone. The dark between the orbits is from air within the ethmoid sinus. Seen within the fat in each orbit are the optic nerve and extraocular muscles: the inferior rectus, medial rectus, lateral rectus, and superior rectus just below the levator palpebrae superioris muscle.

A. T1 axial MRI just above the foramen magnum **B.** T2 axial MRI at the same level in the same patient

8.61 T1 and T2 Axial MRI through the Medulla

This next series of MR images are axial T1-weighted **(A)** and T2-weighted **(B)** sections from the same subject. This section is through the medulla oblongata and inferior part of the cerebellum just superior to the foramen magnum. The vertebral arteries are easily seen entering the skull through the foramen magnum because the CSF that surrounds them is bright on the T2-weighted sequence **(B).** Pathology at this level may also involve cranial nerves IX, X, XI, and XII. The spinal accessory nerve (XI) exits the cervical spinal cord, ascends through the foramen magnum, and then exits the skull through the jugular canal to innervate the trapezius and sternocleidomastoid muscles. Rootlets of the glossopharyngeal (IX), vagus (X), and hypoglossal (XII) nerves exit the brainstem just superior to the foramen magnum.

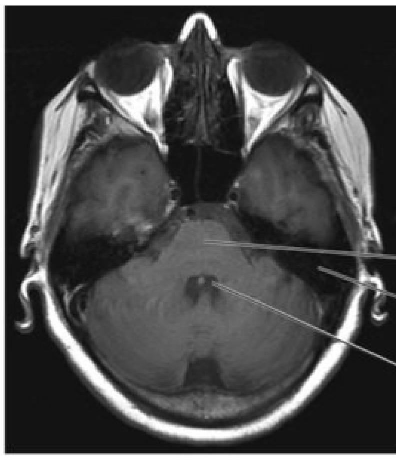

A. T1 axial MRI

B. T2 axial MRI. Note the abducens nerve next to the pons. The insert is from a slightly lower level, showing the facial and vestibulocochlear nerves.

8.62 T1 and T2 Axial MRI through the Cerebellum, Temporal Lobes, and Eye

This section through the orbit and eye highlights the differences between T1- and T2-weighted MRI. Fluid is dark in T1 **(A)** and bright in T2 **(B);** note the vitreous humor of the eye and the CSF. White matter is lighter than gray matter in T1; the reverse is true for T2. Bone, connective tissue, and air have low signal (are dark) in both T1 and T2. Fat is bright in both but a bit lighter here in T1 compared with T2. This section is through the pons, fourth ventricle, and middle of the cerebellum, and the inferior aspect of the temporal lobes is visible. The vertebral arteries have joined to form the basilar artery anterior to the brainstem. Sections through the pons contain cranial nerves, and it is important to look around the brainstem for tumors and other pathology involving these nerves. For example, this level is typical for identifying a vestibular schwannoma. Compare the abducens nerve in **B** with cranial nerves VII and VIII in the insert from a slightly lower level.

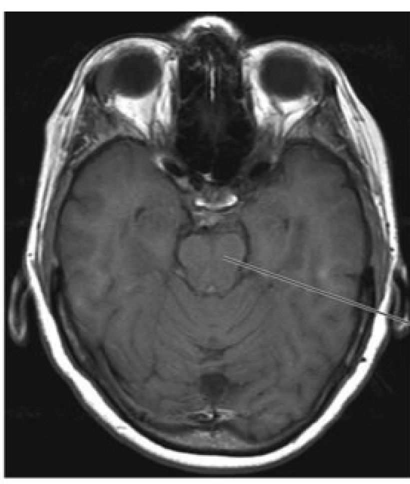

A. T1 axial MRI at the caudal end of the midbrain. The occipital lobe overlaps the top of the cerebellum posteriorly.

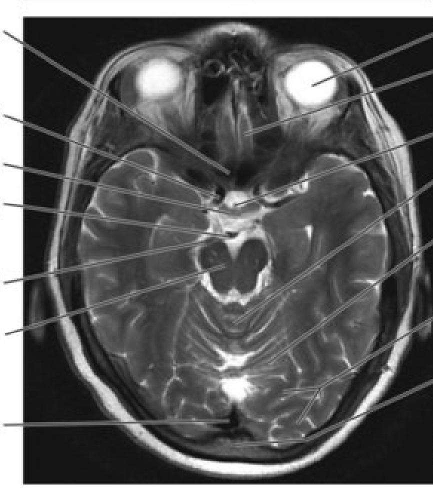

B. T2 axial MRI. Note the basilar and internal carotid arteries, the sources for the cerebral arterial circle of Willis.

8.63 T1 and T2 Axial MRI through the Upper Cerebellum

This plane of section is through the temporal lobes, top of the cerebellum, and inferior aspect of the occipital lobes, where they overlap the cerebellum posteriorly. The confluence of sinuses, also known as the *torcular herophili*, is seen at the level of the tentorium cerebelli, although most of the tentorium is just out of the plane. The section is also through the stalk of the pituitary gland and caudal aspect of the midbrain near the level of the cerebral arterial circle (of Willis). The internal carotid arteries are anterior, and the basilar artery and posterior cerebral arteries are seen posteriorly. The latter are the termini of the basilar artery. A search strategy would include a careful assessment of the arteries for normal anatomical variants, aneurysms, calcifications, and other types of pathology.

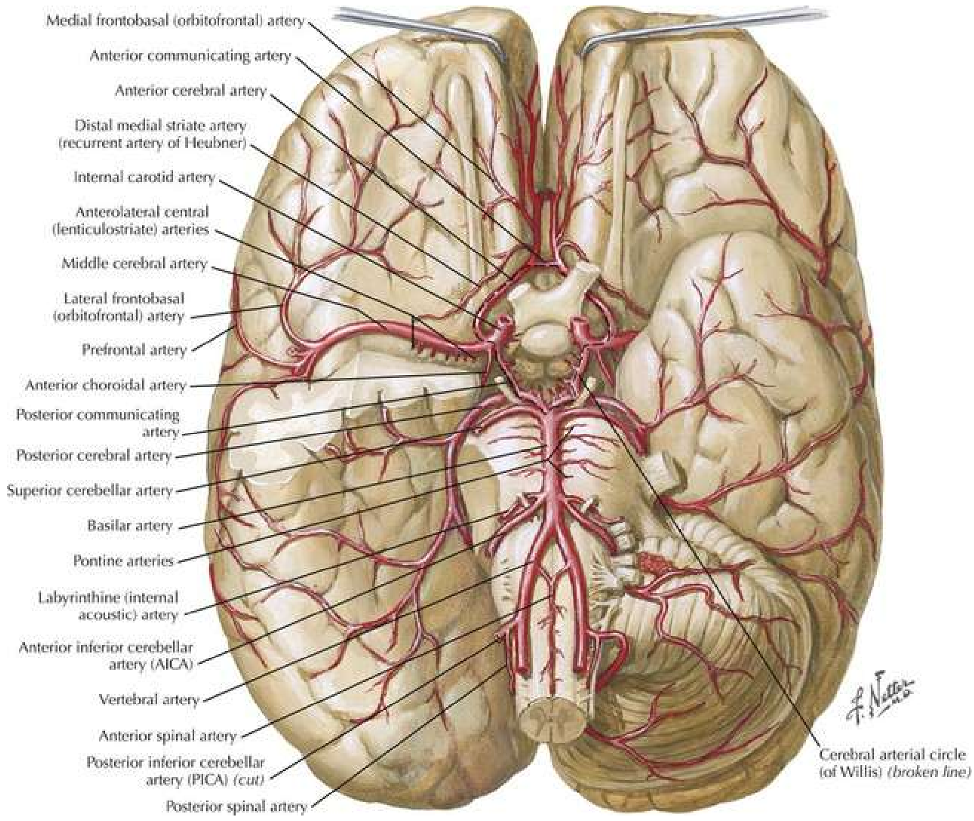

8.64 Arteries of the Brain: Inferior View

The brain receives its blood supply from the vertebral and internal carotid arteries. The vertebral arteries merge at the pontomedullary junction to form the basilar artery that divides into the posterior cerebral arteries at the top of the pons. The posterior vertebrobasilar circulation supplies the brainstem, cerebellum, occipital lobes, and the inferior and medial surfaces of the temporal lobes. The internal carotid arteries continue as the middle cerebral arteries and give off the smaller anterior cerebral arteries. The anterior internal carotid circulation supplies the frontal and parietal lobes and the lateral surface of the temporal lobes. The anterior and posterior circulations both contribute to the circle of Willis, and both supply the choroid plexus in the lateral ventricles. The circle of Willis surrounds the optic chiasm and the inferior surface of the hypothalamus.

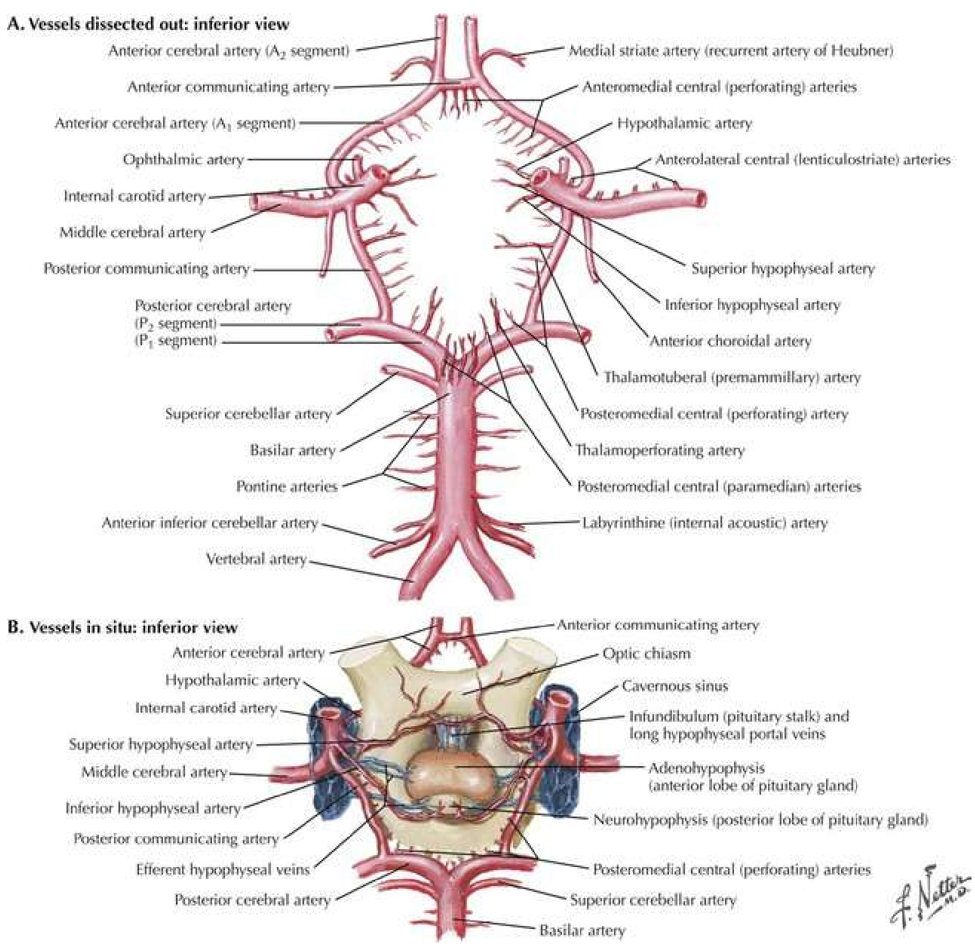

8.65 Cerebral Arterial Circle (of Willis)

Arteries that form the circle of Willis are, from anterior to posterior, the unpaired anterior communicating artery and the paired anterior cerebral, internal carotid, posterior communicating, and posterior cerebral arteries **(A).** The circle of Willis surrounds the optic tracts and the inferior surface of the hypothalamus **(B).** Small perforating or ganglionic arteries arise from the circle of Willis and supply deep structures in the diencephalon and cerebral hemispheres. The hypophyseal arteries that supply the pituitary gland (hypophysis) are branches of the internal carotid arteries rather than direct branches from the circle of Willis **(B).** Hypophyseal veins drain into the cavernous sinus. Hypophyseal portal veins lie in the infundibulum (pituitary stalk).

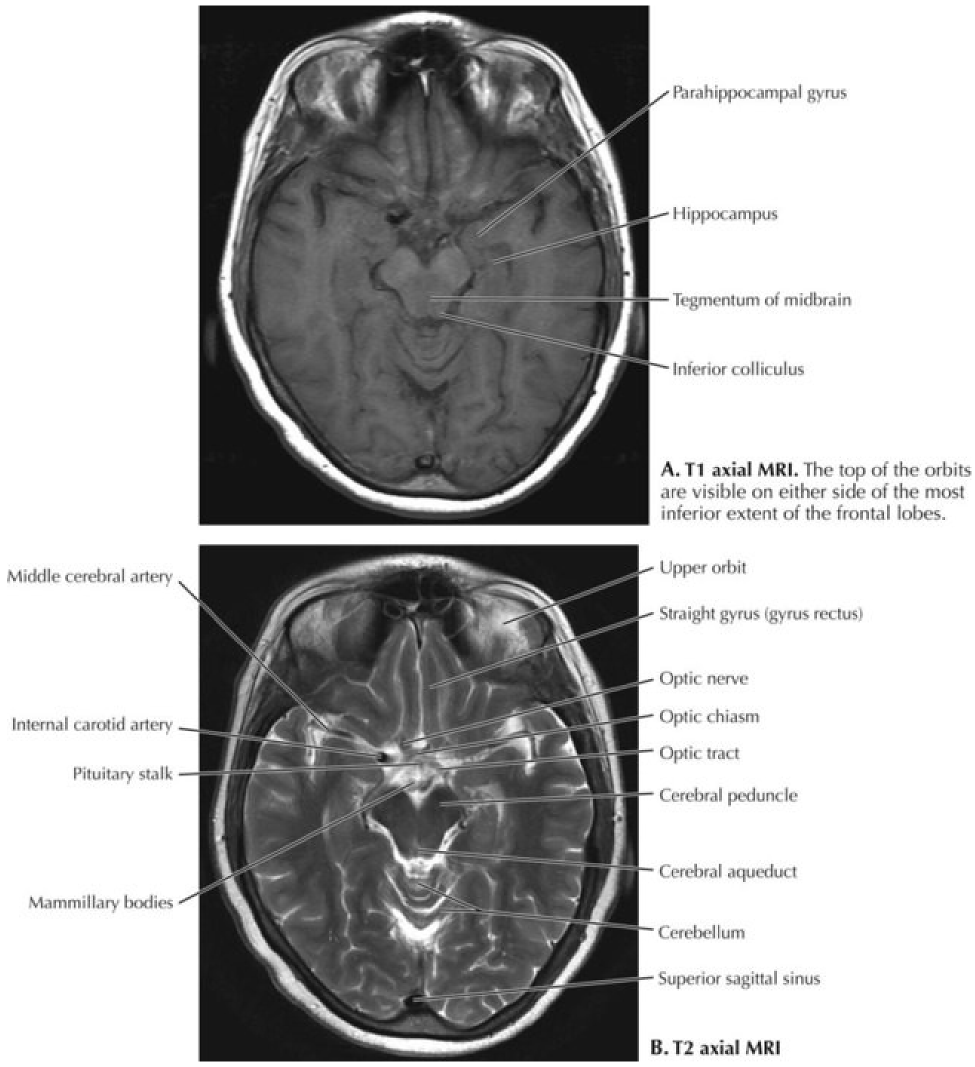

A. T1 axial MRI. The top of the orbits are visible on either side of the most inferior extent of the frontal lobes.

B. T2 axial MRI

8.66 T1 and T2 Axial MRI through the Optic Chiasm

The cerebellum is nearly out of the plane of section, and more of the occipital lobes are seen. The most inferior aspects of the frontal lobes are visible between the orbits. The section captures the optic chiasm and mammillary bodies, the stalk of the pituitary gland, and the origin of the middle cerebral arteries from the internal carotid arteries. The plane is below the third and lateral ventricles and above the fourth ventricle anterior to the cerebellum. It transects the cerebral aqueduct through which CSF passes from the third to fourth ventricle. Although none of the ventricles are normally visible at this level, in a patient with hydrocephalus the enlarged temporal horns of the lateral ventricles may be seen. Their presence would aid in making the diagnosis.

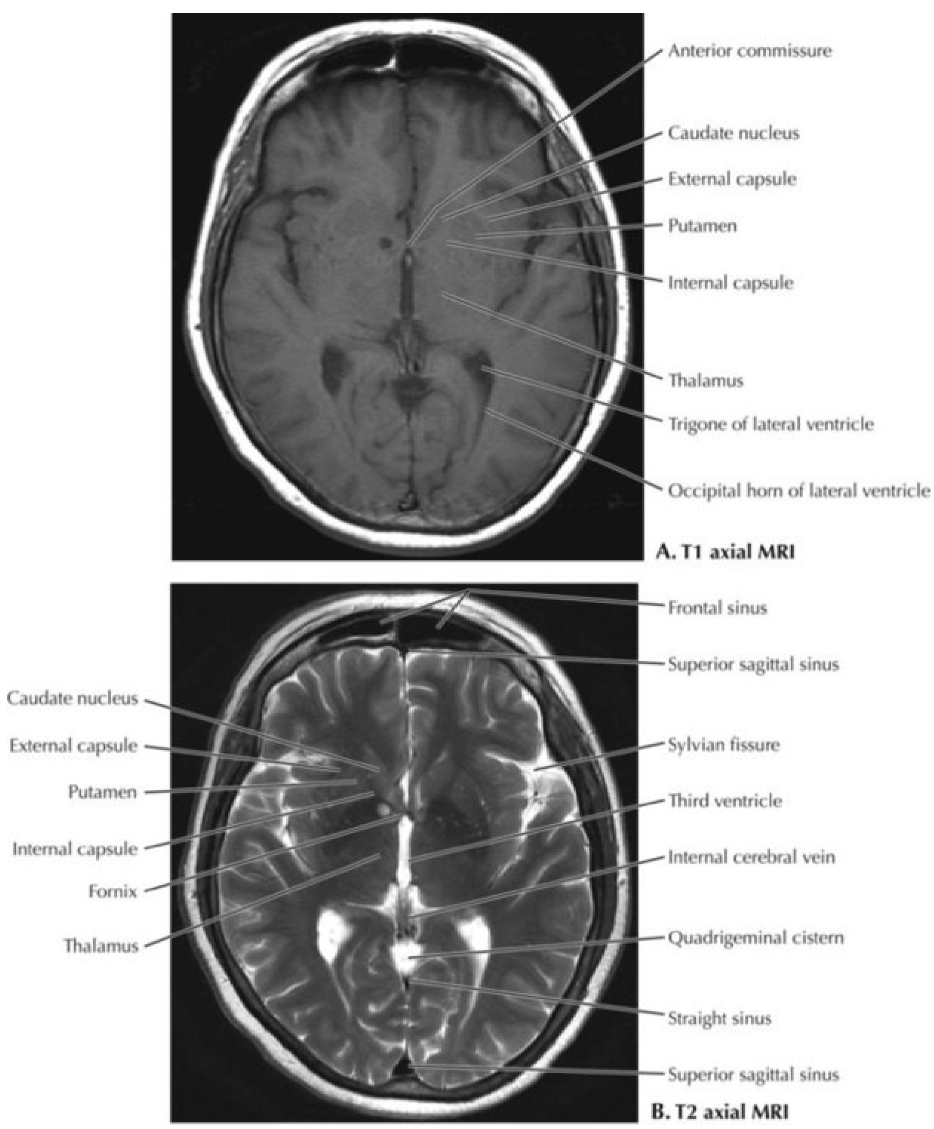

A. T1 axial MRI

B. T2 axial MRI

8.67 T1 and T2 Axial MRI through the Thalamus and Third Ventricle

This section is through the third ventricle flanked on either side by the thalamus. The trigone and occipital horn of the lateral ventricles are visible. Anterior to the thalamus are the caudate nucleus and putamen of the basal ganglia. The anterior limb of the internal capsule passes between the caudate nucleus and putamen. The posterior limb is lateral to the thalamus. The section is near the top of the cerebellum. Most of the tentorium cerebelli is out of the plane, although the straight sinus within it at the intersection of the falx cerebri is cut obliquely **(B)**. The internal cerebral veins are also seen just before they join the great cerebral vein of Galen, which forms the straight sinus when it joins the inferior sagittal sinus. The superior sagittal sinus is seen just before it joins the straight sinus to form the transverse sinuses.

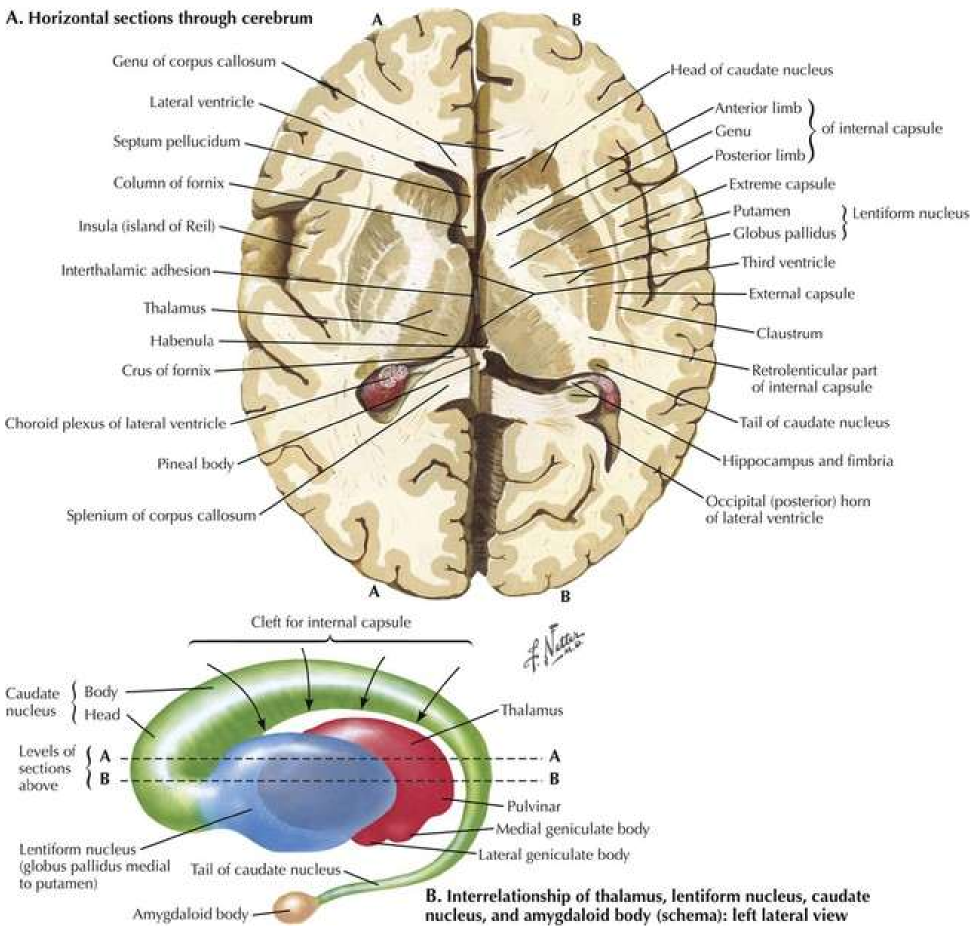

8.68 Transverse (Axial) Section of the Brain at the Level of the Basal Nuclei

Two levels of horizontal sections (**A** and **B**) through the cerebrum illustrate the relationships of the basal nuclei (ganglia), the thalamus, and the internal capsule. Embedded in the white matter of each cerebral hemisphere is a large mass of gray matter, the corpus striatum, which makes up most of the basal nuclei. The corpus striatum consists of the caudate nucleus and the lentiform (lenticular) nucleus that is further subdivided into the putamen laterally and the pale globus pallidus medially. The C-shaped caudate nucleus is named for its resemblance to a long tail as it follows the curvature of the lateral ventricle from the frontal lobe into the temporal lobe. In **B,** the caudate nucleus is seen to be continuous with the putamen. They are also functionally related and referred to as the striatum. Although the tail of the caudate nucleus ends at the amygdala in the temporal lobe, the two are not functionally related. The internal capsule, a V-shaped area of white matter, separates the lentiform nucleus laterally from the caudate nucleus and the thalamus medially. It consists of projection fibers connecting the cortex with subcortical structures.

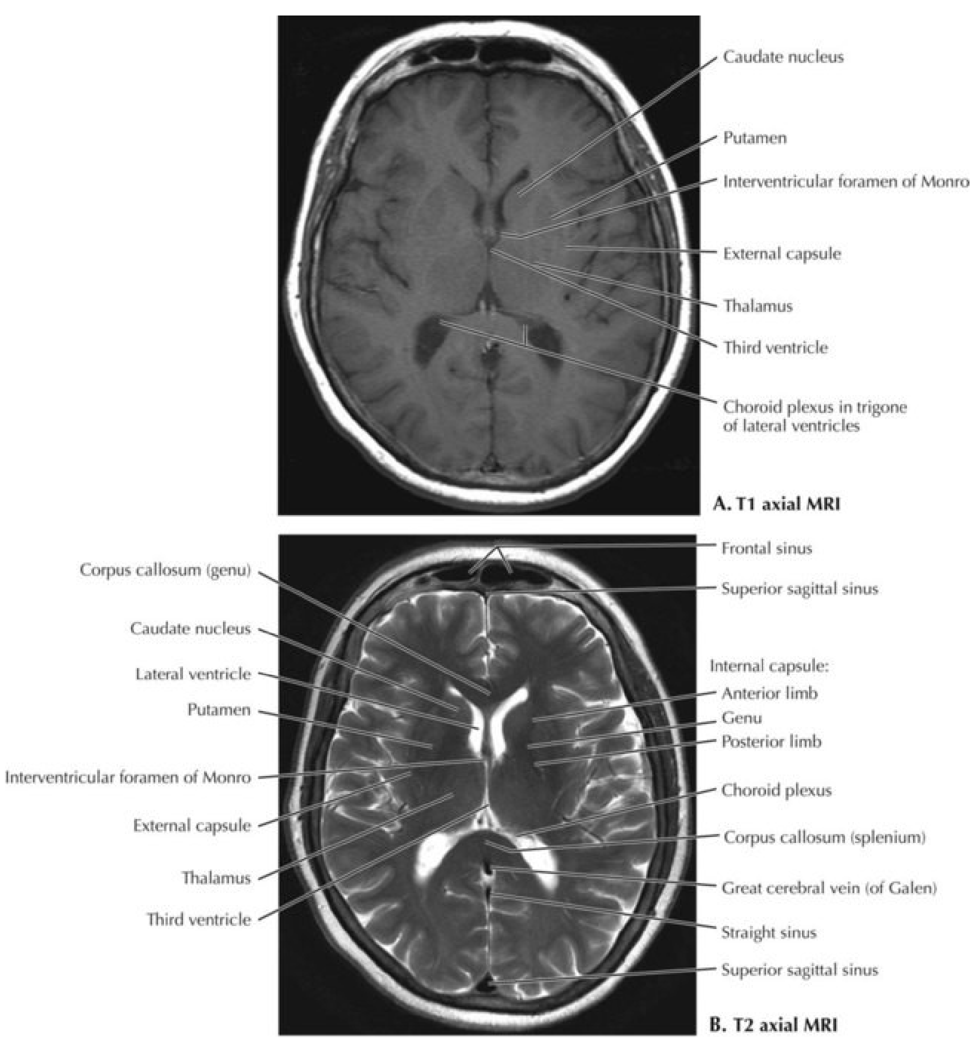

8.69 T1 and T2 Axial MRI through the Thalamus and Lateral Ventricles

This plane of section is near the middle of the cerebrum through the frontal, parietal, and occipital lobes. The frontal sinus is prominent anteriorly within the frontal bone. The section is at the top of the third ventricle between the left and right thalamus at the level of the interventricular foramina of Monro on each side that communicate with the lateral ventricles. Choroid plexus is visible in the trigone of the lateral ventricles posteriorly. The superior sagittal sinus is visible both anteriorly and posteriorly in the falx cerebri between the cerebral hemispheres. The great cerebral vein of Galen approaches the straight sinus in the tentorium cerebelli, although most of the tentorium is below the plane of section between the occipital lobes and cerebellum.

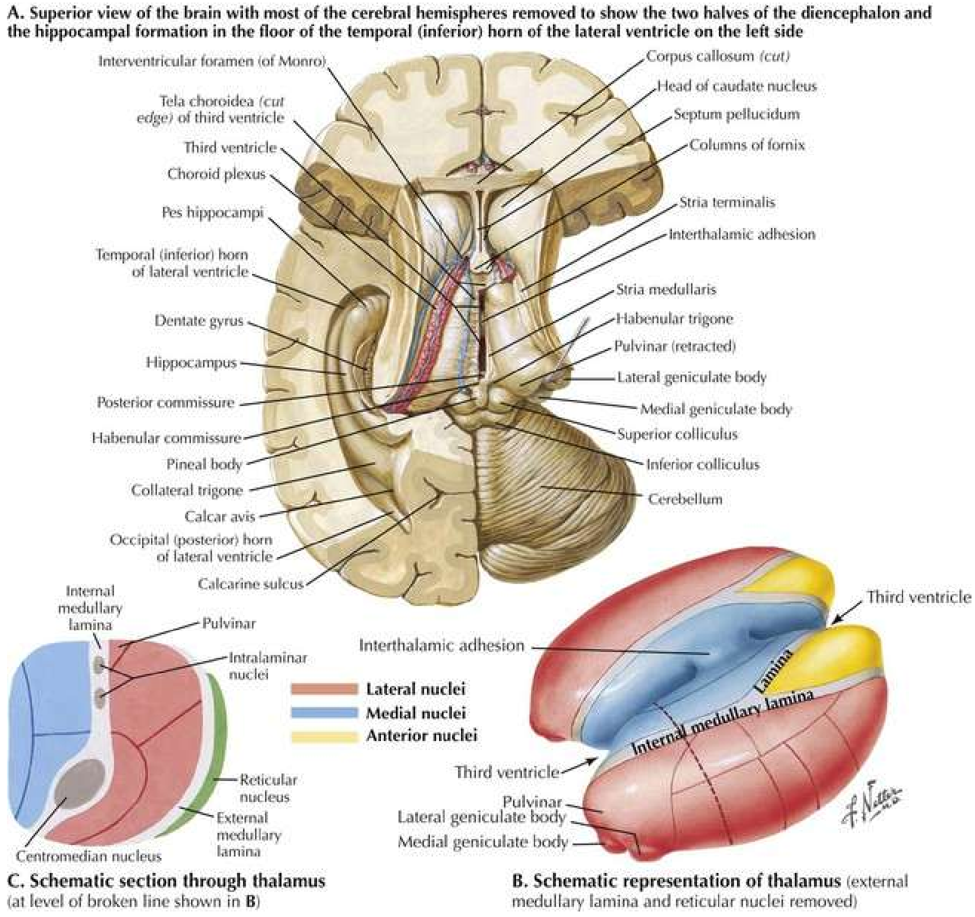

C. Schematic section through thalamus (at level of broken line shown in **B**)

B. Schematic representation of thalamus (external medullary lamina and reticular nuclei removed)

8.70 Thalamus

The vascular tela choroidea forms the roof of the third ventricle between the two halves of the diencephalon and extends laterally to form the choroid plexus of each lateral ventricle. Lying inferior to the roof of the third ventricle at the back of the thalamus is the epithalamus, consisting of the stria medullaris, the habenula, and the pineal gland (body). Posterior and inferior to the diencephalon are the paired superior and inferior colliculi of the midbrain. The internal medullary lamina, a vertical sheet of white matter, divides the thalamus into medial and lateral groups of nuclei and bifurcates anteriorly to enclose the anterior nuclei. The external medullary lamina separates the lateral nuclei from the thin reticular nucleus. The interthalamic adhesion (massa intermedia) is a bridge of gray matter extending across the third ventricle connecting the two halves of the thalamus. Most of the thalamic nuclei form reciprocal connections with specific motor, sensory, or limbic areas of cortex. The intralaminar, midline, and reticular nuclei have diffuse or nonspecific connections with widespread areas of cortex.

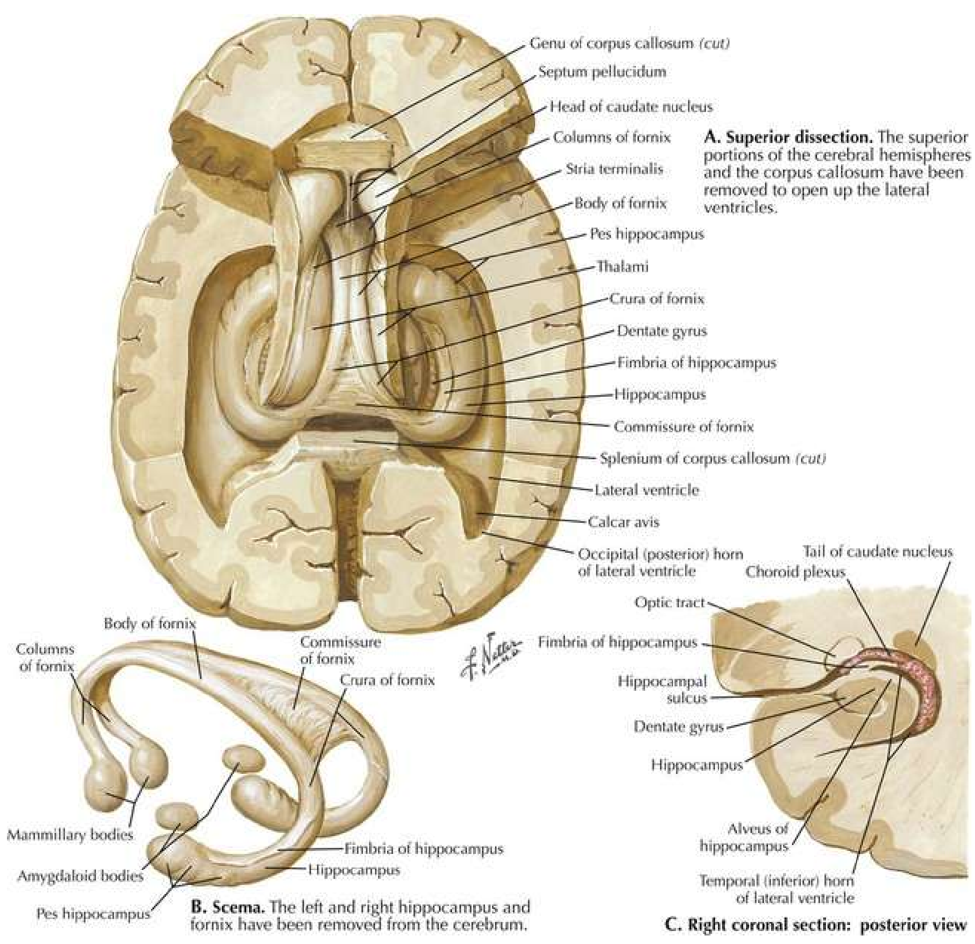

A. Superior dissection. The superior portions of the cerebral hemispheres and the corpus callosum have been removed to open up the lateral ventricles.

B. Scema. The left and right hippocampus and fornix have been removed from the cerebrum.

C. Right coronal section: posterior view

8.71 Hippocampus and Fornix

Bulging into the floor of each temporal horn of a lateral ventricle is the hippocampus (**A** and **B**), a curved, elongated ridge of three-layered archicortex that is continuous with the fornix **(B).** With the adjacent, curving parahippocampal gyrus (not labeled) it resembles the head and body of a seahorse (Gr., hippocampus). Its expanded anterior end resembles a foot with toes and is termed the *pes hippocampus*. Axons leave the hippocampus as the alveus that becomes the fimbria and then the C-shaped fornix that arches anteriorly over the thalamus. The small dentate gyrus medial to the fimbria resembles a row of teeth. Most of the fibers in the columns of fornix synapse in the mammillary body of the hypothalamus. The hippocampus consolidates short-term memories into long-term memories but does not store them.

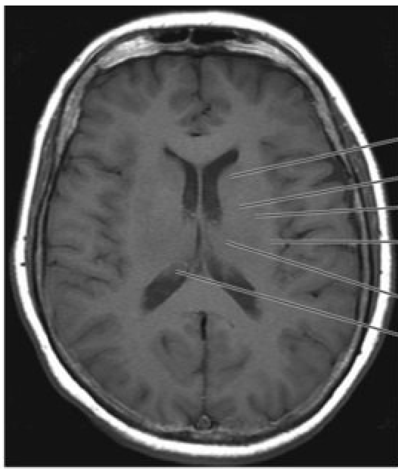

A. T1 axial MRI. Note the prominent choroid plexus.

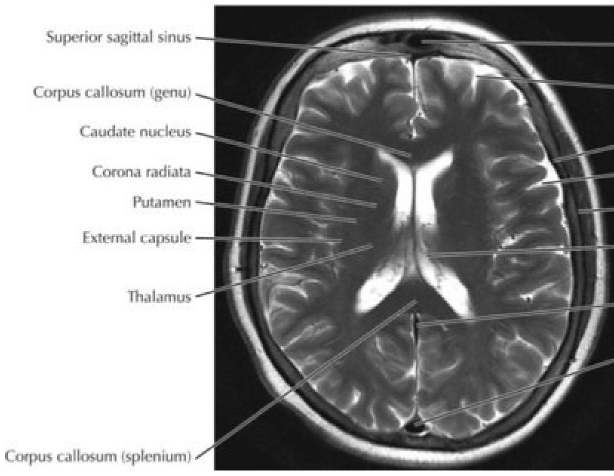

B. T2 axial MRI. The great cerebral vein is visible. It will join the inferior sagittal sinus to form the straight sinus.

8.72 T1 and T2 Axial MRI through the Lateral Ventricles

The lateral ventricles are prominent features in this plane of section. An extensive choroid plexus is visible. Anterior and posterior to the lateral ventricles are the genu and splenium of the corpus callosum, respectively. The great cerebral vein is still seen. The plane is near the top of the frontal sinus, and bright signal of the fatty diploë between the inner and outer tables of compact bone is prominent all around the calvarium. With T1 **(A),** the inner table of bone cannot be distinguished from the CSF in the subarachnoid space. Both appear dark. Note the small size of the superior sagittal sinus near its origin anteriorly compared with its large size near its termination posteriorly as it approaches the confluence of sinuses.

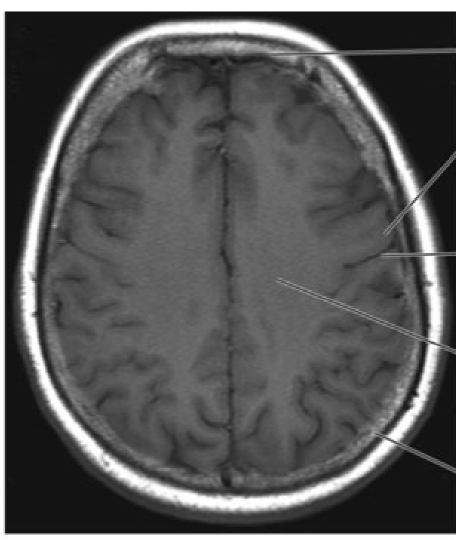

A. T1 axial MRI

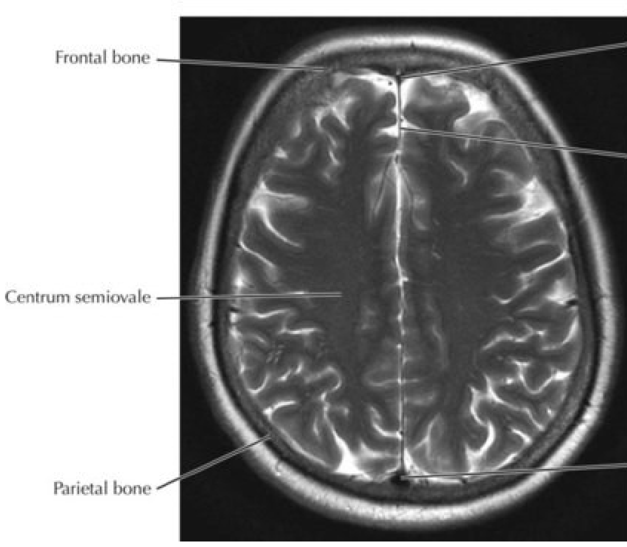

B. T2 axial MRI

8.73 T1 and T2 Axial MRI through the Middle of the Cerebral Hemispheres

This section is through the frontal and parietal lobes just above the occipital lobe. In the interior of the cerebral hemispheres above the lateral ventricles and corpus callosum is the centrum semiovale, the white matter tracts that pass to and from the internal capsule and corpus callosum. Part of the search for lesions, masses, stroke, and other pathology is the evaluation for symmetry of the two hemispheres and the contour of the falx cerebri for possible shift of midline structures. For example, bleeding or a tumor on one side of the brain increases the volume of that hemisphere. Midline structures push the falx cerebri toward the normal side.

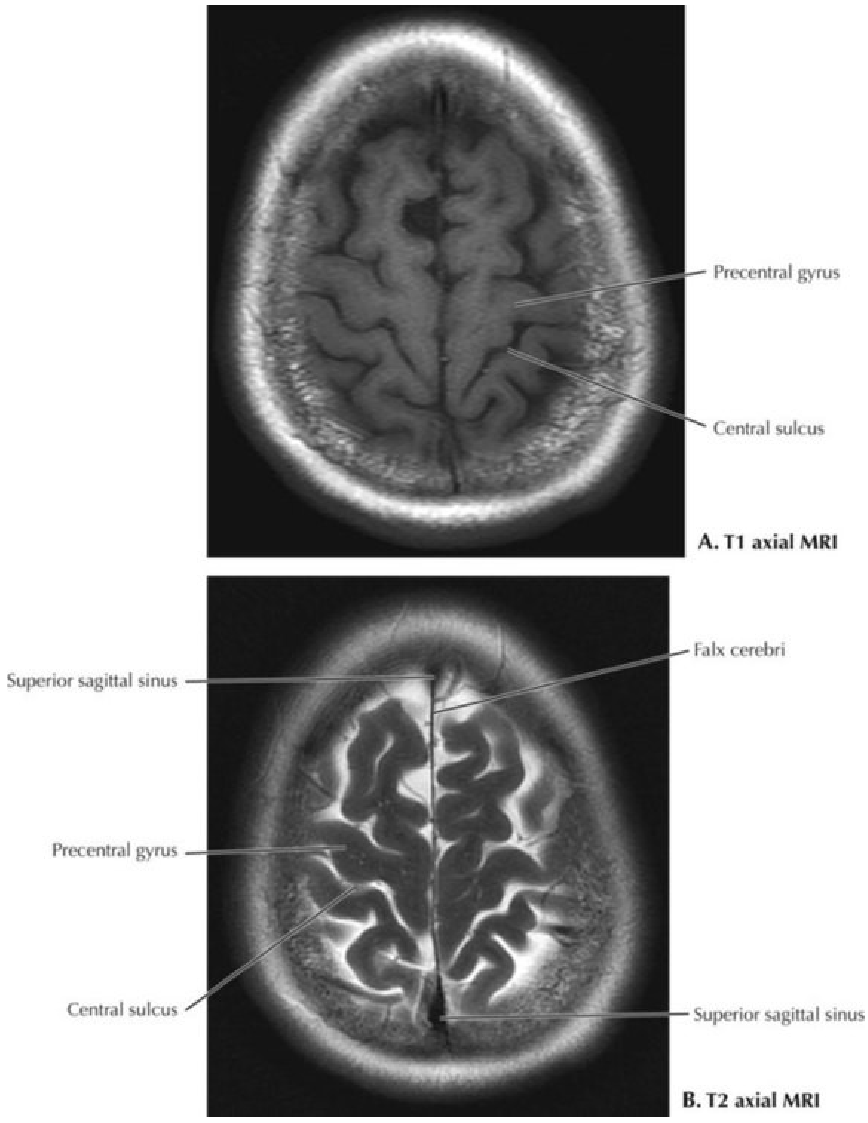

8.74 T1 and T2 Axial MRI through the Thalamus and Lateral Ventricles

A section through the high convexities of the cerebral hemispheres shows the gyri of the frontal and parietal lobes. The falx cerebri is in sharp contrast to the bright cerebrospinal fluid on the T2-weighted MRI **(B).** The profile of the superior sagittal sinus has a more oblique section because the sinus has a more horizontal orientation near the top of the skull. The curving frontal and parietal bones at the top of the calvarium are also sectioned obliquely, and the inner and outer tables of compact bone do not present sharp profiles because of an imaging phenomenon known as *partial volume averaging*.